

TOR SIGNALING:
FROM FRET PROBES DEVELOPMENT TO FUNCTION OF MAP4K3
IN *DROSOPHILA*

BORIS BRYK

2008

Dissertation

submitted to the
Combined Faculties for the Natural Sciences and for Mathematics
of the Ruperto-Carola University of Heidelberg, Germany
for the degree of
Doctor of Natural Sciences

presented by
Boris Bryk, Master of Science
Born in Kiev, Ukraine
Oral-examination: 03.02.2008

TOR SIGNALING:
FROM FRET PROBES DEVELOPMENT TO FUNCTION OF MAP4K3
IN *DROSOPHILA*

Referees: Dr. Carsten Schultz
Prof. Dr. Herbert Steinbeisser

INAUGURAL – DISSERTATION

zur

Erlangung der Doktorwürde

der

Naturwissenschaftlich-Mathematischen Gesamtfakultät

der

Ruprecht – Karls - Universität

Heidelberg

vorgelegt von

Boris Bryk, M.Sc.

aus Kiev, Ukraine

Tag der mündlichen Prüfung:

03.02.2009

**DIE ENTWICKLUNG VON FRET PROBEN ZUR UNTERSUCHUNG DER
TOR SIGNALWEGES UND DIE CHARAKTERISIERUNG VON MAP4K3
IN *DROSOPHILA***

Gutachter: Dr. Carsten Schultz
Prof. Dr. Herbert Steinbeisser

МОИМ РОДИТЕЛЯМ И СЕСТРЕ

Acknowledgements

This work has been carried out in the European Molecular Biology Laboratory – EMBL, in the group of Steve Cohen. I would like to express my gratitude to Steve, who gave me the opportunity to join his lab and contributed greatly to my scientific and personal growth at EMBL. I have learnt a lot during my time in Cohen lab and Steve was always there to answer questions, encourage and give feedback. I admire his scientific insight, dedication, positive and relaxed approach to making science. I feel very privileged to have been able to soak in the atmosphere of EMBL, an outstanding place full of bold ideas, scientific excitement and exceptional people.

I am deeply indebted to Aurelio Teleman for being an endless source of advice and help over the years, who generously hosted me in his lab, after Cohen lab moved to Singapore. Aurelio's contribution is hard to overestimate, as he has been supervising my work on day-to-day basis and I learnt from him how to work, think and organize myself. I am grateful to him for his enthusiasm, scientific guidance and support, which gave me energy and motivation in times of low spirits.

I would like to thank the members of my thesis advisory committee (TAC): Herbert Steinbeisser, Carsten Schultz, Pernille Rorth and Lars Steinmetz for their interest in my work and excellent scientific advice. Thanks to Jochen Wittbrodt for joining my defense committee.

All the Cohen lab members have been a cheerful bunch, making my time in the lab enjoyable and helping me a lot, especially in the beginning, when I was completely lost. Special thanks goes to George Easow for sharing long hours in the lab and outside it, teaching me the “snake dance” and Pandjabi moves and just being a good friend.

Carsten Schultz and his lab were invaluable help in my FRET project. Christiane Jost, Alen Piljic and Gregor Reither were instrumental in providing suggestions, reagents and equipment. The ALMF microscopy facility at EMBL (Timo, Jens, Arne, Stefan and Yury) were great in trying to help with experiments and microscopes.

I would like to express my gratitude to people from the Chemical Core facility, especially Peter Sehr and Joe Lewis, with whom we worked on the screen project that, though is not presented in this thesis, nevertheless was a very educational and positive experience.

Teleman lab at the DKFZ became a new home for me, thanks to everyone, “especialmente muchas gracias!” to Cristina Pallares for commenting on my thesis and her persistence in trying to improve my Spanish.

Too many wonderful people to mention individually including predocs, diving and waterski clubs members, my teammates in the Heidelbergman triathlon were very enjoyable part of my life, proving that life outside the lab exists, even during PhD ☺ I'd like to also mention the EMBL PhD programme office and the canteen staff, who took great care of me.

Many friends, both in Heidelberg and from afar supported and encouraged me in difficult times, particularly David Greenberg for sharing ideas and commenting on my thesis. “Toda raba” to all my Israeli friends, especially Yevgeny Artsev, who stayed “online” and sent their warmth from Israel during the cold German winters. Vielen Dank geht an Rudi Walczak für die Übersetzung der Zusammenfassung. Дякую to Lyuba for sharing many special moments with me.

My deepest gratitude is reserved for my family – my parents and especially my sister for their inexhaustible trust in me. I dedicate this work to my family.

Мама, отец, Сашуня - посвящаю эту работу Вам, без Вас она была бы невозможна.

Table of contents

ACKNOWLEDGEMENTS	1
TABLE OF CONTENTS	3
SUMMARY	5
ZUSAMMENFASSUNG	7
1. INTRODUCTION	9
1.1. OVERVIEW	9
1.2. TOR SIGNALING – INTEGRATION OF EXTERNAL SIGNALS TO COORDINATE METABOLISM AND GROWTH	9
1.3. UPSTREAM REGULATORS OF TOR SIGNALING	11
1.4. DOWNSTREAM OF TOR – REGULATION OF TRANSLATION AND GROWTH.....	14
1.5. METABOLISM REGULATION BY INSULIN/TOR PATHWAY IN DROSOPHILA MELANOGASTER.....	17
2. AIMS OF THE THESIS	20
3. DEVELOPMENT OF A FRET-BASED PROBE FOR TOR SIGNALING	21
3.1. INTRODUCTION - FLOURESCENT PROBES AS TOOLS TO VISUALIZE CELLULAR PROCESSES	22
3.1.1. <i>Fluorescence and Fluorescence Resonance Energy Transfer phenomena</i>	22
3.1.2. <i>Determination of FRET</i>	24
3.1.3. <i>Green Fluorescent Protein and its variants for in vivo labeling</i>	27
3.1.4. <i>Design and uses of FRET probes</i>	30
3.1.5. <i>FlAsH labeling</i>	33
3.2. RESULTS.....	35
3.2.1. <i>Conformational FRET probe strategy</i>	35
3.2.2. <i>Variation of fluorophore pairs and single-tagged 4EBP1</i>	44
3.2.3. <i>A FlAsH labeling approach for making FRET probe</i>	46
3.2.4. <i>FRET measurements using FlAsH labeling</i>	50
3.3. DISCUSSION.....	60
3.3.1. <i>4EBP1 regulation is disturbed by fusion to GFP</i>	60
3.3.2. <i>FlAsH labeled 4EBP1 is functional but produces no FRET</i>	62
4. ANALYSIS OF MAP4K3 FUNCTION IN DROSOPHILA MELANOGASTER	66
4.1. INTRODUCTION - AMINO ACID SIGNALING AND FAT METABOLISM.....	67
4.1.1. <i>Nutrient signaling by TORC1</i>	67
4.2. RESULTS.....	71
4.2.1. <i>Identification of the Drosophila MAP4K3 mutant</i>	71
4.2.2. <i>Phenotypic characterization of MAP4K3 mutant</i>	73
4.2.3. <i>Overexpression of MAP4K3</i>	79
4.2.4. <i>Genetic interactions</i>	81
4.2.5. <i>MAP4K3 molecular mechanism</i>	82
4.3. DISCUSSION.....	86
4.3.1. <i>MAP4K3 regulates growth</i>	86
4.3.2. <i>MAP4K3 affects fat metabolism</i>	87
4.3.3. <i>TOR activity status and possible mechanism</i>	88
4.3.4. <i>Metabolism and growth, a close relationship</i>	90
5. CONCLUSIONS	93
6. OUTLOOK	95
7. MATERIALS AND METHODS	97
7.1. CHEMICALS AND SOLUTIONS.....	97
7.2. MOLECULAR BIOLOGY AND CLONING.....	97
7.3. PLASMIDS.....	97
7.4. PCR, RT-PCR AND QUANTITATIVE REAL-TIME PCR.....	99
7.4.1. <i>PCR reaction</i>	99
7.4.2. <i>RNA isolation</i>	100

7.4.3.	<i>First-strand cDNA synthesis – Reverse Transcription</i>	100
7.4.4.	<i>PCR reaction on cDNA</i>	101
7.4.5.	<i>Quantitative real-time RT-PCR</i>	101
7.5.	WESTERN BLOT.....	103
7.6.	CAP PULL-DOWN AND CO-IMMUNOPRECIPITATION	105
7.7.	CELL CULTURE.....	106
7.8.	MICROSCOPY AND FRET	107
7.8.1.	<i>Ratiometric FRET measurement</i>	107
7.8.2.	<i>Image analysis</i>	108
7.8.3.	<i>Acceptor photobleaching</i>	108
7.8.4.	<i>Sensitized emission</i>	108
7.8.5.	<i>FLAsH labeling and BAL experiments</i>	109
7.9.	FLY GENETICS	110
7.9.1.	<i>Fly husbandry</i>	110
7.9.2.	<i>Fly strains</i>	110
7.9.3.	<i>Ectopic expression using GAL4/UAS system</i>	112
7.10.	FAT MEASUREMENTS.....	112
7.11.	SIZE MEASUREMENT	113
7.11.1.	<i>Growth controlled condition</i>	113
7.11.2.	<i>Body weight</i>	113
7.11.3.	<i>Growth rate/pupation</i>	114
7.11.4.	<i>Wing size and cell size measurement</i>	114
7.12.	STATISTICS.....	114
	APPENDIX	115
	LIST OF FIGURES	115
	LIST OF OIGONUCLEOTIDES USED FOR CLONING AND PCR	116
	REFERENCES	120

Summary

Cells in a multicellular organism need to monitor their environment for nutritional cues, growth and stress signals in order to adapt their metabolism and growth to the changing conditions. The Target of Rapamycin (TOR) signaling pathway is an evolutionary conserved cellular protein network that controls responses to these signals. TOR signaling is a major research topic because of its role in several prevalent human disorders, including cancer and diabetes, but our understanding of TOR pathway is still far from complete. This work is aimed at improving our understanding of TOR signaling in two ways: by developing new research tools to dissect the dynamics of TOR signaling in cells and by characterizing the function of a novel component in the TOR pathway.

The first chapter presents the project to develop a probe, based on the Fluorescence Resonance Energy Transfer (FRET) method, for measuring TOR activity in cell culture. I used several approaches to design a FRET probe, based on a substrate of TOR kinase called 4EBP1. These probes did not prove to be useful because fusions to fluorophore domains abolished biological regulation of 4EBP1. An alternative strategy whereby a small tag was introduced into 4EBP1 and then used for *in vivo* labeling, could solve this problem. Unfortunately, when this probe was expressed in the cells, its interaction with a corresponding partner did not produce a reliable FRET signal, as determined by three different methods. Nevertheless, the obtained results can be used as a basis for future attempts to develop probes for TOR kinase.

The second chapter describes the genetic analysis of the MAP4K3 function in *Drosophila*. MAP4K3 is a new component of the TOR pathway proposed to mediate nutrient sensing by TOR. I identified a strong hypomorphic MAP4K3 mutant and investigated the phenotypes caused by absence of this protein. MAP4K3 mutant flies were viable but weak. Mutant animals demonstrated delayed growth, reduced cell and organ size. Furthermore, they were lean, displaying reduced fat, which could be rescued by genetically increasing TOR activity. This suggests that the observed metabolic defect is due to low TOR

activity. The mechanism of MAP4K3 action may involve the MAP kinase pathway and/or modifying activity of Rag GTPases, which can interact with MAP4K3 in cell culture. These results establish MAP4K3 as a regulator of metabolism and growth and open up new possibilities for manipulating TOR signaling.

Zusammenfassung

Die Zellen eines vielzelligen Organismus müssen ihre Umgebung auf Nahrungs-, Wachstums- und Stresssignale überwachen, um ihren Stoffwechsel und ihr Wachstum den sich wandelnden Bedingungen anzupassen. Der Rapamycin (TOR) Signalweg stellt ein evolutionär konserviertes zelluläres Proteinnetzwerk dar, welches die spezifischen Reaktionen der Zelle auf obige Reize kontrolliert. Die Signalübertragung durch TOR ist wegen seiner Rolle in mehreren weit verbreiteten menschlichen Krankheiten, darunter Krebs und Diabetis, ein wichtiges Forschungsgebiet, aber unser Verständnis des TOR Signalweges ist immer noch lückenhaft. In der vorliegenden Arbeit werden zwei Ansätze verfolgt, um unser Verständnis des TOR Signalweges zu erweitern: die Entwicklung neuer Werkzeuge zur Untersuchung des dynamischen Verhaltens des TOR Signalweges in Zellen und die funktionelle Charakterisierung einer neuen Komponente des TOR Signalweges.

Das erste Kapitel stellt ein Projekt vor, im Rahmen dessen eine neue Sonde entwickelt wurde, die auf dem Prinzip des Fluorescence Resonance Energy Transfer (FRET) beruht und mit deren Hilfe die TOR Aktivität von Zellen in Kultur gemessen werden sollte. Ich habe mehrere unterschiedliche Versuche unternommen, die Sonde auf dem TOR Kinase Substrat 4EBP1 basierend zu entwickeln. Diese Sonden konnten jedoch nicht für die Messungen verwendet werden, da die Fluorophordomäne die biologische Regulation des 4EBP1 beeinträchtigte. Durch eine andere Strategie, bei der ein kleinerer Affinitäts "tag" in 4EBP1 eingeführt und für die *in vivo* Markierung verwendet wurde, konnte dieses Problem jedoch behoben werden. Leider zeigte diese FRET-Sonde, wenn sie in Zellen exprimiert wurde, aber das Problem, bei Interaktion mit ihrem entsprechenden Bindungspartner kein zuverlässiges FRET Signal zu liefern, was durch drei unterschiedliche Methoden nachgewiesen wurde. Die gewonnenen Ergebnisse können jedoch als Ausgangspunkt für zukünftige Versuche genutzt werden, Sonden für die TOR Kinase zu entwickeln.

Das zweite Kapitel beschreibt die genetische Untersuchung der Funktion von MAP4K3 in *Drosophila*. MAP4K3 ist eine neue Komponente des TOR Signalweges, der die Funktion zugeschrieben wird, das Aufspüren von

Nährstoffen durch TOR zu vermitteln. Ich habe eine starke hypomorphe Mutation in MAP4K3 identifiziert und den Phänotyp untersucht, den das Fehlen dieses Proteins verursacht. Fliegen mit der MAP4K3 Mutation waren lebensfähig, aber schwach. Sie wiesen ein verzögertes Wachstum und eine geringere Zell- und Organgröße auf. Weiterhin waren sie übermäßig dünn und besaßen einen verminderten Körperfettanteil, was durch genetische Erhöhung der TOR Aktivität aufgehoben werden konnte. Dies legt nahe, dass der beobachtete Stoffwechseldefekt auf zu geringer TOR Aktivität beruht. Es ist möglich, dass für den Wirkmechanismus von MAP4K3 der MAP Kinase Signalweg eine Rolle spielt oder die Modulierung der Aktivität von Rag GTPasen, welche mit MAP4K3 in Zellkultur interagieren können. Die vorliegenden Ergebnisse etablieren MAP4K3 als einen Stoffwechsel- und Wachstumsregulator und eröffnen neue Möglichkeiten, den TOR Signalweg zu manipulieren.

1. Introduction

1.1. Overview

All cells must constantly assess their environment for various cues, such as availability of nutrients for growth or signs of stress that may interfere with normal growth. Successful evaluation of environmental conditions is crucial for taking appropriate decisions that may determine whether the cell lives or dies. Therefore, cells have evolved complex and robust mechanisms that enable them to detect, process and respond to environmental cues. Such mechanisms are implemented by networks of interacting proteins that transduce signals activating or repressing the necessary processes in the cell. Many of these signaling cascades often use phosphorylation – the transfer of a phosphate group, as means to propagate a signal. Kinases, the enzymes mediating phosphate transfer, are central players of these signaling pathways and understanding of the function and regulation of kinases is a primary goal of cell and molecular biology.

This thesis deals with Target Of Rapamycin (TOR) kinase signaling, a pathway that has emerged as a critical node integrating many extracellular and intracellular cues to regulate growth and metabolism. After a general introduction to TOR signaling in and its functions, I will describe the two projects that constitute this thesis. The first project deals with developing a TOR kinase *in vivo* probe based on fluorescent visualization of biochemistry in live cells. The second project takes a genetic approach to assess the function of a new gene responsible for mediating nutrient sensing by TOR in *Drosophila melanogaster*.

1.2. TOR signaling – integration of external signals to coordinate metabolism and growth

TOR is an evolutionary conserved Ser/Thr kinase first identified in yeast as a target of the immunosuppressant drug Rapamycin (Heitman et al., 1991).

Rapamycin is produced by *Streptomyces hygroscopicus*, a bacterium found in soil of the Easter Island (in local language - Rapa Nui), from which the name Rapamycin arises. Every eukaryotic genome so far examined (including yeasts, algae, slime mold, plants, worms, flies and mammals) has contained a *TOR* gene. *Saccharomyces cerevisiae* have two *TOR* genes, while mammals possess a single gene producing a protein called mammalian Target of Rapamycin - mTOR (Wullschleger et al., 2006).

Since its discovery in the early 90's, TOR has been implicated in a long list of fundamental cellular processes and attracts ever increasing scientific attention. The literature is extensive; the number of publications in PubMed having the keyword "TOR" is approaching 8000, with new articles published every week. TOR kinase integrates cues from both outside and inside the cell, including hormones, availability of nutrients, energy status, and hypoxia. TOR kinase regulates a wide variety of processes including growth and proliferation, translation and ribosome biogenesis, metabolism and autophagy (Sarbasov et al., 2005). Naturally, I will focus my attention on the processes regulated by TOR that are relevant to my work.

One of the reasons TOR has become such a hot topic of research is its important role in development and disease. TOR is essential for organismal development, and its deficiency and in *C.elegans* and *D.melanogaster* leads to developmental arrest (Long et al., 2002; Oldham et al., 2000; Zhang et al., 2000). Knockout of mTOR in mice results in embryonic lethality (Gangloff et al., 2004). Phenotypes of TOR mutant animals resemble phenotypes of amino acid starvation, highlighting its role in nutrient sensing.

Dysregulation of the mTOR signaling pathway has been connected to a number of diseases, most prominently cancer and metabolic diseases. Many upstream regulators of TOR as well as downstream effectors are causally involved in cancer and the TOR pathway is considered an important target in cancer therapy (Bjornsti and Houghton, 2004a, b; Sabatini, 2006). Being regulated by insulin and feeding back to insulin signaling, mTOR is also an important player in metabolic disorders such as diabetes and obesity (Manning, 2004).

1.3. *Upstream regulators of TOR signaling*

TOR functions as a multiprotein complex, where members of the complex define its identity and function. Two distinct complexes have been described. TOR complex 1 (TORC1) is a rapamycin-sensitive one that in mammals contains, in addition to mTOR kinase, raptor and mLST8 proteins and regulates ribosomal biogenesis, protein synthesis and growth. TOR complex 2 (TORC2) is insensitive to rapamycin, contains rictor, mLST8 but not raptor and it is thought to regulate the actin cytoskeleton (Bhaskar and Hay, 2007). I will not further consider TORC2 as it is not directly connected to my work. Therefore, I will use the terms TOR and TORC1 interchangeably throughout this thesis.

Insulin/growth factors regulation of TOR

A simplified model of mammalian TOR signaling is presented in Figure 1. Molecular mechanisms of TOR regulation have been elucidated to a different extent for various upstream regulators. Insulin/IGF (Insulin-like Growth Factor) pathway is connected to TOR signaling, which is considered to have evolved later in multicellular organisms on top of the more ancient nutrient regulation of TOR. Cells must coordinate their actions with other cells within a tissue or an organ to allow coordinated behavior during development and growth. In animals, this is accomplished in part via insulin. Insulin and related hormones (e.g. IGF) are systemic hormonal signals that bind to the receptors on the cell surface and initiate a signaling cascade inside the cell. Activated insulin receptor promotes phosphorylation of insulin receptor substrate (IRS) and its recruitment to the cell membrane, which is needed for recruitment and activation of phosphatidylinositol 3-phosphate kinase (PI3K). In the cell membrane PI3K bound to IRS adds an additional phosphate group on its substrate phosphatidylinositol-4,5-phosphate (PIP₂) to produce phosphatidylinositol-3,4,5-phosphate (PIP₃). PIP₃ is a signaling molecule, which is recognized by a special protein domain called PH (for Pleckstrin Homology) domain. The concentration of PIP₃ is controlled by PI3K and PTEN – a phosphatase that antagonizes PI3K activity by removing a phosphate from PIP₃.

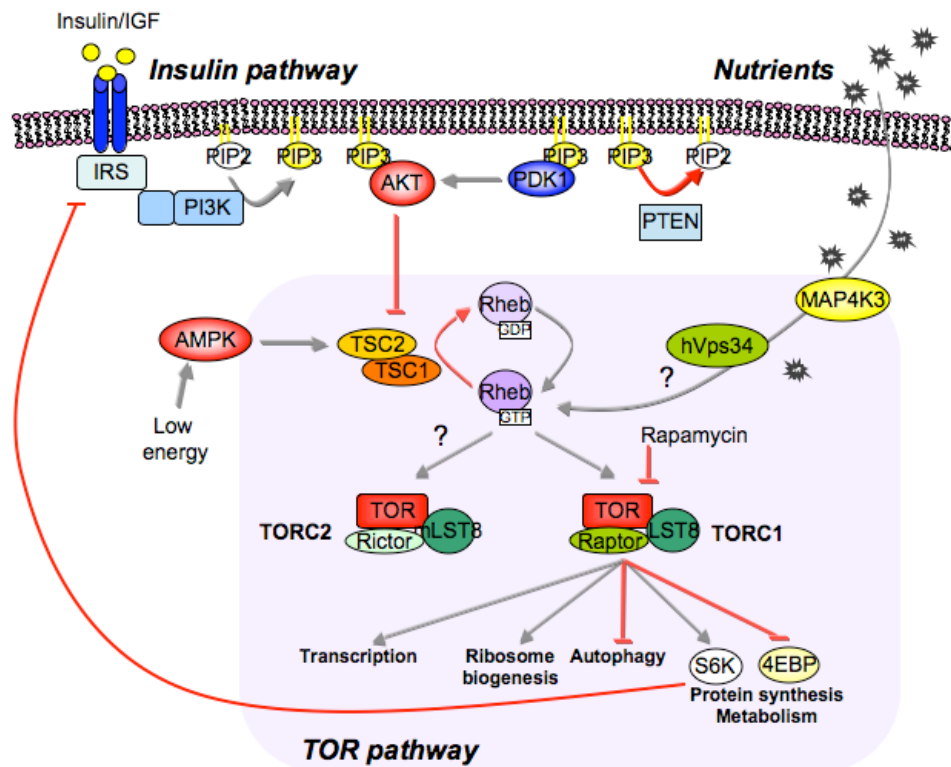


Figure 1 Model of mammalian TOR signaling

Two distinct mTOR complexes exist in the cell. Rapamycin-sensitive mTOR complex 1 controls cell growth and size through regulation of a variety of indicated processes and rapamycin insensitive mTOR complex 2, which is thought to control cell shape. mTORC1 is integrating inputs from growth factors/Insulin, nutrients and energy status, while factors regulating mTORC2 are largely unknown (see text for details). Grey arrows indicate activation, red bars – inhibition.

PIP3 production triggers translocation to the cell membrane of PDK1 (phosphoinositide-dependent protein kinase 1) and AKT kinase (also designated as PKB – Protein Kinase B), both of which possess PH domains. Colocalization at the membrane allows efficient activation of AKT by PDK1 by phosphorylation on the so-called activation loop. AKT is a very important cellular kinase and links insulin and TOR signaling through TSC1/2 complex and Rheb (Hay and Sonenberg, 2004).

Tuberous sclerosis proteins TSC1 (hamartin) and TSC2 (tuberin) act as a heterodimer that negatively regulates mTOR signaling by inactivating Rheb (Ras homolog enriched in the brain). TSC complex act as a GTPase Activating Protein (GAP) of Rheb, promoting GTP hydrolysis by Rheb and thus its inactivation. TSC2 is phosphorylated and functionally inactivated by

AKT in response to insulin. Rheb can bind and activate TORC1 although the precise mechanism remains elusive (Long et al., 2005a; Manning, 2004).

TSC complex is a component where additional inputs into TOR signaling feed in, such as energy status and stress. TSC2 is positively regulated by AMP-activated protein kinase (AMPK). AMPK is activated in response to low cellular energy (high AMP/ATP ratio) and downregulates mTORC1 activity through TSC complex (Inoki et al., 2003). This couples energy status with protein synthesis, ribosome biogenesis and growth – all energy dependent processes. Other kinds of stress, such as hypoxia and DNA damage have been implicated in deactivation of mTORC1 activity by TSC stimulation (Brugarolas et al., 2004; Feng et al., 2005; Reiling and Hafen, 2004).

Other regulators working through TSC complex

Additionally, TSC2 can be phosphorylated by other kinases activated by growth factors, such as ERK2 (Ma et al., 2005) and its downstream kinase RSK (Roux et al., 2004) and also p38 activated kinase MK2 (Li et al., 2003). ERK and p38 kinases are part of the MAP (Mitogen-activated Kinase) signaling pathway, implying that it may have cross-talk with TOR (for further detail, see the introduction to MAP4K3 function in *Drosophila*). The phosphorylation sites of MAP kinases are different from those of AKT and are not conserved in *Drosophila*, while AKT's phosphorylation sites are. Although it is clear that TSC complex is a central regulator of TORC1, our understanding of all the inputs going through this node and their relative importance is still far from complete. There is an urgent need to develop new tools that would complement existing biochemical and genetic methods to unveil the complex regulatory circuits controlling TOR signaling. During my PhD I worked toward developing such a tool: a fluorescence based probe to assess mTOR activity in cells.

Nutrients regulation of TOR

TORC1 is regulated by nutrients, especially amino acids. Starvation of amino acids leads to rapid dephosphorylation of TORC1 substrates, and is reversed by re-addition of amino acids. In physiological terms this makes perfect sense – sensing amino acids is necessary for protein production since amino acids

are the building blocks for proteins. Although nutrient sensing is the most conserved function of TORC1, it is still poorly understood. Reports vary as to whether any of the classical upstream regulators of TOR are involved. The emerging consensus is that TSC complex is not required for amino acid signaling to TOR, while Rheb is required, although it is not clear whether it is actively participating or just needs to be present in the cell. Budding yeast *S. cerevisiae* lack functional orthologs of TSC and Rheb, while still being sensitive to amino acids, suggesting that amino acids can signal directly to TORC1.

It has recently been proposed that some newly discovered proteins such as hVps34 and MAP4K3 mediate the amino acid stimulation of mTORC1 (Byfield et al., 2005; Findlay et al., 2007; Nobukuni et al., 2005). I will describe these findings in more detail in the introduction to the MAP4K3 in *Drosophila*. Since amino acid sensing by TOR is so poorly understood we decided to test the function of MAP4K3 – a new candidate gene for mediating amino acid signaling to TOR in the whole organism context, using *Drosophila melanogaster* as a model.

1.4. Downstream of TOR – regulation of translation and growth

TOR signaling regulates a stunning array of cellular functions. These include translation, ribosome biogenesis, macroautophagy, transcription, metabolism, and actin organization (Bhaskar and Hay, 2007; Sarbassov et al., 2005; Wullschleger et al., 2006). How is TOR regulating all these cellular processes? To answer this we need to look at the substrates of TOR. There are surprisingly few substrates known for TOR and the best-characterized ones are those involved in control of translation. 4EBP1 and p70 S6K are commonly used as a readout of TORC1 activity.

4EBP1 is a negative regulator of translation. Specifically, it can block translation initiation, the first step of protein synthesis. 4EBP1 stands for eIF4E binding protein1, a repressor of eukaryotic translation initiation factor 4E (eIF4E). The 5' end of nearly all mRNAs possesses a cap structure (m⁷GpppN, in which “m” represents a methyl group and “N”, any nucleotide)

that is specifically recognized and bound by eIF4E. The assembly of a ribosome on mRNA starts with eIF4E binding of the cap structure. eIF4E is a bridging element between the cap and another initiation factor, eIF4G. eIF4G is a large scaffold protein connecting eIF4E with the rest of the translation initiation machinery. 4EBP1 has an eIF4E binding motif similar to the one in eIF4G and is able to repress translation by binding eIF4E and thereby preventing it from association with eIF4G as depicted in Figure 2A (Hay and Sonenberg, 2004; Proud, 2007).

Mammals have three 4EBPs: 4EBP1, 4EBP2, and 4EBP3, encoded by three separate genes, whereas *Drosophila* expresses only one 4EBP. 4EBP1 is the best-studied one and its binding to eIF4E is regulated by phosphorylation via mTOR (Figure 2).

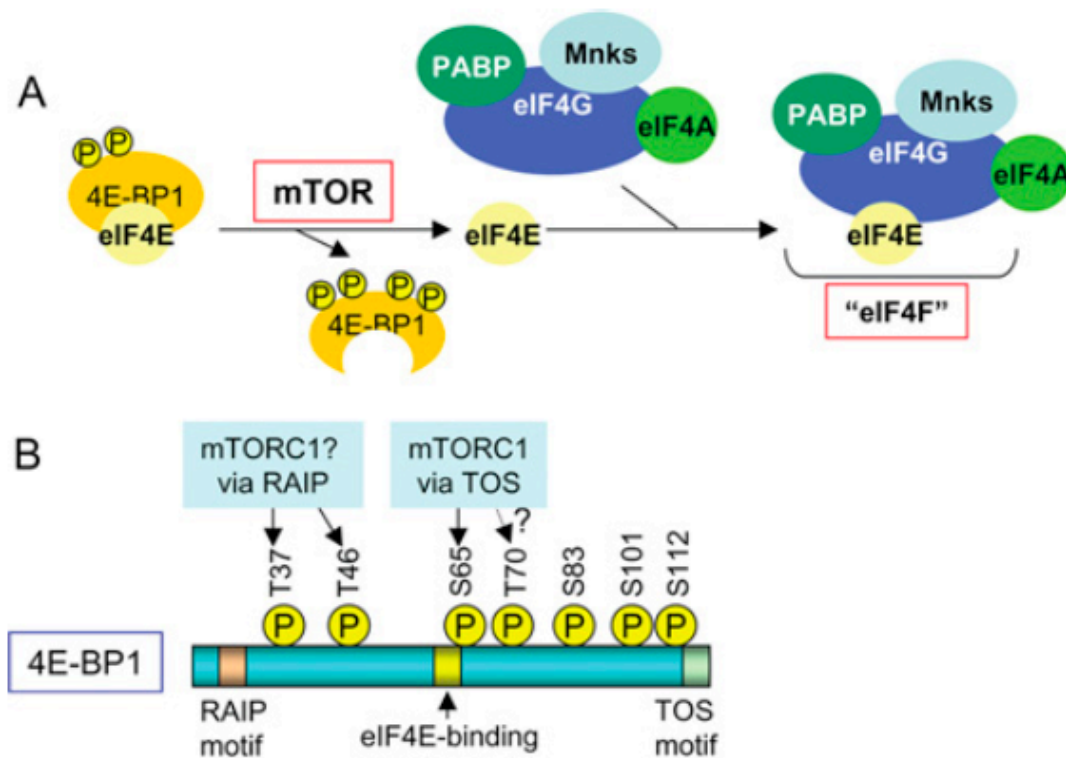


Figure 2 4EBP1 binding to eIF4E is regulated by TORC1 mediated phosphorylation

(A) When hypophosphorylated 4EBP1 is bound to eIF4E, translation is blocked. Upon mTOR activation, it is hyperphosphorylated and dissociates from eIF4E allowing the latter to interact with eIF4G and the rest of the translation initiation machinery to form eIF4F complex, necessary for efficient

translation. (B) 4EBP1 model showing important motifs and phosphorylation sites. Adapted from (Proud, 2007).

The phosphorylation pattern of 4EBP1 is complex and not entirely clear. The following phosphorylation sites have been identified in 4EBP1: Thr37, Thr46, Ser65, Thr70, Ser83, Ser101, and Ser112 (residue numbers are for the human protein, subtract 1 for sites in rat and mouse). The first four are the most important and phosphorylation of these sites in cells occurs in an ordered fashion, with that of Thr37 and Thr46 occurring first, followed by Thr70, and finally Ser65. The sites on 4EBP1 differ in sensitivity to rapamycin treatment of cells: phosphorylation of Thr70 and Ser65 generally shows a greater decrease in response to rapamycin than does phosphorylation of Thr37 and Thr46 (Gingras et al., 2001; Mothe-Satney et al., 2000). Two motifs in 4EBP1 are essential for the efficient phosphorylation in cells. The first is a TOS (target of rapamycin signaling) motif formed by the last five C-terminal amino acids, Phe-Glu-Met-Asp-Ile. TOS motif is thought to bind to raptor, which supposedly mediates substrate specificity of TORC1, and is needed for phosphorylation of Ser65 and Thr70. Phosphorylation of Thr37/Thr46 does not require the TOS motif, but depends instead on an N-terminal RAIP (Arg-Ala-Ile-Pro) motif (Proud, 2007; Tee and Proud, 2002; Wang et al., 2005).

The complex hierarchical phosphorylation of 4E-BP1 and its dependence on two distinct motifs leads one to question whether all the mTOR-regulated sites in 4E-BP1 and S6K1 are really direct targets for phosphorylation by mTOR itself.

S6K1, a ribosomal protein S6 (rpS6) kinase, is another “classical” TORC1 substrate. Rapamycin inhibits activation of S6K1 in response to insulin, and the drug reduces rpS6 phosphorylation in multiple cell types. S6K1 belongs to the AGC family of protein kinases and requires phosphorylation at two sites for its full activation, a site in a C-terminal hydrophobic motif and a site in the T loop of the kinase domain. mTORC1 mediates phosphorylation of Thr389 within the hydrophobic motif, whereas PDK1 is responsible for phosphorylation of the T loop (Harris and Lawrence, 2003; Wullschleger et al., 2006). Activated S6K phosphorylates rpS6 and thus promotes efficient translation through increased translation of a subset of mRNAs, although how it does so remains unclear. Importantly, when activated S6K can

phosphorylate IRS and attenuate signaling through the insulin pathway. This negative feedback loop has been proposed to play a role in the development of insulin resistance in diabetes and obesity. For instance, when mTORC1 is activated by high levels of nutrients, activated S6K is decreasing PI3K signaling by phosphorylating and inactivating IRS.

Although much understanding has been gained regarding TOR signaling, present knowledge and understanding of this system remains insufficient to allow disruption of cancer and metabolic diseases.

1.5. *Metabolism regulation by Insulin/TOR pathway in Drosophila melanogaster*

Physiological significance of TOR signaling lies in its control of essential cellular functions – metabolism and growth. Dysregulation of metabolism is associated with major human diseases such as diabetes, obesity, cardiovascular disease and some cancers (Baker and Thummel, 2007). The impact of these on human health is hard to overestimate and this drives large amount of interest and efforts into understanding the underlying mechanisms of metabolism regulation.

Insulin is a key regulator of energy homeostasis. It is a systemic hormone that in mammals regulates the balance between dietary intake, storage and release of energetic currency of the body, carbohydrates and lipids, according to the organism's needs. Upon food intake, glucose and other nutrients (amino acids, lipids) levels rise in the circulation and trigger insulin secretion from pancreas. Insulin, through activating of intracellular signaling cascade, elicits specific responses in different tissues of the organism to promote nutrient uptake and storage. Glucose is taken up mainly by the muscle and adipose tissues but also liver and other tissues. In the liver insulin is inhibiting glycogen breakdown and gluconeogenesis. When nutrients influx is low and energy needs are high, glucose levels fall and insulin goes down, while other hormones such as glucagon, adrenaline and corticosteroids promote hepatic glucose production (Rosen and Spiegelman, 2006).

Insulin signaling inside cells is responsible for execution of the response to insulin. When tissues responses to insulin are not efficient, this results in a state known as insulin resistance. Insulin resistance is manifested in high glucose levels and is one of the hallmarks of diabetes mellitus and obesity (Biddinger and Kahn, 2006).

One of the tissues where insulin resistance produces significant problems for the organism is the adipose tissue. Adipose tissue is the main form of energy stores in the organism. It is closely connected with glucose homeostasis, too much fat (obesity) is associated with insulin resistance and hyperglycemia. Although fat tissue is only responsible for a fraction (10-15%) of glucose uptake from circulation, with most glucose being taken up by muscle (Kahn, 1996), adipocytes can affect glucose levels by a number of endocrine and non-endocrine mechanisms (Rosen and Spiegelman, 2006). Insulin stimulates glucose transport, lipogenesis, fatty acids uptake and maturation of adipocytes. This is achieved by complex intracellular signaling cascades regulating existing proteins and also changes in translation and transcription. Under starvation, insulin activity is low and lipids in adipose tissue are mobilized to provide energy for organism's activity.

Insulin signaling is conserved in *Drosophila* and because it usually has less redundancy in various components of insulin signaling *Drosophila* is becoming increasingly popular model for metabolic studies (Baker and Thummel, 2007). Insect fat body is an organ that combines functions of mammalian liver and white adipose tissue; it stores glycogen and lipids which are mobilized in the times of need.

Recent studies in flies established that Insulin-Like Peptides (ILPs) and Adipokinetic Hormone (AKH) analogs of mammalian insulin and glucagon, respectively, regulate carbohydrate and lipid homeostasis in a manner similar to mammalian systems, highlighting conservation of energy metabolism regulation in *Drosophila* (Brogiolo et al., 2001; Broughton et al., 2005; Kim and Rulifson, 2004; Lee and Park, 2004). Ablation of cells producing some of seven *Drosophila* ILPs results in diabetic-like phenotypes (Rulifson et al., 2002). On the contrary, ablation of cell producing AKH results in decrease of circulating trehalose (main blood sugar in *Drosophila*), while ectopic AKH

expression in fat body leads to elevated trehalose and reduction of fat through increased lipolysis (Lee and Park, 2004).

Insulin signaling activates an array of cellular effectors. One of the key effectors is PI3 kinase, which acts through at least two branches: transcriptional control via inactivation of transcriptional activator FOXO and control of translation and metabolism via TOR kinase (Baker and Thummel, 2007). Reduction of insulin signaling in fat body genetically by inhibiting PI3K activity mimics starvation (Britton et al., 2002) and dTOR mutants exhibit morphology changes in fat body typical for starvation (Zhang et al., 2000). Numerous mutants connected to the Insulin/TOR pathway have metabolic phenotypes (Bohni et al., 1999; Colombani et al., 2003; Luong et al., 2006; Teleman et al., 2005a, b; Tsukiyama-Kohara et al., 2001; Um et al., 2004), establishing TOR signaling as a major conserved regulator of metabolism. Results from MAP4K3 mutant analysis presented in this thesis provide additional support to this function and add a link between nutrient sensing, metabolism and growth.

2. Aims of the Thesis

In order to understand a complex biological system such as TOR signaling we need to achieve a number of goals. Firstly, to identify all functional components that constitute the underlying physical framework of the interacting proteins. Secondly, to decipher the nature of interactions between the individual components and regulatory modules that they constitute, such as protein complexes composition and function of the individual proteins in the complex (enzyme-substrate, activator-effector, etc.) Thirdly, we need to understand the regulation and biological function at the whole system level, including dynamics of activation and inhibition, relative importance of different inputs, crucial components and information flow through the network (amplification vs. attenuation, linear vs. circuitry, etc.)

My thesis aims at contributing to this task using three different approaches to generate new tools and characterize novel components of TOR signaling. The first goal was to develop a tool that would visualize mTORC1 signaling in live cells. Based on recent successes of *in vivo* fluorescent labeling I aimed to develop a sensor for a cell culture assay that would allow monitoring of TORC1 activity *in vivo*, in a spatially and temporally resolved manner, a task impossible till now. There are several reasons why it would be useful to have a readout for TORC1 activity: (1) one method for identifying components of the pathway is to do RNAi screening in cells, however this requires a readout for TORC1 activity; (2) to study the dynamics of TORC1 pathway activation; and (3) to visualize TORC1 activation *in vivo* to see if there are any spatial patterns to its activation – one can assume it is not uniformly active in tissues, but depends on local nutrient level, oxygen levels, etc..

I then employed a classical genetic approach, using the advantages of *Drosophila melanogaster* as a model organism, to analyze the function of a newly identified component of TOR signaling on the whole organism level. Lastly, I utilized a chemical biology strategy to discover novel small molecule inhibitors for an important TOR dependent protein-protein interaction. This last project is still at the early phase, so I will not discuss it in this thesis, as this work will be followed and published later.

3. Development of a FRET-based probe for TOR signaling

3.1. Introduction - Fluorescent probes as tools to visualize cellular processes

3.1.1. Fluorescence and Fluorescence Resonance Energy Transfer phenomena

Observation has been at the heart of biological sciences, especially since Antonie van Leeuwenhoek designed his first microscope in the 17th century. Microscopy has contributed enormously to our understanding of biology ranging from whole organism processes such as embryonic development, to the cellular level processes such as cell division, and down to the molecular level such as observing localization of labeled molecules within the cell. In modern biology proteins are typically labeled with fluorescent molecules. Fluorescence based methods enable visualization of signaling events *in vivo* and provide spatio-temporal information, which is critical for understanding signaling networks (Aoki et al., 2008; Miyawaki, 2003).

Fluorescence is a physical phenomenon that results from ability of atoms and molecules to absorb light at a certain wavelength and to subsequently emit light of longer wavelength. This process is schematically illustrated by Jablonski diagram in Figure 3. It shows possible routes by which an excited molecule can return to its ground state via higher energy singlet and triplet states. A rapid return results in fluorescence and a delayed return results in phosphorescence. The time difference between excitation and emission is called the fluorescence lifetime. Although the entire molecular fluorescence lifetime, from excitation to emission, is measured in only billionths of a second, it can be measured using dedicated equipment. During its fluorescence lifetime an excited electron loses some energy due to collisions with surrounding molecules, called vibrational relaxation (non-radiative) until it reaches the lowest excited energy level from where it can return to the ground state by releasing the rest of the energy in the form of a photon (radiative). This photon has a longer wavelength (lower energy) than the excitation photon because some energy is lost due to non-radiative processes

(vibrational relaxation). The difference between excitation and emission wavelength is called Stokes-shift (Wolf, 2003).

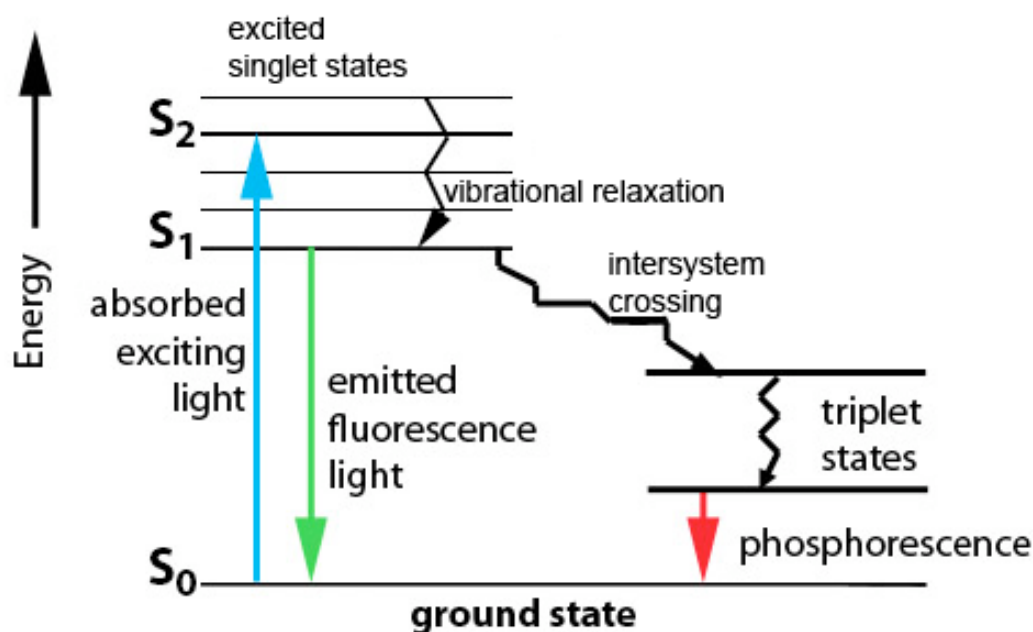


Figure 3 Jablonski diagram

Fluorescence occurs when a molecule absorbs a quantum of light and an electron goes from ground state to one of the excited states. A return from the higher energy state can occur via fluorescence with emission of a photon. Alternatively, an intersystem crossing to a triplet state can occur and electrons return to the ground state by phosphorescence. Part of the energy is lost in a non-radiative way, through vibrational relaxation.

In large molecules with many electrons and many nuclei there are many vibrational levels which causes their excitation and emission spectra to seem continuous rather than consisting of the sharp bands observed in atomic spectra.

Instead of the returning to the ground state and radiating a photon, an excited electron can transfer the energy non-radiatively to a neighboring molecule, if certain criteria are met. This phenomenon was first described by Förster and hence it is called Förster (or Fluorescence) Resonance Energy Transfer (FRET) (Förster, 1948). FRET is based on a long range dipole-dipole interaction which are limited to distances up to 10 nm (100 Å). This is the scale on which many biological interactions take place, which was the reason

for the renewed interest in this photo-physical phenomenon, which was previously used as a “spectroscopic ruler” (Stryer, 1978). For resonance energy transfer to occur, three specific conditions must be met. (1) The emission spectrum of the fluorophore, also called the donor, must overlap the acceptor molecule’s (which is usually also a fluorophore) absorbance spectrum. (2) The emission dipole of the donor and the absorption dipole of the acceptor must not be oriented perpendicular to each other. If the emission dipole of the donor is perpendicular to the absorption dipole of the acceptor, there will be no FRET. (3) Donor and acceptor molecules must reside within 10 nm (100 Å) of each other. Förster showed that the efficiency of resonance energy transfer, or FRET efficiency (the fraction of the photon energy absorbed by a fluorescent molecule that is transferred to an acceptor through dipole-dipole interactions), has a sixth power dependence on the distance between the donor and the acceptor as described by an equation:

$$E = \frac{R_0^6}{R_0^6 + r^6} \quad (\text{Eq.1})$$

where E is FRET efficiency, R_0 is the Förster Radius and r is the distance between the fluorophores. Because of such strong dependence of the efficiency on the distance, FRET is very sensitive to a change in a distance between donor and acceptor. For example, doubling of the distance reduces the transfer rate 64 times. The Förster Radius, R_0 , summarizes other factors influencing the transfer rate such as the effect of the solvent, relative orientations of the transition dipoles and a degree of overlap between the emission spectrum of the donor and excitation spectrum of the acceptor. FRET is maximal when donor emission and acceptor excitation dipoles are parallel to each other. For a mixture of molecules with random relative orientations due to rotation diffusion factor $k=2/3$ is usually assumed. From Eq.1 Förster Radius is the distance at which half of the energy is transferred to the donor.

3.1.2. Determination of FRET

Many different methods have been developed or proposed for determining

FRET efficiency, some of them theoretically quite complex and requiring special instrumentation (Jares-Erijman and Jovin, 2003; Sekar and Periasamy, 2003). The methods for measuring FRET can be divided by the principle into 3 groups: (i) methods that measure changes in donor fluorescence; (ii) methods that monitor changes in acceptor fluorescence; (iii) methods that use the orientation of the fluorophores as a readout for FRET. Each one of those has its advantages and disadvantages and I will describe the most common ones.

Methods that monitor donor fluorescence are very popular and include acceptor photobleaching and fluorescent lifetime imaging (FLIM). They compare donor intensity (acceptor photobleaching) or lifetime (FLIM) in the presence or absence of the acceptor. As the acceptor is quenching donor fluorescence or decreasing the donor's fluorescent lifetime due to FRET one can calculate FRET efficiency by comparing samples with and without the donor. Acceptor photobleaching is a straightforward approach in which the sample is illuminated with strong light or a laser that leads toward photo-destruction of the acceptor, and donor fluorescence intensity is compared before and after bleaching. This method is easy to implement on both wide-field and confocal microscopes but it is not suitable for time-lapse experiments as the donor is destroyed. Care should be taken to make sure that no fluorophore movement occurs during the bleaching process, which can take some time; this is especially difficult to achieve in live samples.

FLIM is a method that measures FRET by monitoring changes in a donor's fluorescent lifetime, that is, how rapidly a population of fluorophores emits light after a short excitation pulse, the fluorescent lifetime of a donor should become shorter if FRET is occurring (Lakowicz et al., 1992). FLIM requires some specialized instrumentation that is not available in most laboratories. The advantage of measuring the fluorescence lifetime of chromophores is that this parameter is directly dependent upon excited-state reactions but independent of chromophore concentration and light-path length, conditions that are difficult to control inside a cell (Bastiaens and Squire, 1999).

The sensitized emission method for measuring FRET involves monitoring

acceptor emission as a result of donor excitation. This seems to be the most straightforward method of measuring FRET but has caveats in practice. The emission spectra of most fluorophores have long tails towards longer wavelengths, which makes it difficult to separate donor and acceptor emission completely (bleed-through). The contribution of the donor emission to the sensitized emission channel has to be experimentally determined and corrected for in the evaluation of the data (unmixing). In addition, excitation wavelengths that are used to excite donors can excite acceptors in some cases, which also needs to be corrected for. Using this method, intensity calculated in the corrected FRET image not only encodes information about the amount of FRET in the sample, but also depends of the amount of sample present, the excitation intensity, the excitation wavelength, and the instrumentation used (filters, objectives, detectors, etc.). Thus, the FRET signal measured is not typically comparable to that obtained in experiments conducted on other microscopes or even to other experiments on the same microscope with different samples or parameters used.

One simplified method that does not calculate absolute FRET efficiency but detects relative change in FRET is measuring the ratio of acceptor-donor fluorescence, so called ratiometric FRET measurement (Wouters et al., 2001). It is applicable for cases where there is a constant stoichiometry between donor and acceptor molecules as in the case where both donor and acceptor fluorophores are on the same molecule (Adams et al., 1991; Miyawaki et al., 1997).

Measuring FRET by fluorescent polarization microscopy compares the orientation of the molecules excited (by linearly polarized light) with the orientation of the molecules that emit fluorescence (in response to excitation). Since fluorescent lifetimes are usually much shorter than rotation times in solution, especially for slow-moving fluorophores such as fluorescent proteins, in the absence of FRET, the molecule excited is the molecule emitting fluorescence, and thus its orientation will be highly correlated. If FRET occurs, the molecule excited may be different from the molecule emitting, and thus the correlation between their orientations will

decrease substantially (Rizzo and Piston, 2005). This method is relatively new and still needs to be fully established.

There is no one perfect method for FRET determination and they all suffer from certain assumptions and technical limitations. One must choose a single method based on the specifics of the experimental system and available instruments and it is advisable to employ several different methods to validate each other.

3.1.3. Green Fluorescent Protein and its variants for *in vivo* labeling

FRET's renewed popularity in the last decades stems from two factors. Firstly, the wealth of biochemical data from various protein-protein interaction methods (yeast two-hybrid, cell extract pull-down assay, and immunostainings) needs to be confirmed *in vivo*. Secondly, at the same time *in vivo* fluorescent labeling using genetically encoded Fluorescent Proteins (FP) has been developed and provides the tools for *in vivo* technology.

The first fluorescent protein, later termed GFP (Green Fluorescent Protein) was purified from a jellyfish *Aequorea Victoria* 1962 by Shimomura *et al* (Shimomura *et al.*, 1962). It took over 30 years until the gene encoding GFP was introduced and expressed in other organisms such as *E.coli* and *C.elegans* (Chalfie *et al.*, 1994). Later Roger Tsien and his lab contributed to our understanding of the chemistry of the fluorescence properties of GFP. He has made extensive contributions to the development of GFP variants with fluorescence emission in the whole visible spectrum, with increased brightness and photostability and improved folding properties along with rapid maturation of their chromophores (Heim *et al.*, 1995; Heim *et al.*, 1994; Heim and Tsien, 1996; Tsien, 1998).

Notably, this year the impact of GFP discovery and characterization was acknowledged by awarding Shimomura, Chalfie and Tsien a Nobel prize (http://nobelprize.org/nobel_prizes/chemistry/laureates/2008/index.html).

GFP is a 238 amino acid protein (Prasher *et al.*, 1992). Residues 65-67 (Ser-Tyr-Gly) in the GFP sequence spontaneously form the fluorescent chromophore, which is located inside the beta-barrel structure of the protein as depicted in Figure 4 (Brejci *et al.*, 1997)



Figure 4 Ribbon diagram of the wtGFP structure

The α -helices are shown in red, the β -strands are shown in green, and the chromophore is shown as a ball-and-stick model (adapted from Brejc *et al.*, 1997).

The fluorophore forms post-translationally in an oxygen-dependent cyclization reaction. Since no other cellular factors are needed GFP can be expressed in any aerobic cell or organism.

Original wild-type GFP was greatly improved by mutagenesis to make it brighter, more photostable, less sensitive to environment (such as pH and ion concentration). Fast folding of the protein and fluorophore maturation was also achieved. In addition many spectral variants of GFP with shifted excitation/emission maxima have been developed to enable labeling of cellular components with different colors (Chudakov *et al.*, 2005). A commonly used red-shifted variant is EYFP (Enhanced Yellow Fluorescent Protein), which contains the mutation T203Y. The excitation peak is shifted to 512 nm and the emission to 525 nm. Additional mutations in the periphery of the fluorophore increase the extinction coefficient (V68L) and accelerate folding (S72A) (Ormo *et al.*, 1996). Another EYFP variant called Citrine has increased photostability and decreased pH and chlorine sensitivity (Griesbeck *et al.*, 2001). Further mutations at the fluorophore or surrounding region have created several more colors based on the wtGFP. Cyan fluorescent protein

(ECFP) is a blue-shifted variant, which has an excitation maximum at 434 nm and an emission maximum at 475 nm (Heim and Tsien, 1996) and is the most commonly used variant together with EYFP as a FRET pair. Recently other naturally fluorescent proteins have been described from various marine organisms, in the search for more options in the red part of the spectrum. Other advances include development of photoactivatable and photoswitchable FPs to provide maximum flexibility and control (Chudakov et al., 2005; Shaner et al., 2007).

For FRET applications, the donor-acceptor pair should ideally fulfill several criteria: The donor should have a large quantum yield (the ratio of the number of photons emitted to the number absorbed), the spectral overlap should be as large as possible and the donor should have a large Stokes shift to allow a selective excitation of the donor. ECFP-EYFP (or Citrine) is a well-characterized pair that has been used extensively and this is the reason it was used in this thesis. wtGFP and all its derivatives have a weak tendency to dimerise, which may interfere with the performance of FRET probes. To solve the potential problem stemming from dimerization so called “monomeric” versions of GFP variants have been created, in which residue 206 has been mutated from Ala to Lys (Zacharias et al., 2002). However, it has even been shown that in some cases this dimerization property can contribute to the performance of the probe (Jost et al., 2008). Therefore, it must be determined experimentally whether monomeric or wt variants perform better. A list of selected GFP variants used in this thesis is presented in Table 1.1.

Table 1.1 GFP-variants compared to the wt-GFP

Name	Excitation [nm]	Emission [nm]
wt-GFP	395 472	504
GFP ²	396	510
ECFP	433	475
EYFP	514	527
Citrine	516	529

Note that wt-GFP has two excitation peaks.

3.1.4. Design and uses of FRET probes

The main advantage of the FRET technology is the ability to visualize biochemistry *in vivo* in space and time. FRET probes have been developed to visualize many different processes in the cell, from Ca⁺⁺ concentration fluctuations to membrane receptor activation during growth (Wouters et al., 2001). The design of FRET probes is limited only by the imagination of the researchers and many creative approaches have been employed. FRET probes based on GFP variants can generally be classified in two groups. The first group is intermolecular FRET probes, where donor and acceptor are on a separate molecules, genetically fused to proteins (domains) of interest, that are able to interact with each other. Upon binding of two interacting partners, donor and acceptor come to proximity allowing FRET. The second group includes intramolecular FRET probes, where both donor and acceptor are part of the same molecule. Usually one or more domains can change conformation to separate or juxtapose the probes. In response to the binding of a particular ligand, or upon specific modification, the intramolecular interaction of domains leads to a change in the spatial orientation and distance between the FPs, resulting in visible changes in the FRET effect. The interacting domains can be both sandwiched between donor and acceptor, or one may be on a separate molecule that binds its partner under specific conditions (for instance, when phosphorylated). These basic designs are illustrated in Figure 5.

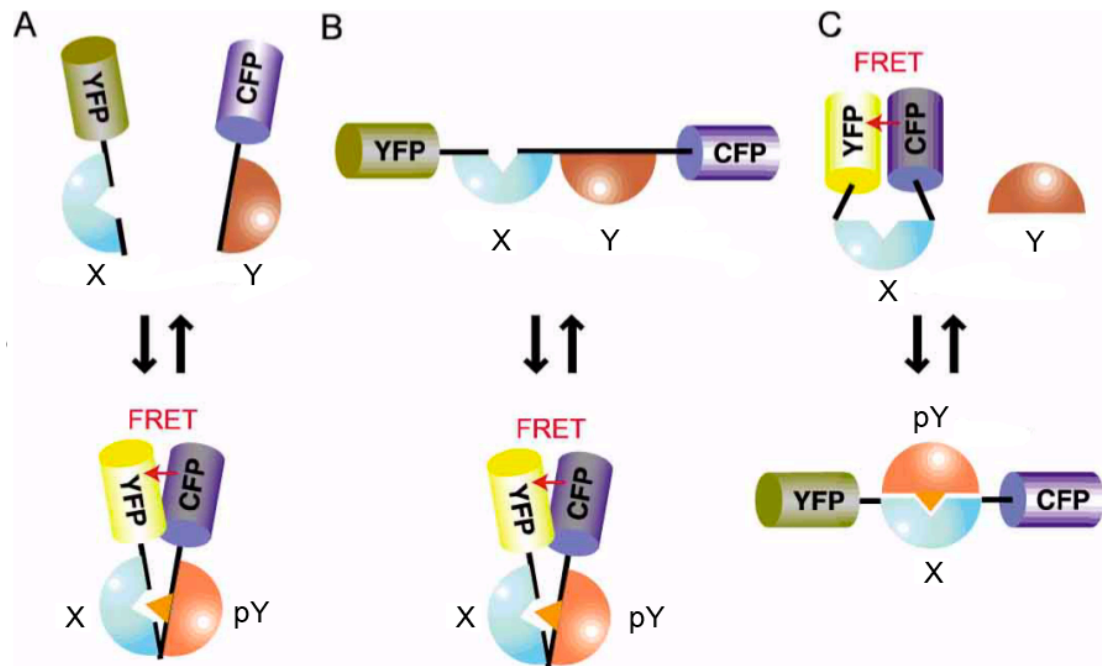


Figure 5 Structure of FRET probes

Domain X binds domain Y, when it is phosphorylated – pY. Possible designs of FRET probes are presented: (A) Intermolecular FRET probe (B) Intramolecular FRET probe (C) Intramolecular FRET probe, when only domain X is part of the probe and Y is not. Note that in (C) binding results in loss of FRET as opposed to (A) and (B). Modified from (Kurokawa et al., 2004).

Intramolecular FRET probes became popular following successful demonstration of this approach in Ca^{2+} signaling (Miyawaki et al., 1997). Many different probes, monitoring tyrosine and serine/threonine kinase activities, small GTPases and intracellular second messengers (lipids, ions, etc) have been developed (see (Aoki et al., 2008) for the full list). These so called conformational FRET probes have a number of advantages. They have a stoichiometrically stable ratio of donor and acceptor and thus allow simple acceptor/donor intensity ratio representing FRET efficiency, without complicated correction factors. Additionally if both domains are on the same molecule, their local concentrations are very high and they can find each other easily, increasing FRET efficiency. Moreover, perturbation of endogenous signaling is also lower than in other designs, since the domain will predominantly react intramolecularly without interfering with endogenous components. The disadvantage of intramolecular FRET probes are that it is

difficult to design a well-functioning probe, since the magnitude of change is usually not large.

Intermolecular FRET probes are easy to make and usually have a better signal/noise ratio since there is no “baseline” FRET when the proteins are not bound. On the other hand, since the concentration of the donor and acceptor are not known, one must perform spectral corrections for measuring FRET, which makes the experiments and analysis more complicated and creates room for errors. In addition there is a greater chance that fusions of donor and acceptor will interact and perturb endogenous signaling processes, especially when overexpressed.

Although FRET is becoming more and more popular to study protein-protein interactions *in vivo*, many articles have debated about the best way to detect it and warned of numerous caveats in interpreting the results (Berney and Danuser, 2003; Piston and Kremers, 2007; Vogel et al., 2006). Several general limitations are well known for FRET approaches. Sensitivity or dynamic range is usually low, especially for intramolecular FRET probes. There is no way to predict the efficiency of FRET and to achieve a satisfactory FRET probe may require extensive optimization to achieve a signal that can be reliably detected above the background noise level (Hires et al., 2008). FRET efficiency typically lies within tens of percents, rarely reaching 50% in best probes (Berney and Danuser, 2003; Kurokawa et al., 2004). This limits applicability of these probes in systems where small changes have to be measured reliably and also as readout for High Throughput Screening (HTS), where high signal/noise ratio is required. Perturbation of endogenous signaling by introducing artificial components, capable of interacting or competing with cellular signaling is always a concern. Integrity of the probes in the cell can also be an issue. Due to different efficiencies of folding, maturation and proteolysis, different species of the incomplete or non-fluorescent probe can co-exist within the cell, attenuating the signal or increasing the background (Miyawaki, 2003).

Despite many limitations, FRET remains probably the best approach to visualize protein-protein interactions in living cells. Researchers have to be aware of them and interpret the results cautiously with consideration of possible caveats, such as dynamics of acceptor abundance, random FRET,

and donor-acceptor stoichiometry. Universal use of proper controls and standards should improve the comparability of results from different laboratories.

3.1.5. FIAsH labeling

One of the known drawbacks of GFP-variants' fusions is that the resulting chimeric protein is altered in a way that disrupts its biological function. Although in many cases the biological function is preserved, because of the modular structure of proteins, sometimes relatively the large GFP domain (~25 Kd) can cause steric obstruction and affect the protein structure of regulation (Villardaga et al., 2003). Therefore small fluorescent tags are highly desirable for labeling proteins.

FIAsH (Fluorescein Arsenical Hairpin binder) technology utilizes a small tetracysteine motif to label proteins in cells. This approach was also pioneered by the Tsien lab (Griffin et al., 1998). Arsenoxides are known to have a high affinity for thiols, including closely spaced cysteines. FIAsH, containing two arsenoxides, has a high affinity for four appropriately spaced cysteines. The rigid spacing of the two arsenoxides enables FIAsH to bind with high specificity to the small tetracysteine motif introduced into proteins (Figure 6). The optimized tetracysteine motif has the 12 amino acids FLNCCPGCCMEP and binds FIAsH with high affinity.

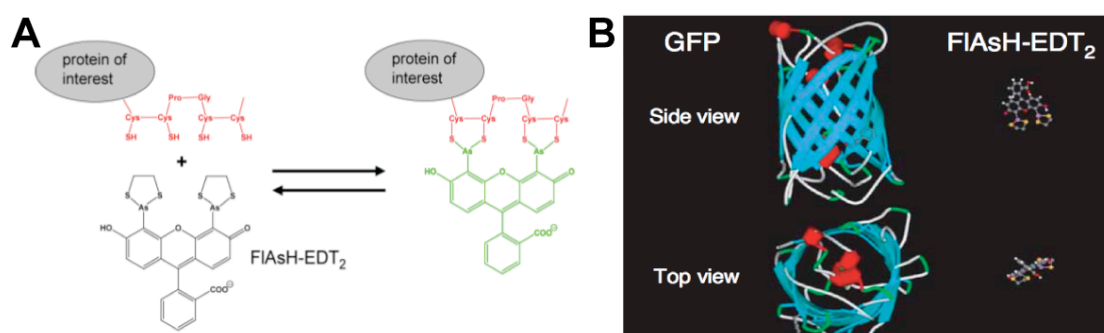


Figure 6 FIAsH labeling and comparison to GFP

(A) Non-fluorescent FIAsH-EDT₂ becomes fluorescent upon binding to the tetracysteine motif, introduced into the protein of interest. (B) Size comparison of FIAsH-EDT₂ with GFP domain. Much smaller size is an advantage as it is less likely to affect protein function. Modified from (Hoffmann et al., 2005).

A useful property of FIAsh is that the molecule becomes fluorescent only upon binding to the tetracysteine motif, so that only labeled protein produces fluorescent signal. FIAsh is added to the cells as FIAsh-EDT₂ adduct, to protect reactive arsenicals. However, it can bind to cysteines on other proteins in the cell, producing significant background staining (Stroffekova et al., 2001).

When attached to a protein FIAsh has an excitation peak at 508 nm and emission peak at 528 nm, which makes it a good FRET acceptor for CFP. FIAsh was successfully used together with CFP as a FRET pair to monitor G-protein coupled receptor dynamics (Hoffmann et al., 2005) and in a protein kinase C FRET probe (Jost et al., 2008).

This prompted me to try a FIAsh approach for making a TOR kinase FRET probe to overcome the difficulties of GFP-fusions as FRET probes.

3.2. Results

3.2.1. Conformational FRET probe strategy

Developing FRET-based probe for TOR kinase started with choosing a strategy, as there were several options available. First we decided which protein would be used as a basis for the probe and then what kind of probe to do. We chose 4EBP1 as one of the best studied substrates of TOR. Upon stimulation with insulin TOR phosphorylates 4EBP1 on multiple sites (some are phosphorylated directly by TOR and others are TOR dependant) causing 4EBP1 to decrease its affinity to eIF4E (Gingras et al., 1999). Phosphorylated 4EBP1 dissociates from eIF4E and thus allows efficient translation. 4EBP1 has no defined structure in solution but upon binding to eIF4E at least part of it becomes structured as it has to adopt a structure supporting interaction with eIF4E (Marcotrigiano et al., 1999). This prompted us to try to make a conformational FRET probe based on 4EBP1. Conformational FRET probes exploit the changes in the 3D structure of a protein; by placing donor and acceptor fluorophores on a protein in such a way that their distance from each other, and hence FRET efficiency, will change upon a change in protein conformation. Conformational FRET probes have a number of advantages over other FRET probe designs, in particular that by hanging both donor and acceptor on one protein, the stoichiometry, and thus relative concentration of the two is fixed, allowing FRET monitoring by a ratio of accetor/donor fluorescence upon donor excitation. Therefore, we decided on a conformational FRET probe attaching ECFP as a donor and Citrine as an acceptor to the ends of 4EBP1.

The domain composition of our conformational FRET probe based on 4EBP1 is depicted in Figure 7A. In the dephosphorylated state, the conformational FRET probe based on 4EBP1 is expected to bind to eIF4E and adopt a structured conformation. Since we don't know how this structured conformation will affect the distance between the two fluorophores, we don't know whether to expect a decrease or an increase in FRET relative to the unstructured state. Based on the structure of a 4EBP1 peptide bound to eIF4E, which adopts extended L-shape conformation I would expect that the

two fluorophores will be separated further from each other than in solution when unbound 4EBP1 exists as a random coil. As GFP variants have an intrinsic tendency to dimerization, they would probably associate with each other leading to more FRET. This scenario, where free 4EBP1 probe shows more FRET than bound is depicted in Figure 7B.

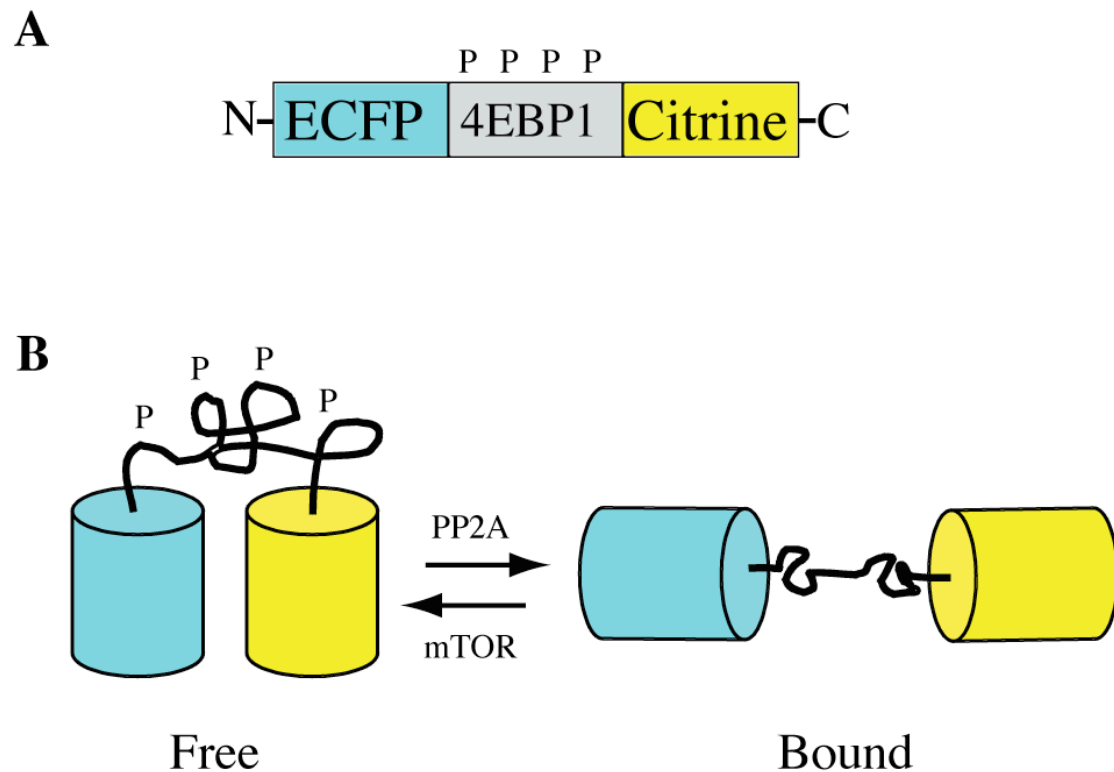


Figure 7 Schematic of a conformational ECFP-4EBP1-Citrine FRET probe

(A) Domain structure of the ECFP-4EBP1-Citrine FRET probe. P denotes 4 main phosphorylation sites on 4EBP1.

(B) Hypothetical model for conformational change induced by binding to eIF4E. Unphosphorylated probe is bound to eIF4E with donor and acceptor separated by a partially structured 4EBP1. Upon phosphorylation by mTOR, binding is lost and 4EBP1 adopts random coil conformation, which allows two fluorophores to come close together, leading to FRET.

Initially I tried to work with the *Drosophila* 4EBP ortholog to work in the S2 (Schneider's 2) cells but because S2 cells are very small, poorly adherent and because most of the literature of 4EBP is about the mammalian cells we decided to switch to the mammalian system. We started with HEK 293 cells as these are readily transfected and have been used for studying the TOR

pathway before, meaning that they have all the necessary components of the Insulin/TOR pathway.

Figure 8 shows regulation of endogenous 4EBP1 in HEK 293 cells. 4EBP1 was detected with the antibody against the total protein migrates in several distinct bands, which correspond to differently phosphorylated protein species. Dephosphorylated 4EBP1 is in the first lane after overnight serum starvation runs as a double band. Insulin stimulation, which activates TOR kinase, leads to phosphorylation of 4EBP1 and a shift up in its electrophoretic mobility. Treatment with PBS to deprive cells of amino acids and thus inactivate TOR or addition of Rapamycin to specifically inhibit TOR, leads to further dephosphorylation, which is not very clear from the lysate blot but is evident from the phosphospecific antibodies in Figure 8B.

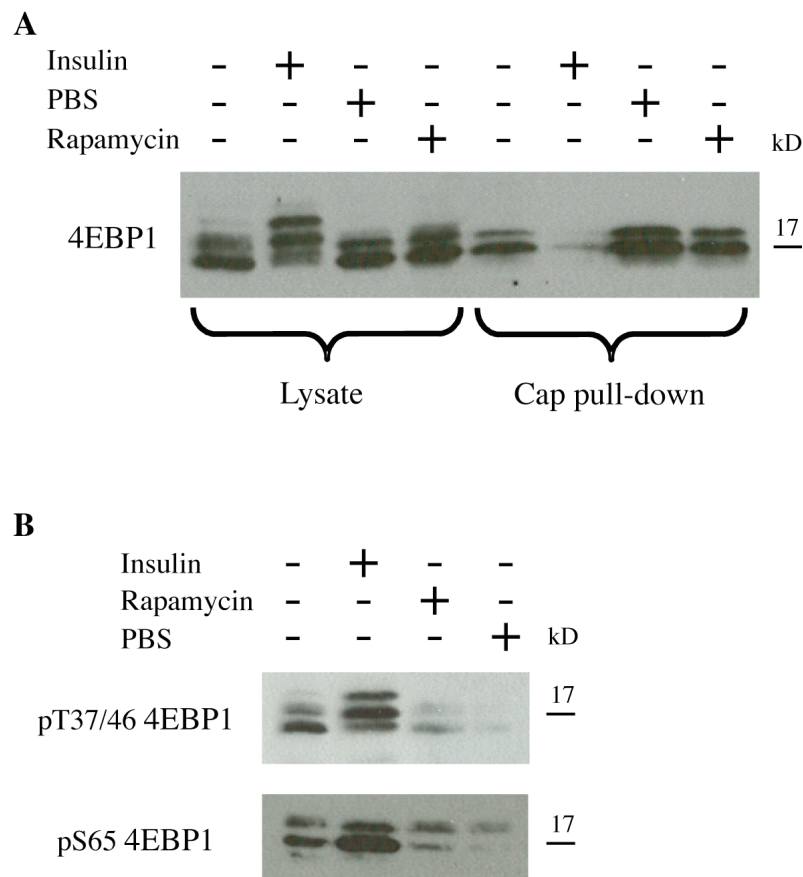


Figure 8 Regulation of endogenous 4EBP1 in HEK 293 cells

Cells were starved of serum for 16 hours and treated with 1mg/ml Insulin, 100nM Rapamycin or incubated in PBS for 30 min as indicated. Cell lysate or cap-beads bound fraction was analyzed by Western blot with total (A) or phosphospecific (B) 4EBP1 antibodies.

Both Rapamycin and PBS treatment decrease phosphorylation of 4EBP1 on Thr37/46 and Ser65 with PBS having a stronger effect. The functional significance of 4EBP1 phosphorylation is assessed by a Cap pull-down assay, where lysate is incubated with beads conjugated with m7GTP cap structure. This structure is recognized and bound by eIF4E and if it is bound by 4EBP1 the whole complex is pulled down. Insulin stimulation almost completely abolishes binding, while both PBS and Rapamycin increase the amount of 4EBP1 that is bound to eIF4E.

Human 4EBP1 was amplified by PCR and inserted into the pCDNA3 vector between ECFP and Citrine. This ECFP-4EBP1-Citrine FRET probe had to be tested to make sure that it still retains the physiological regulation of 4EBP1 and thus can faithfully reflect TOR activity. In HEK293 cells ECFP-4EBP1-Citrine FRET probe phosphorylation was increased by insulin and decreased by PBS treatment on both Thr37/46 and Ser65 in a manner similar to the endogenous 4EBP1 (Figure 9B). This suggests that it is still recognized by mTOR and the PP2A phosphatase. Unfortunately binding to eIF4E was impaired and no longer regulated by insulin and PBS. Insulin did not decrease the amount of ECFP-4EBP1-Citrine in the cap pull-down and after PBS treatment we actually observed less ECFP-4EBP1-Citrine bound to eIF4E, which is contrary to expectations (Figure 9A). One possible explanation for this could be that if the amount of eIF4E in the cell is limiting and if endogenous 4EBP1 binds eIF4E better than the FRET probe, then binding of the FRET probe would be impaired. To overcome this potential problem, I cotransfected eIF4E together with ECFP-4EBP1-Citrine using the same promoter in order to provide similar amounts of eIF4E. This solved the problem of competition with endogenous 4EBP1 (compare lanes 6 and 9) but binding of ECFP-4EBP1-Citrine was still constitutive and not regulated by Insulin or PBS (lanes 7-9).

Constitutive binding of the conformational FRET probe was a discouraging result but the possibility still existed that phosphorylation alone would change the conformation of 4EBP1 and lead to a change in FRET. It is known that sometimes a single phosphate group can lead to a significant change in a

protein structure and to a change in FRET (Nagai et al., 2000), although this is usually the case for proteins with a well defined structure.

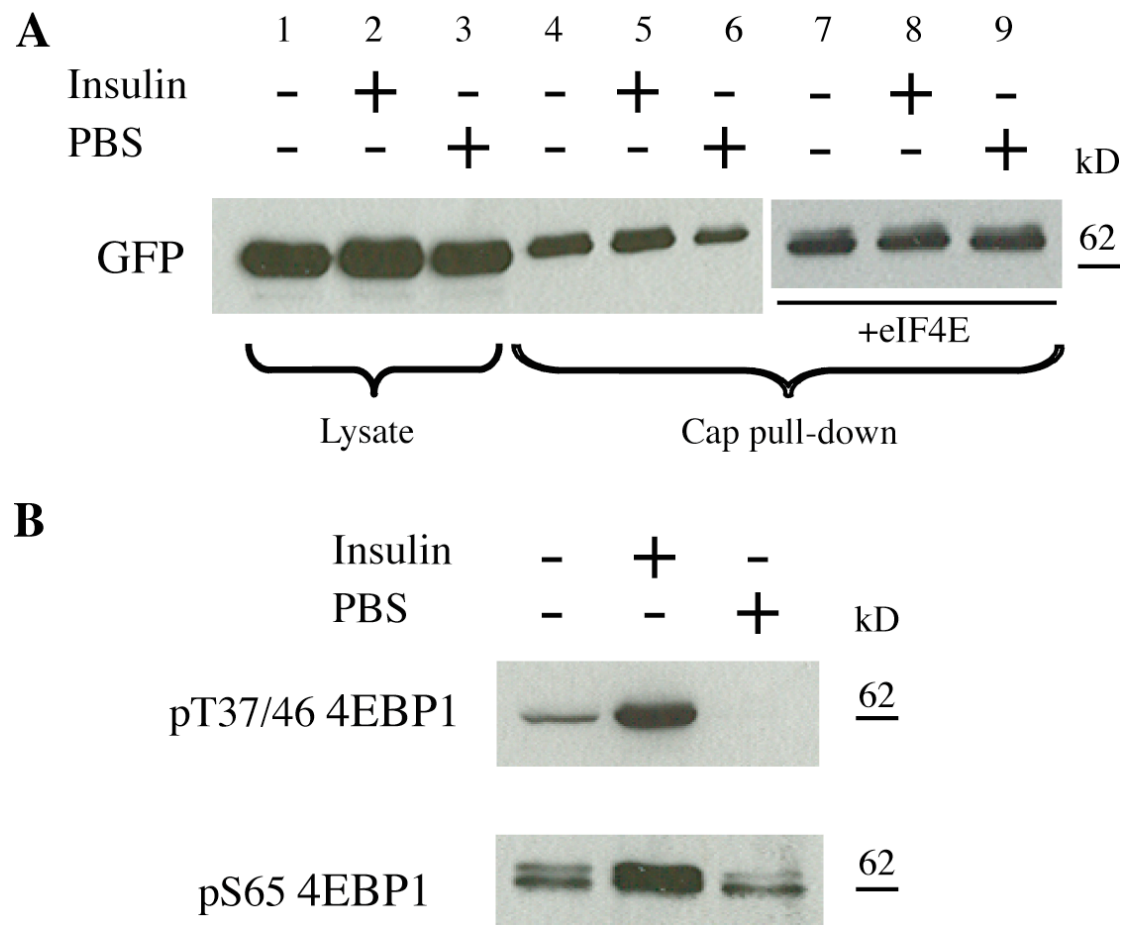


Figure 9 Regulation of ECFP-4EBP1-Citrine in HEK 293 cells

Cells were transfected with ECFP-4EBP1-Citrine alone or cotransfected with eIF4E, after 24 hours starved of serum for 16 hours and treated with 1mg/ml Insulin or incubated in PBS for 30 min. Cell lysate or cap-beads bound fraction was analyzed by Western blot with anti-GFP (A) or phosphospecific 4EBP1 (B) antibodies.

In order to test if phosphorylation can change FRET for ECFP-4EBP1-Citrine probe I performed ratiometric measurement of FRET, using a widefield automated microscope. Figure 10 shows a representative panel of FRET measurements, measured as a ratio of Citrine/ECFP. Insulin was added to the cells to stimulate Insulin/mTOR pathway and to promote 4EBP1 phosphorylation. After that, Rapamycin was added to inhibit mTOR and promote dephosphorylation. There was no consistent change in the Citrine/ECFP ratio in response to either stimulation or inhibition of mTOR kinase. This could indicate that there is no change in the relative position of

the fluorophores following phosphorylation/dephosphorylation of 4EBP1 or that the change is so small that it is not detectable by the method that I employed.

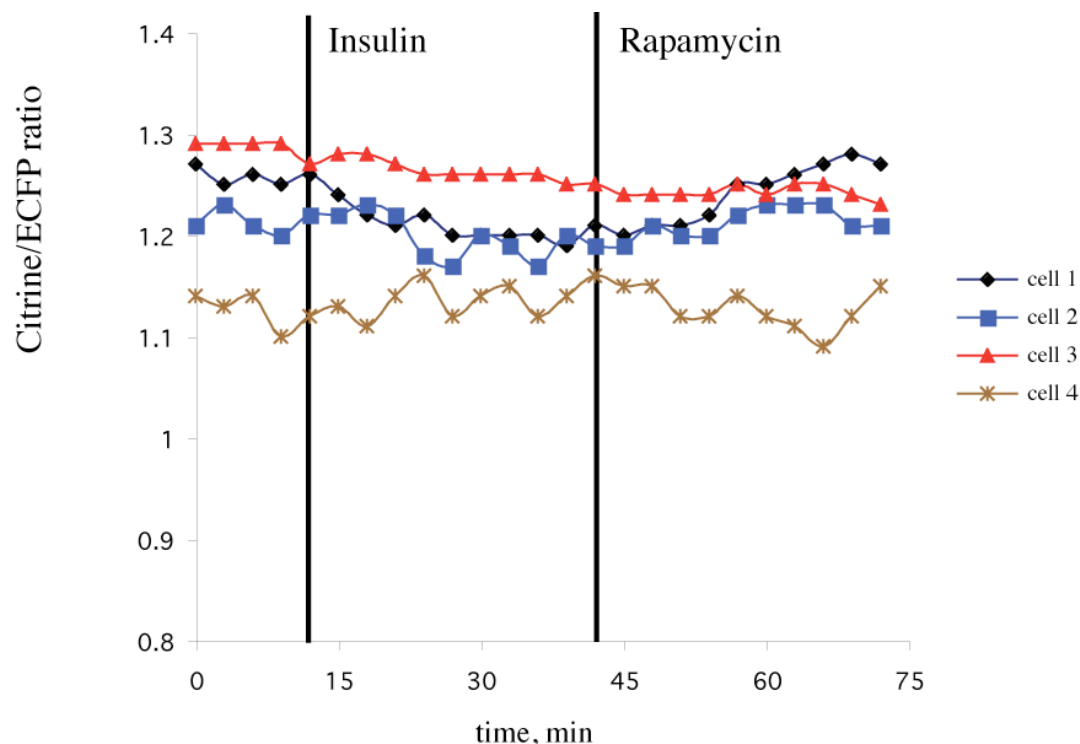


Figure 10 Ratiometric FRET measurement of the ECFP-4EBP1-Citrine sensor in HEK 293 cells

Cells were starved of serum for 16 hours and imaged under the widefield microscope. Following excitation of the ECFP, ECFP (donor) and Citrine (acceptor) emissions were captured and after subtraction of the background Citrine/ECFP ratio was calculated. At indicated times 1mg/ml Insulin or 2 μ M Rapamycin was added. Each color represents a single cell.

One possible problem is that high levels of expression of the FRET probe are higher than physiological capacity of the cells to regulate it. Then only a small fraction of the FRET probe is phosphorylated, binding and even if it has a change in FRET, this change is masked by a much larger fraction of non-regulated pool of FRET probe molecules. To try to overcome this, I selected stable cell lines with low level of fluorescence hoping to get the FRET probe expression to more physiological levels. Figure 11 shows an example of response to insulin stimulation of the stable HEK293 cells. Addition of HEPES buffer as a control or Rapamycin didn't change the FRET ratio, while addition of insulin resulted in a decrease of the Citrine/ECFP ratio. Rapamycin

pretreatment of the cells 10 min before insulin addition was not able to block the decrease as would be expected if the response was dependent on the mTOR kinase. It is noteworthy that the signal to noise ratio was not very good for the stable cells, as is evident from “jumps” in the graphs, while no manipulation was done. This most likely stems from the fact that the signal is low, since the cells were selected for their low expression levels.

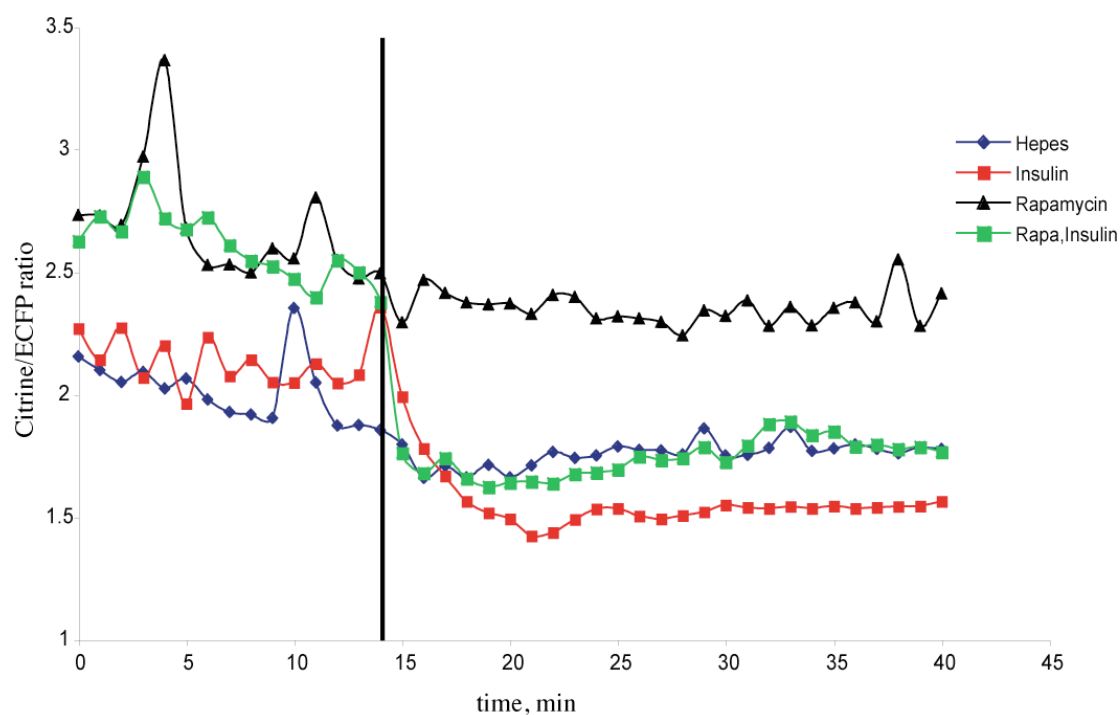


Figure 11 Ratiometric FRET measurement of the ECFP-4EBP1-Citrine sensor in stable HEK 293 cells

Cells were starved of serum for 16 hours and imaged under the widefield microscope. Following excitation of the ECFP, ECFP (donor) and Citrine (acceptor) emissions were captured and after subtraction of the background Citrine/ECFP ratio was calculated. At the indicated time (vertical line) 30mM HEPES buffer, pH7.2, 1mg/ml Insulin or 100nM Rapamycin was added. For the Rapa, Insulin sample cells were pretreated with Rapamycin 10 min before Insulin treatment. Each graph represents average of 4-6 cells.

Despite low signal/noise ratio, the response to insulin was reproducible and convincing but could not be blocked by either Rapamycin or Wortmannin, an inhibitor of PI3 Kinase (data not shown). This remained a mystery until a more careful analysis revealed that insulin addition changed the background fluorescence of the medium. This change was slight and came unnoticed in my initial analyses. I initially corrected background by calculating the mean value of the area without cells and subtracting it from all the images in the

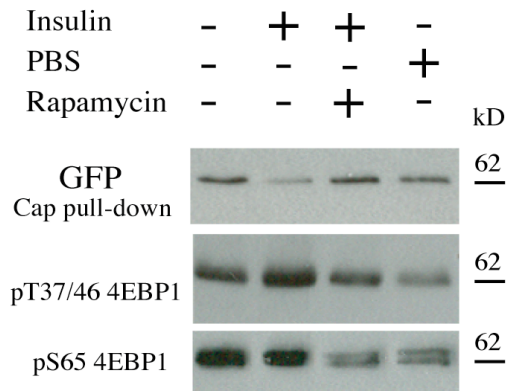
time series for each channel, in a so called “global” background correction. This of course is only valid if the background remains stable throughout the entire experiment. Insulin for an unknown reason slightly changed the background fluorescence and the change was different for the donor and acceptor channel. Given that the signal from the cells was not very strong this background change led to a visible drop in the Citrine/ECFP ratio. After I determined what was causing the artifact of FRET ratio decrease, I started to correct each image in the time series using the “local” background from the same image, which eliminated the artifact of insulin addition. After this proper background correction no significant change in FRET ratio was left, indicating that there was no FRET change upon phosphorylation of the probe. Figure 12B shows an example of background correction. Left panel – global background correction, insulin addition artifact is apparent as a drop in the ratio. Right panel – local background correction, after correction no response to insulin is present. In conclusion stable HEK293 cells did not show a FRET response.

In parallel another cell line was tested to determine whether cell line specific factors may influence 4EBP1 regulation and hence my FRET probe performance. I used HeLa cells that were better suited for microscopy in comparison to HEK293, which were weakly adherent and often detached. Figure 12A shows that in HeLa cells the ECFP-4EBP1-Citrine FRET probe is phosphorylated in the expected manner, namely insulin increases phosphorylation, which is blocked by Rapamycin and PBS treatment reduced the amount of phosphorylated protein. Moreover, in a cap pull-down there was a slight decrease in the amount of the bound ECFP-4EBP1-Citrine FRET probe after insulin stimulation, although PBS failed to increase the binding. Unfortunately, ECFP-4EBP1-Citrine FRET probe did not show response to insulin (except for the background artifact) in HeLa cells (representative example shown in Figure 12B).

All these results taken together suggest that the binding of the ECFP-4EBP1-Citrine FRET probe is affected in a way that does not allow regulation by Insulin/mTOR pathway. Although phosphorylation of the ECFP-4EBP1-Citrine

FRET probe is similar to the endogenous 4EBP1 it does not translate into detectable FRET signal.

A



B

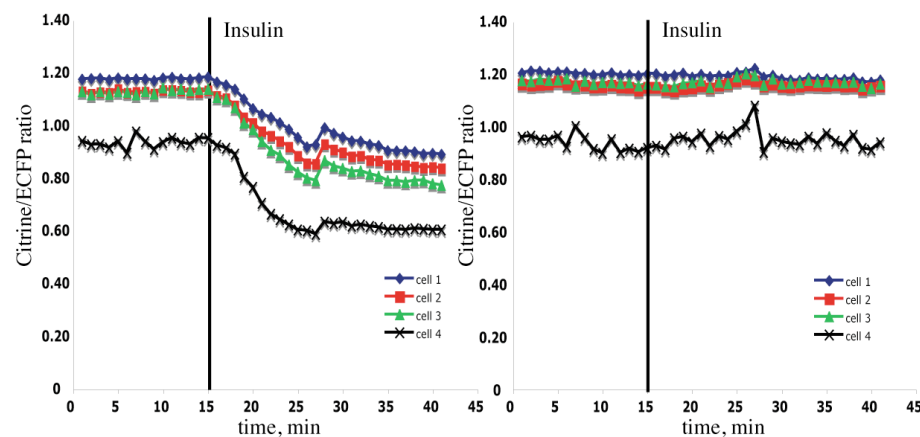


Figure 12 Biochemical analysis and FRET measurement of the ECFP-4EBP1-Citrine sensor in HeLa cells

(A) Cells were transfected with ECFP-4EBP1-Citrine and eIF4E, after 24 hours starved of serum for 16 hours and treated with 1mg/ml Insulin or incubated in PBS for 30 min, where indicated, pretreated for 30 min with 100nM Rapamycin. Cell lysate or cap-beads bound fraction was analyzed by Western blot with indicated antibodies.

(B) Cells were starved of serum for 16 hours and imaged under the widefield microscope. Following excitation of the ECFP, ECFP (donor) and Citrine (acceptor) emissions were captured and Citrine/ECFP ratio was calculated. Left panel – global background correction, Insulin addition artifact is evident. Right panel – local background correction. At indicated time (vertical line) 1mg/ml insulin was added. Each graph represents a single cell.

3.2.2. Variation of fluorophore pairs and single-tagged 4EBP1

The conformational FRET probe design with ECFP and Citrine yielded a probe that was phosphorylated in the correct way but the binding to eIF4E was not regulated anymore. As the FRET phenomenon is not very predictable, there are examples of probes where simply changing the donor-acceptor pair can make a difference between a working or a “dead” probe (Christiane Jost, personal communication). Therefore, I tried using the GFP²-EYFP combination as an alternative donor-acceptor pair. GFP² a variant of GFP with particularly large Stokes shift, has an excitation maximum at 399nm, which allows specific donor excitation without cross-excitation of the acceptor. It was reported to have better FRET efficiency than a CFP-YFP pair (Zimmermann et al., 2002). Another factor affecting FRET is that GFP and its derivatives are weak dimers, so I also tried using the “monomeric” version of the fluorophores to test whether this makes a difference.

4EBP1 was amplified by PCR and inserted into between EYFP and GFP² to give a EYFP-4EBP1-GFP² FRET probe or to a vector containing monomeric versions of EYFP and GFP² to give a mEYFP-4EBP1-mGFP² FRET probe. The A206K mutation abolishes the intrinsic affinity of all GFP variants to dimerize and have been shown to influence FRET probe performance (Zacharias, 2002). The resulting probes were transfected into HeLa cells and FRET change was measured by monitoring EYFP/GFP² ratio. Insulin stimulation was not able to change the FRET ratio in either EYFP-4EBP1-GFP² or mEYFP-4EBP1-mGFP² FRET probe (Figure 13). EYFP-4EBP1-GFP² FRET probe shows a slow non-specific decrease of the EYFP/GFP² ratio which could be due to a focus drift. Thus changing the fluorophore pair did not make the probe sensitive to phosphorylation.

An alternative strategy to develop FRET probe would be a probe based on intermolecular instead of intramolecular FRET, where donor and acceptor fluorophores are on different proteins. Intermolecular FRET is based on a concept of two interacting partners, each containing one fluorophore. When they bind each other, this brings the fluorophores in proximity of each other resulting in FRET. Since 4EBP1 is a small protein, addition of two GFP domains, one on each end, might be too disturbing, whereas addition of only

one at one end might allow 4EBP1 to still function correctly. Since 4EBP1 regulation was abolished by fusing it to two fluorophores, I went on to test whether it is possible to fuse it to one fluorophore and keep the regulation.

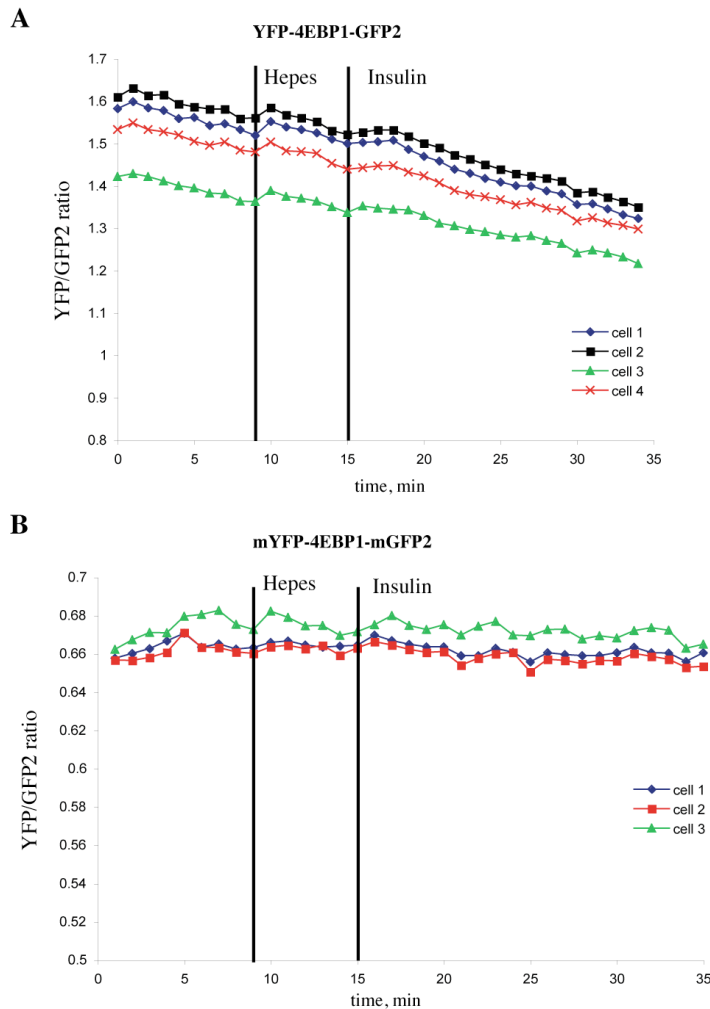


Figure 13 Ratiometric FRET measurement of the YFP-4EBP1-GFP2 sensor in HeLa cells

Cells were starved of serum for 16 hours and imaged under the widefield microscope. Following excitation of the GFP2, GFP2 (donor) and YFP (acceptor) emissions were captured and after subtraction of the background YFP/GFP2 ratio was calculated. At indicated times (vertical line) 30mM HEPES buffer, pH7.2, 10 μ g/ml Insulin was added. Each color represents a single cell.

I produced an N-terminal ECFP fusion and a C-terminal Citrine fusion of 4EBP1 with the idea to fuse the partner for FRET to eIF4E if one of these constructs shows proper regulation. Figure 14 show that none of the two constructs is behaving as an endogenous 4EBP1 in cap pull-down, although the phosphorylation pattern is similar. This result suggests that 4EBP1 binding is sensitive to artificial modifications and does not tolerate large domains at either N- or C-terminus.

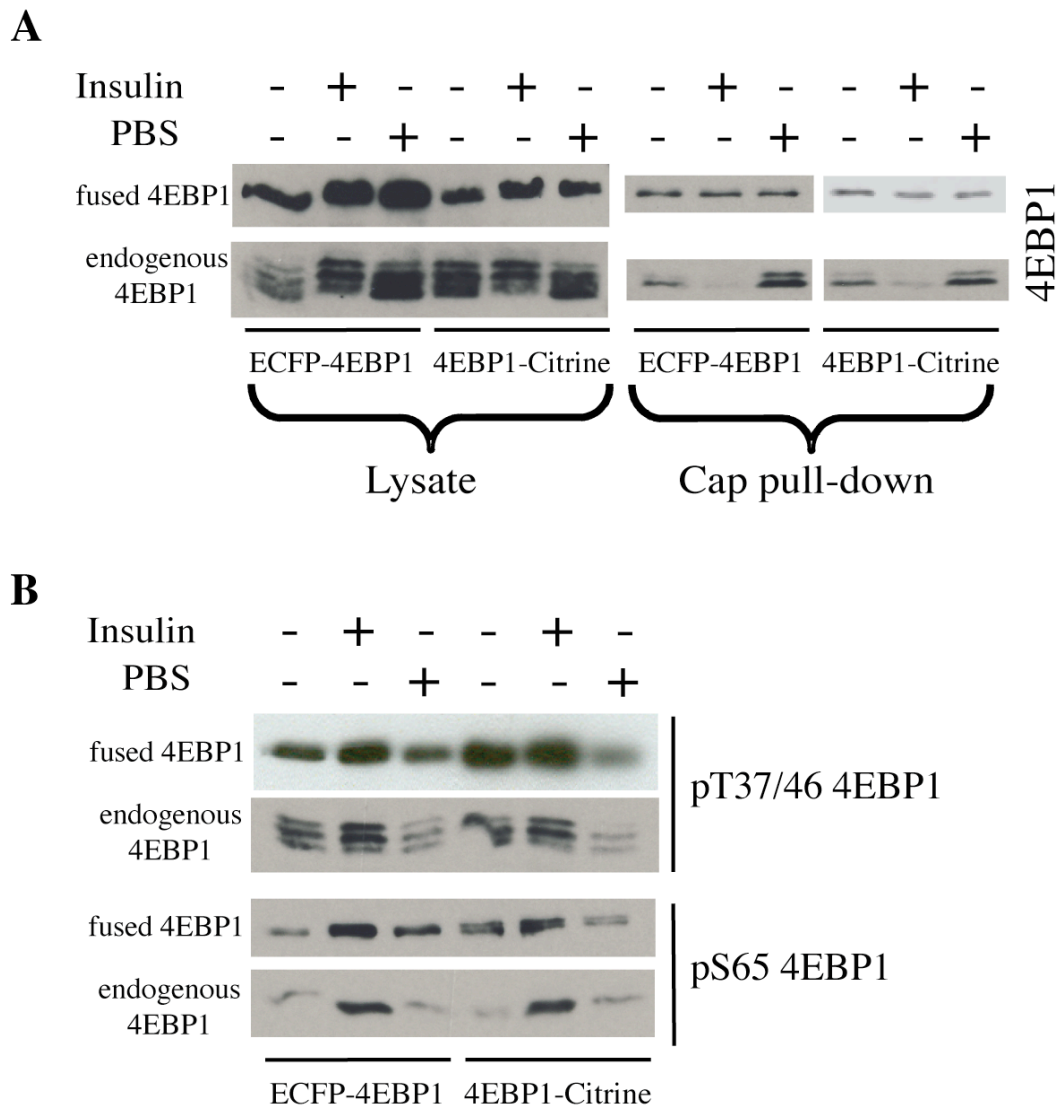


Figure 14 Regulation of ECFP-4EBP1 and 4EBP1-Citrine in MCF7 cells

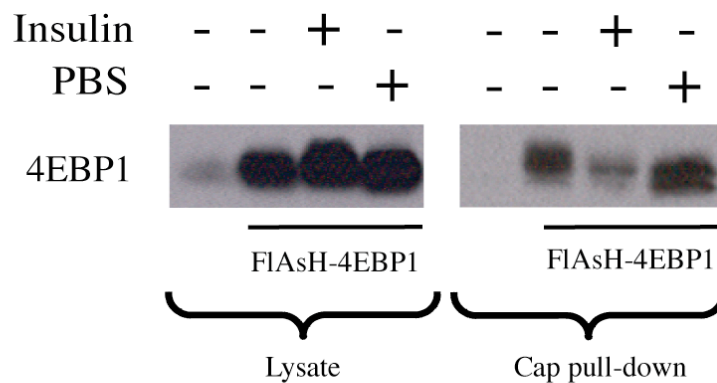
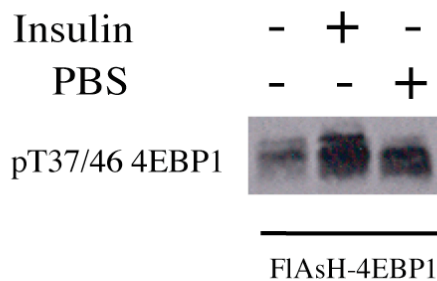
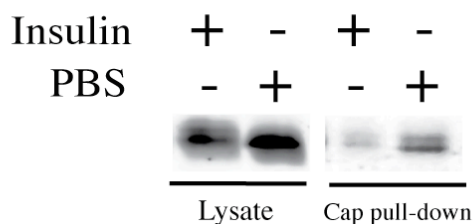
Cells were co-transfected with eIF4E and with ECFP-4EBP1 (N-terminus fusion) or 4EBP1-Citrine (C-terminus fusion), after 24 hours starved of serum for 16 hours and treated with 10 μ g/ml Insulin or incubated in PBS for 30 min. Cell lysate or cap-beads bound fraction was analyzed by Western blot with total (A) and phosphospecific (B) 4EBP1 antibodies.

3.2.3. A FIAsh labeling approach for making FRET probe

After it became clear that 4EBP1 binding to eIF4E is altered by fusing it to GFP-variant fluorophores, I began looking for alternatives. A new method, called FIAsh labeling appeared promising as it only required a small linear motif and was shown to function in the cases where larger GFP derivatives

had interfered with biological function (Andresen et al., 2004). FIAsh is a fluorescent dye that becomes fluorescent only when bound to the tetracysteine motif on a peptide or a protein and it is very small compared to GFP. FIAsh can be used as an acceptor for FRET, for example with the ECFP as a donor. I introduced the optimized tetracysteine motif FLNCCPGCCMEP at the N- and C-terminus of 4EBP1. First FIAsh-4EBP1 needed to be tested to ensure that its binding is physiological. In contrast to the previous attempts with GFP moieties, in HeLa cells after stimulation with insulin FIAsh-4EBP1 binding to eIF4E was reduced, while PBS treatment increased the amount of the bound FIAsh-4EBP1 in the cap pull-down (Figure 15A). The phosphorylation pattern was also similar to endogenous 4EBP1 (Figure 15B). Finally, labeled FIAsh-4EBP1 could be directly visualized by scanning a non-reducing gel containing protein from FIAsh labeled cells (Figure 15C). Encouragingly, FIAsh-4EBP1 binding to eIF4E was weaker after Insulin treatment than it was after PBS, as expected for the endogenous 4EBP1 protein. In lysate a characteristic shift down after PBS was evident, indicating proper phosphorylation regulation. FIAsh-4EBP1 behavior was also tested in MCF7 cells, yielding similar results (data not shown). I continued with HeLa cells, since they showed greater transfection efficiency. These results suggest that FIAsh labeled 4EBP1 is functional and can be used for intermolecular FRET.

Encouraged with successful proof that FIAsh-4EBP1 phosphorylation and binding was regulated in a physiological manner, I cloned the corresponding FRET partner – ECFP at the N- and C-terminus of eIF4E. These fusions also had to be tested for their ability to bind cap and 4EBP1 to ensure that eIF4E biological function and regulation is preserved in these constructs. HeLa cells were transfected with ECFP-eIF4E and eIF4E-ECFP and immunoprecipitations were performed. Both proteins were able to bind cap, although eIF4E-ECFP binds cap much more weakly than ECFP-eIF4E (Figure 16A, left). This could be caused by a steric hindrance, because C-terminus of eIF4E is close to the cap binding pocket and ECFP domain might interfere with the binding.

A**B****C****Figure 15 Biochemical analysis of the FIAsh-4EBP1 fusion in HeLa cells**

(A) Cells were transfected with FIAsh-4EBP1, and after 24 hours treated with 10 μ g/ml Insulin or incubated in PBS for 30 min. The cell lysate or cap-beads bound fraction was analyzed by Western blot with 4EBP1 antibody. Note that almost no signal is visible for the non-transfected cells, meaning that endogenous 4EBP1 contributes very little to the total signal.

(B) Same samples as in (A) detected with phosphorylation-specific Thr37/46 4EBP1 antibody.

(C) Direct scan of the non-reducing gel electrophoresis. Lysate or cap-bound fraction of FIAsh-4EBP1 transfected HeLa cells were separated on a gel and labeled FIAsh-4EBP1 was visualized with Bio-Rad Molecular Imager Pharos FX.

Glutathione-sepharose beads were used to control for non-specific binding to the beads. To test whether eIF4E fusions could bind 4EBP1, I immunoprecipitated them with an anti-GFP antibody that crossreacts with

ECFP, and detected whether 4EBP1 had coimmunoprecipitated (Figure 16A, right). Cells transfected with GFP served as a control. Both N- and C-terminal labeled eIF4E were able to bind 4EBP1. I then checked if ECFP-eIF4E and eIF4E-ECFP could bind 4EBP1 in a manner regulated by PBS and insulin.

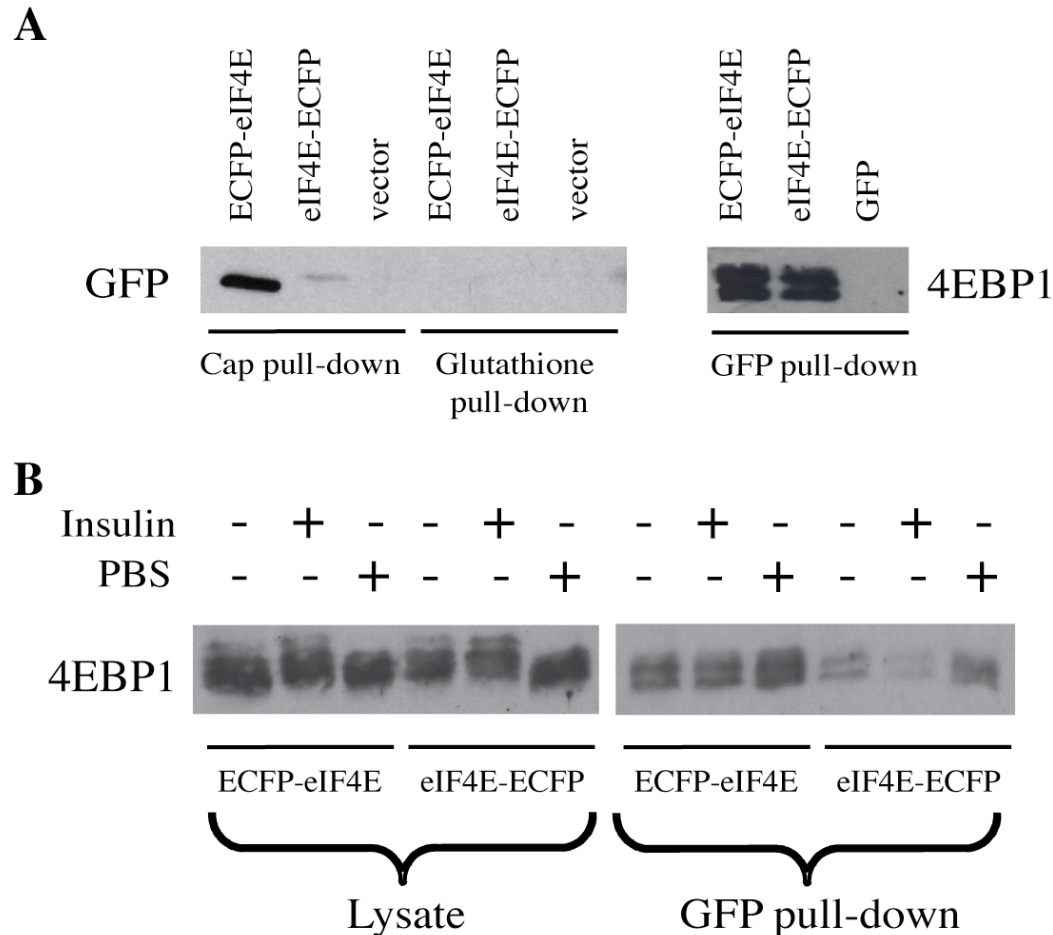


Figure 16 eIF4E fusions bind cap and 4EBP1 in HeLa cells

- (A) Cells were transfected with ECFP-eIF4E (N-terminal) or eIF4E-ECFP (C-terminal) or empty vector, lysed and tested for the ability to bind cap-beads or Glutathione-beads as a control (left panel). After immunoprecipitation with GFP antibody, the ability to bind 4EBP1 was tested by detecting bound 4EBP1 (right panel). GFP also served as a control.
- (B) Cells were transfected with ECFP-eIF4E (N-terminal) or eIF4E-ECFP (C-terminal), after 24 hours starved of serum for 16 hours and treated with 10 μ g/ml insulin or incubated in PBS for 30 min. Cell lysate or anti-GFP immunoprecipitated material was analyzed by Western blot with 4EBP1 antibody.

Figure 16B shows endogenous 4EBP1 in cell lysate, as a control that the treatments worked and the right panel shows the amount of 4EBP1 pulled

down in the anti-GFP precipitation. ECFP-eIF4E bound more 4EBP1 after PBS treatment, as should be the case, but it didn't respond to insulin, while eIF4E-ECFP bound more 4EBP1 after PBS and less after Insulin treatment, thus demonstrating normal regulation.

These results indicated that FIAsh labeled 4EBP1 can be phosphorylated by mTOR and that 4EBP1 binding to eIF4E labeled with ECFP is regulated by mTOR phosphorylation. Therefore we proceeded to test whether changes in FRET can be detected upon interaction between the labeled partners.

3.2.4. FRET measurements using FIAsh labeling

For intermolecular FRET, the magnitude of FRET is directly proportional to the amount of binding between the interacting partners: the more molecules are in complex with each other, the more FRET we expect. Therefore, I wanted to see if under the conditions of maximal binding there is detectable FRET. Conveniently enough, FIAsh labeling is done in a salt solution similar to PBS (Hank's Buffered Salt Solution - HBSS), which means that after the labeling the cells are in starved of serum and we expect 4EBP1 to be bound to eIF4E and thus the maximal amount of FRET. I started with acceptor photobleaching technique, which monitors FRET by the increase of the donor fluorescence after the acceptor is destroyed by a strong illumination. I tested all 4 possible combinations of N- and C-terminal tagged 4EBP1 and eIF4E, trying to maximize the probability of fluorophore orientation favoring FRET. Cotransfection of ECFP with FIAsh-4EBP1, where we expect no interaction served as a negative control. FRET efficiency is calculated according to the following formula:

$$\text{FRET}_{\text{eff}} = (D_{\text{post}} - D_{\text{pre}}) / D_{\text{post}}, \text{ for all } D_{\text{post}} > D_{\text{pre}}$$

where D_{pre} is the donor fluorescence before the bleaching and D_{post} is the donor fluorescence after the bleaching .

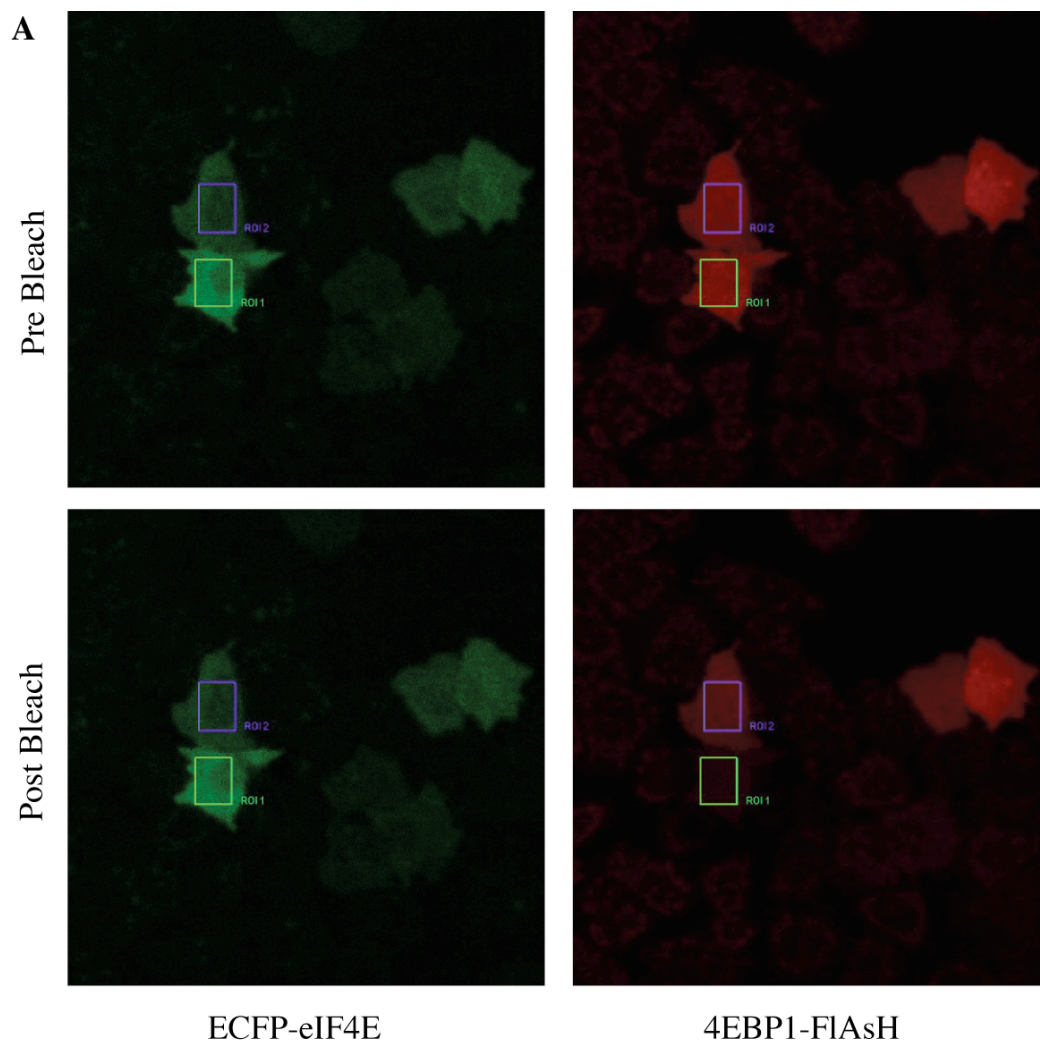
In general, acceptor photobleaching on live cells was quite variable and poorly reproducible. Figure 17 shows an example of an acceptor photobleaching experiment using ECFP-eIF4E and 4EBP1-FIAsh. A cell containing ROI_1

(Region Of Interest) is bleached, and FRET efficiency is calculated from the donor (ECFP-eIF4E) channel. A cell containing ROI_2 is not bleached and serves as a control to estimate noise of the live imaging. FRET efficiency in this example is 0 for both bleached and unbleached cells. From the signal in ROI_2 it is clear that the post bleaching images for both donor and acceptor are weaker also in the non-bleached area, for an unknown reason. In other cases the same donor-acceptor combination showed apparent FRET efficiency of up to 7%. However, FRET efficiency for cells where acceptor was not bleached was similar or even greater than in the cell where acceptor was bleached (up to 10%). Moreover, negative control samples, containing ECFP and 4EBP1-FIAsH also showed up to 3% FRET efficiency, which was clearly an artifact of measurement, since we expect no interaction between these proteins. We concluded that this technique has too much variability and too low signal/noise ratio to be useful. Table 3.1 summarizes the data from all acceptor photobleaching experiments. N-terminal FIAsH-4EBP1 did not show any FRET with either eIF4E construct, while C-terminal 4EBP1-FIAsH presented values that varied between 0 and 7% FRET efficiency. Notably, non bleached cells displayed FRET efficiency in a similar range.

Table 3.1 FRET efficiency, measured by acceptor photobleaching

Donor	Acceptor	Number of cells measured	FRET efficiency, %	FRET efficiency, %, non bleached cells
ECFP-eIF4E	FIAsH-4EBP1	3	all 0	ND
ECFP-eIF4E	4EBP1-FIAsH	4	0, 1, 1, 7	0, 0.4, 7, 10
eIF4E-ECFP	FIAsH-4EBP1	3	all 0	ND
eIF4E-ECFP	4EBP1-FIAsH	3	4, 4, 5	0, 1.6, 1.5
ECFP	4EBP1-FIAsH	2	0, 3	ND

FRET efficiency is shown for individual cells, ND – Not Determined.

**B**

ROI	ROI_1	ROI_2
D pre	98.65	42.80
D post	90.79	39.27
A pre	105.03	93.52
A post	22.43	69.18
FRETeff (%)	0.00	0.00

Figure 17 FRET measurement by Acceptor photobleaching

- (A) Cells were cotransfected with ECFP-eIF4E and 4EBP1-FIAsH, labeled with FIAsH after 36 hours and imaged using confocal microscopy. Pre and post bleaching images are shown for donor (ECFP-eIF4E) and acceptor (4EBP1-FIAsH) channels. FRET efficiency was calculated for in indicated Regions Of Interest (ROI) inside the bleached region (ROI 1) and outside (ROI 2).
- (B) Quantification of the ROIs shown in (A). Fluorescence values for Donor (D) and Acceptor (A) channels are displayed pre and post bleaching as well as FRET efficiency calculated from these values.

A factor leading to the low FRET efficiency, observed by acceptor photobleaching experiments could be a difference in fluorophore strength between ECFP and FIAsH. ECFP is much brighter than FIAsH and it is possible that even if the FRET efficiency is high for the FIAsH, the increase in the ECFP donor fluorescence after bleaching is small and is hard to detect. I therefore tried to estimate FRET using sensitized emission method, which calculates FRET based on the acceptor fluorescence after donor excitation. Sensitized emission is conceptually straightforward but technically challenging method for FRET measurement. The challenge is that when detecting sensitized emission from the acceptor upon donor excitation one must correct for a number of factors, mainly for the donor emission overlapping with the acceptor emission (bleed-through) and the direct excitation of the acceptor when exciting the donor. These corrections can be made using samples containing only donor and only acceptor fluorophores. One must assume that these correction factors are invariable within the image and between different cells and this is of course an approximation, so one must take the values with a grain of salt and test them by relevant biological assays.

Table 3.2 summarizes the results for the sensitized emission FRET measurements. 3 out of 4 combinations showed FRET with the ECFP-eIF4E

Table 3.2 FRET efficiency, measured by sensitized emission

Donor	Acceptor	Number of cells measured	FRET efficiency, %
ECFP-eIF4E	FIAsH-4EBP1	11	3,7,14,5,6,12,14,16,14,21,24
ECFP-eIF4E	4EBP1-FIAsH	5	0,0,2,5,7
eIF4E-ECFP	FIAsH-4EBP1	6	all 0
eIF4E-ECFP	4EBP1-FIAsH	5	1,3,4,4,5
ECFP	4EBP1-FIAsH	5	0,0,15,15,17

FRET efficiency is shown for individual cells.

FIAsh-4EBP1 combination showing highest values (on average 12%). Unfortunately the negative control also showed up to 17% FRET, demonstrating that biological variability causes noise in the similar range of the FRET measured in experiments.

As a biological test, I decided to perform stimulation with Insulin and inhibition of Rapamycin to see if these can change the FRET efficiency, as observed through sensitized emission. If the calculated FRET values are indeed reflecting the interaction between labeled 4EBP1 and eIF4E, then we expect a change upon Insulin stimulation and Rapamycin inhibition of TOR. I used ECFP-eIF4E and FIAsh-4EBP1 combination, which appeared most promising, often showing relatively high calculated FRET. Unfortunately, as shown in Figure 18 neither insulin nor Rapamycin were able to change FRET significantly, suggesting that the calculated FRET is not biologically relevant.

The graph of FRET efficiency against time is a good example to how noisy this method is in live cells. From one point to the next calculated FRET efficiency can change 2-fold, probably due to rearrangement of fluorophores in the cells, cells movements and focus changes associated with it. Figure 19 shows the same kind of experiment on a negative control sample (ECFP and FIAsh-4EBP1). One of the two cells showed no response to either insulin or Rapamycin, while another cell displayed an artifact of addition after both treatments.

In conclusion sensitized emission data did not confirm that the intermolecular FRET occurs, as calculated FRET was not responsive to physiological stimulation or inhibition that biochemically was shown to affect the interaction between the labeled proteins.

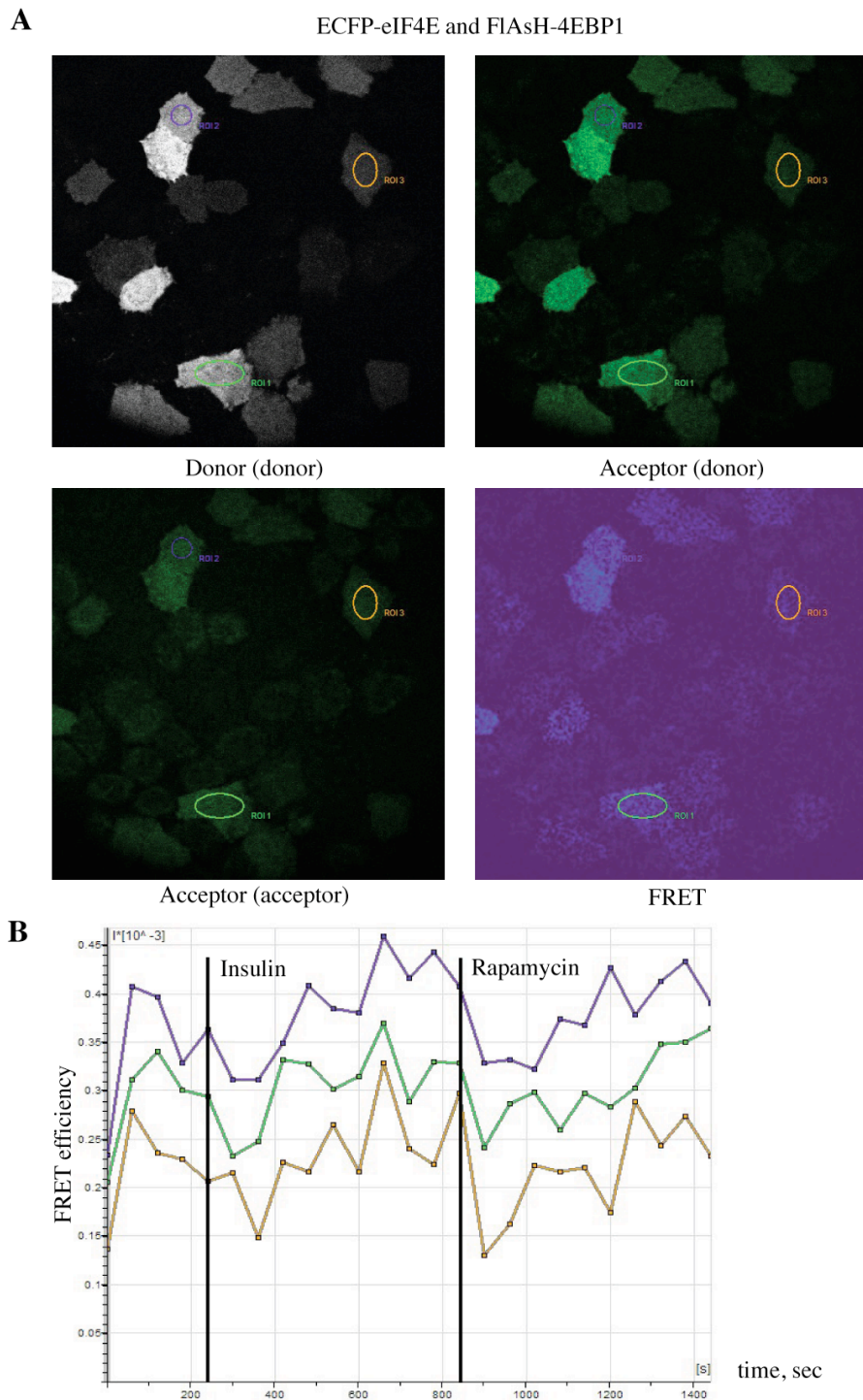


Figure 18 FRET measurement by Sensitized Emission

Cells were cotransfected with ECFP-eIF4E (N-terminal) and FIAsh-4EBP1 (N-terminal), after 36 hours labeled with FIAsh and imaged using confocal microscopy. (A) Images are shown for donor (ECFP-eIF4E), acceptor (4EBP1-FIAsh), sensitized emission – acceptor emission (donor excitation) and calculated FRET. FRET efficiency was calculated in indicated Regions Of Interest (ROI) and plotted in (B). At indicated times (vertical line) 10 μ g/ml Insulin or 20 μ M Rapamycin was added. Labels indicate emission channel, upon excitation in parenthesis.

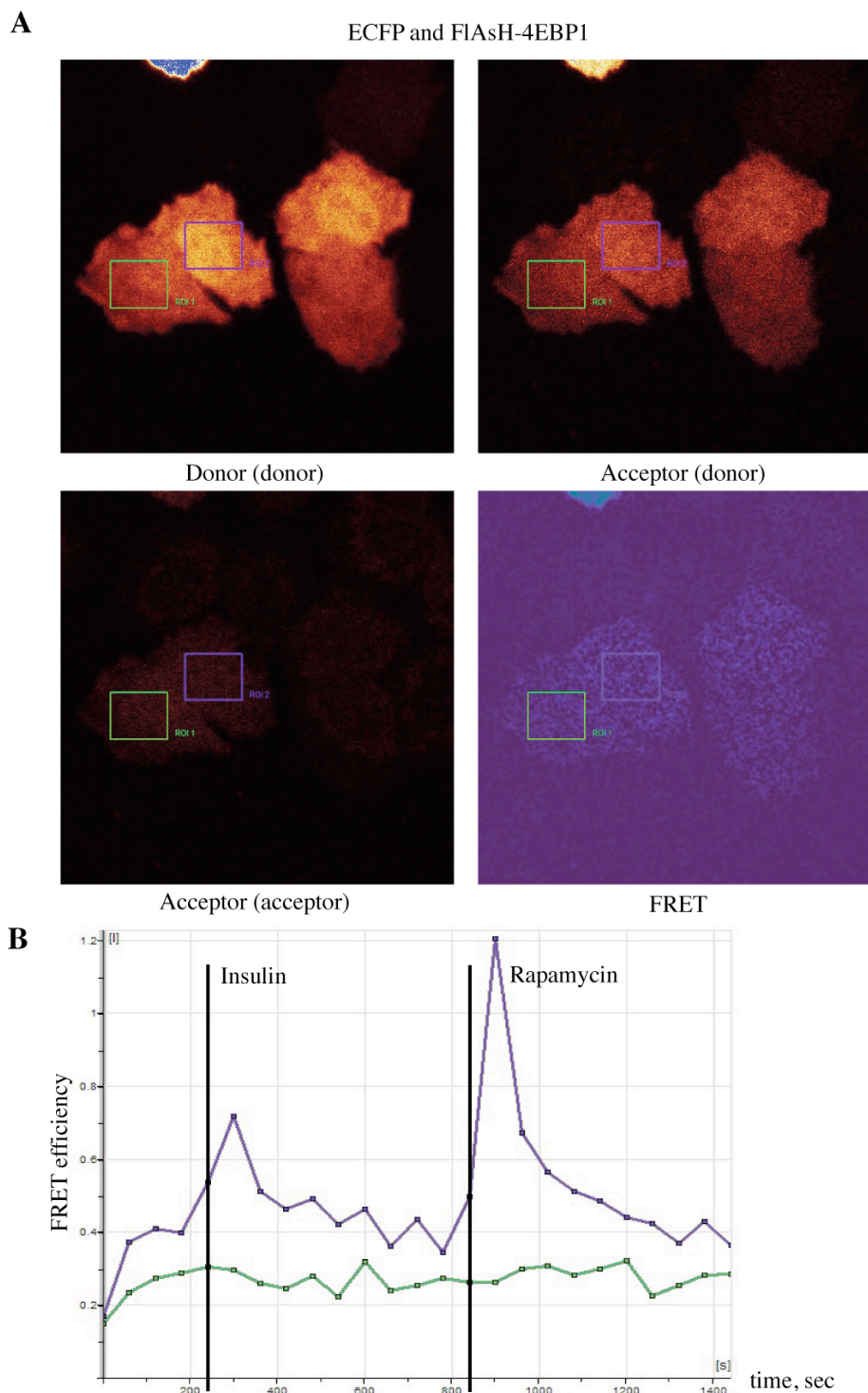


Figure 19 FRET measurement by Sensitized Emission – Negative control

Cells were cotransfected with ECFP and FIAsh-4EBP1 (N-terminal), labeled with FIAsh after 36 hours and imaged using confocal microscopy. (A) Images are shown for donor (ECFP), acceptor (4EBP1-FIAsh), with sensitized emission – acceptor emission (donor excitation) and calculated FRET. FRET efficiency was calculated in indicated Regions Of Interest (ROI) and plotted in (B). At indicated times (vertical line) 10 μ g/ml Insulin or 20 μ M Rapamycin was added. Labels indicate emission channel, upon excitation in parenthesis.

Finally, I tested the intermolecular FRET approach by chemically bleaching FIAsH. This type of FRET measurement has a similar principle to acceptor photobleaching but the bleaching is chemical, using BAL (British-Anti-Lewisite, 2,3-dimercapto-1-propanol) – a chemical with a higher affinity for arsenicals than EDT or FIAsH. It strips FIAsH off the tetracysteine motif very effectively and thus destroys the acceptor. This should lead to an increase of the donor (ECFP) fluorescence if there is any FRET (Adams et al., 2002). Addition of 5mM BAL leads to the rapid drop in FIAsH fluorescence and simultaneous increase the ECFP for a well-characterized KCP-F probe (Jost et al., 2008)(Figure 20).

Negative control (ECFP and FIAsH-4EBP1) did not exhibit an increase in donor channel upon BAL addition, while positive control KCP-F did as expected (Figure 21A). Disappointingly, all the combinations of FIAsH labeled 4EBP1 and ECFP labeled eIF4E displayed no elevation in donor channel after BAL, indicating that no FRET takes place between these fluorophores (Figure 21B). This is surprising given the small size of the proteins and the fact that both proteins have been labeled on each end and all combinations tested. One possible explanation could be that dipoles of the fluorophores are arranged at an angle that does not allow FRET.

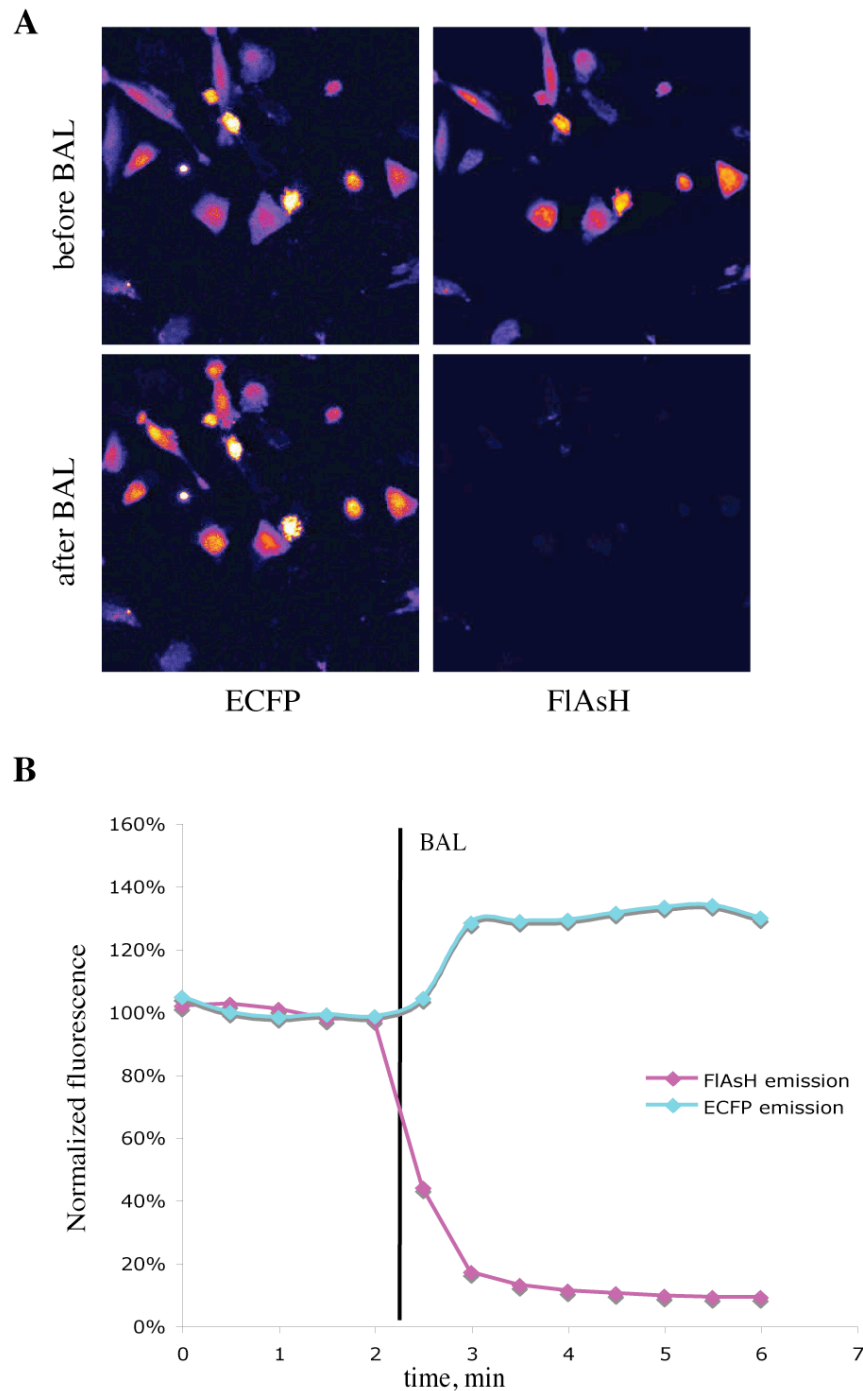
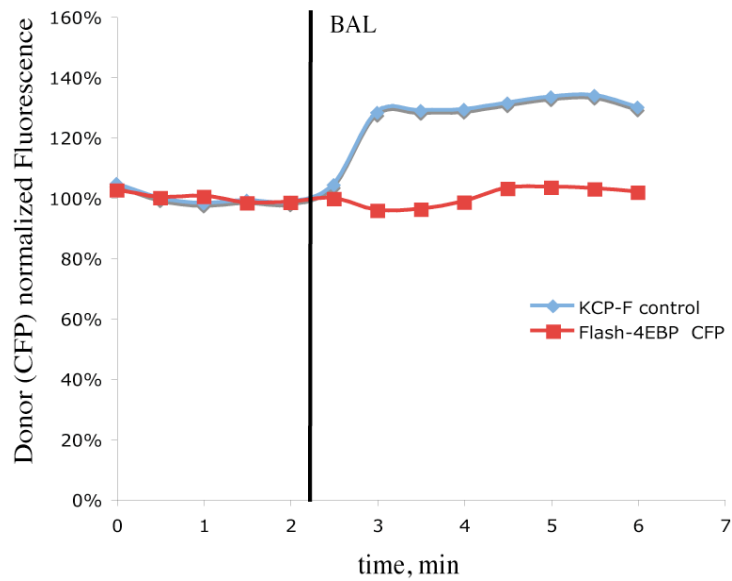


Figure 20 FRET test by destroying FIAsH with BAL – KCP-F

Cells were transfected with KCP-F, after 36 hours labeled with FIAsH and imaged using confocal microscopy. (A) Pseudocolored images are shown for donor (ECFP) and acceptor (FIAsH) before and after addition of BAL. Note that donor fluorescence is completely destroyed by BAL. (B) Normalized fluorescence of donor and acceptor plotted against time. FIAsH is disappearing in less than a minute with a corresponding increase in ECFP signal.

A



B

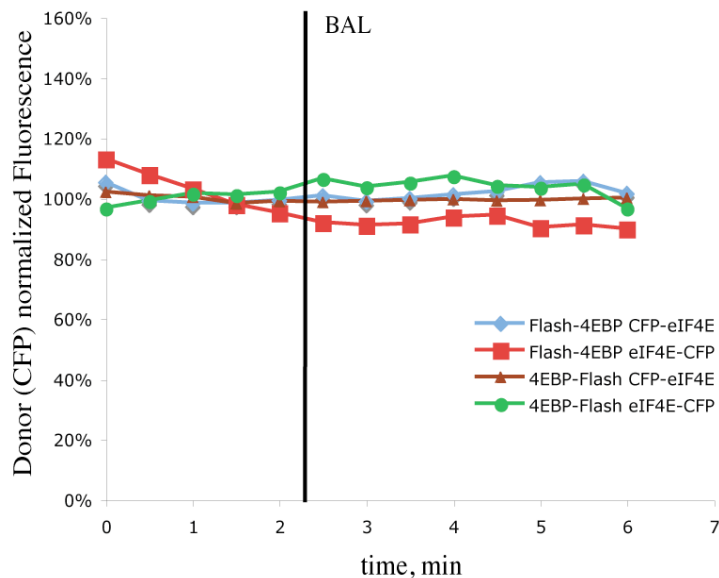


Figure 21 4EBP1 fusions to FIAsH do not show FRET

Cells were cotransfected with indicated combinations of 4EBP1 fused to FIAsH and eIF4E fused to ECFP or ECFP alone, after 36 hours labeled with FIAsH and imaged using confocal microscopy. (A) Positive control KCP-F shows an increase in donor fluorescence after addition of BAL while negative control (ECFP alone with FIAsH-4EBP1) doesn't. (B) None of the combinations of 4EBP1 fused to FIAsH and eIF4E fused to ECFP shows FRET.

3.3. Discussion

3.3.1. 4EBP1 regulation is disturbed by fusion to GFP

Development of the FRET probe for TOR signaling proved to be challenging. The conventional strategy of a conformational probe based on GFP variants as a FRET pair did not work, because inserting 4EBP1 in between ECFP and Citrine abolished regulation of binding to eIF4E. The ECFP-4EBP1-Citrine fusion was still recognized by TOR kinase and phosphorylated properly. At least a fraction of FRET probe was able to bind to eIF4E, as shown by cap pulldowns, but this fraction does not respond to phosphorylation by TOR. This is most probably because addition of two globular GFP domains changes the ability of 4EBP1 to bind eIF4E. An alternative explanation would be that because of overexpression, TOR cannot phosphorylate all available FRET probe molecules and there is always an unphosphorylated fraction that binds. This is not likely to be the case, because then we would still expect the increase in binding after inhibition of TOR (starvation with PBS or rapamycin), which is not occurring (Figure 9A, last lane). Of course one would have to ensure that there is enough eIF4E to bind in the cell, which was achieved by cotransfection of eIF4E together with FRET probe.

Given a small size of 4EBP1 (12 KDa) it is easy to imagine that addition of two 25 KDa GFP domains can change its behavior. As turned out in subsequent experiments one GFP domain was still too much, irrespective of which end of the protein it was attached to. 4EBP1 tagged with one GFP-variant at either end of the protein was also binding constitutively and not regulated by TOR activation or inhibition. Since 4EBP1 is unstructured in solution, it is conceivable that it needs its dynamic conformation to make proper contacts with eIF4E and a bulky GFP domain restricts its conformational freedom and thus affects binding properties to eIF4E.

Surprisingly, phosphorylation of all tested FRET probes was similar to the endogenous 4EBP1, indicating that it can be recognized by TORC1. For TORC1, raptor was proposed to act as an adaptor protein, recognizing the TOS motif and thus bringing TORC1 substrates to the TOR kinase. In 4EBP1,

the TOS motif is at the very C-terminus, but apparently it can still function in the FRET probe fusion with GFP domain fused directly after it.

Many FRET probes for kinases utilize a strategy where a short peptide sequence (either a generic consensus or a known substrate) is sandwiched between a FRET pair and phosphorylation of the peptide triggers a conformational change, leading to a change in FRET (Schleifenbaum et al., 2004). Sometimes to create a larger conformational change, a phosphotyrosine or phosphoserine binding domain is included to recognize and bind phosphorylated substrate (Kurokawa et al., 2001) (Sasaki et al., 2003; Zhang et al., 2001). When we considered possible FRET probe designs we decided to use full-length 4EBP1 to preserve all its regulatory sequences for the best specificity.

Phosphorylation alone of the FRET sensor was not enough to see a change in FRET. This is consistent with the idea that conformational change in 4EBP1 is induced by binding to eIF4E and free 4EBP1 in solution has no stable structure. This was the case in HEK293 and HeLa cells in transient transfection and also in stable line of HEK 293 cells selected for low levels of FRET probe expression. The idea behind selecting low-expressing cell line stemmed from observation that sometimes there was weak response to insulin in dim cells and selecting cells with low expression would increase the fraction of probe that was responding to stimulation. Later it turned out that it was an effect of Insulin addition (changing background fluorescence), which was more evident in cells with low signal. This example highlights the importance of proper controls and caveats in interpreting FRET probes results.

Alternative FRET pair of GFP² as a donor and YFP as an acceptor, did not produce FRET change either, which strengthens the conclusion that it is the presence of the GFP domain that affects the binding and using an another FRET pair cannot solve this issue. Using “monomeric” mutants of GFP did not make a difference in this case, suggesting that a tendency to dimerize does not play a role in this FRET probe, probably because its primary problem is inability to undergo binding in a regulated manner.

3.3.2. FIAsH labeled 4EBP1 is functional but produces no FRET

Tetracystein motif of 12 amino acids used for FIAsH labeling did not interfere with binding, supporting that it was indeed a steric problem in the GFP fusions that affected binding. This was a very encouraging development allowing to explore the possibility to make an intermolecular FRET probe. Unfortunately, despite having properly regulated binding to eIF4E, FIAsH labeled 4EBP1 did not show FRET response. This was tested by a number of different approaches such as: acceptor photobleaching, sensitized emission and chemical bleaching of the acceptor.

Acceptor photobleaching and sensitized emission data were not conclusive, because they were badly reproducible and signal to noise ratio was low. In live cell imaging there are many factors that influence the signal; if the signal is not strong enough to overcome fluctuations from the biological variance and measurement and analysis imprecision, the usefulness of the approach is limited. This was the case for acceptor photobleaching, where calculated FRET efficiency was varying from cell to cell and was comparable to the negative control samples. For most of the combinations of N- and C-terminally labeled 4EBP1 and eIF4E FRET efficiency was zero or low (not exceeding 7%), suggesting that if there is FRET happening, it is not very efficient and would be hard to detect reliably.

I then focused my attention on sensitized emission method, thus concentrating on the acceptor (FIAsH). It was possible that because FIAsH had weaker fluorescent signal than ECFP, more of FIAsH would participate in FRET and detecting sensitized emission could be a better way to assess FRET. Indeed, one of the combinations (ECFP-eIF4E and FIAsH-4EBP1) did show more apparent FRET than others, but it was not responsive to stimulation with insulin. In addition signal/noise ratio was low and negative control samples gave similar FRET values. Sensitized emission method uses correction factors for calculating FRET, which are prone to introduce mistakes. The factors are calculated from control cells with specific parameters of brightness, expression levels and stoichiometry of fluorophores

and then are applied to the cells that may have slightly different parameters. Also such factors as donor and acceptor brightness and stoichiometry are influencing FRET detection. Ideal donor/acceptor stoichiometry is 1:1 and FRET can still be detected for the ratios varying from 0.1 till 10 (Chen et al., 2006). In reality, there is no way to know the stoichiometry in the cell for intermolecular FRET, as protein concentrations will depend on multiple parameters, such as expression efficiency, stability and degradation dynamics.

Acceptor chemical bleaching with BAL proved unambiguously that there is no FRET happening between differently labeled 4EBP1 and eIF4E. Chemical bleaching strips FIAsh completely off the protein, making it non-fluorescent. This happens very fast, and it is a better method than photobleaching, because there is no danger of bleaching the donor. All combinations looked like the negative control, namely there was no increase in the donor channel, after destroying the acceptor fluorescence. It is surprising that none of the combination of N- and C-terminally labeled 4EBP1 and eIF4E produced any measurable FRET. Given the small size of 4EBP1 and also eIF4E and analysing at the structure of eIF4E with 4EBP1 peptide bound (see Figure 22) it is plausible that there would be some FRET between the two. Although we cannot predict the location of full-length 4EBP1 N and C termini, eIF4E N-terminus is facing the side where 4EBP1 binds and it is quite flexible, because it is not visible in the structure (Tomoo et al., 2005). Based on the structure only the central part of 4EBP1 containing the eIF4E binding motif becomes structured upon binding, leaving a lot of flexibility to the fluorophore fused to either N or C terminus. Still despite biochemical proof of binding between the two partners there is no FRET occurring based on the chemical bleaching experiment.

The absence of FRET could be attributed to the unfavorable orientation of dipoles of the FRET pair, which is an unpredictable parameter. In addition, non-stoichiometric ratio between the fluorophores with excess of non-interacting fluorophores can mask FRET.

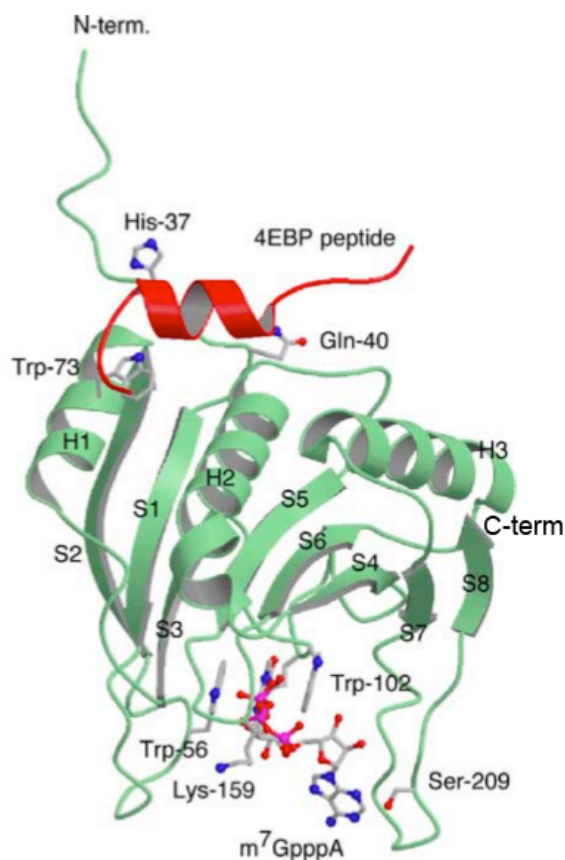


Figure 22 Structure of eIF4E with 4EBP1 peptide and cap analog

Structure of the ternary complex of m⁷GpppA – eIF4E – 4E-BP1 peptide. eIF4E is shown in green, 4EBP1 peptide in red. Some residues important for interactions and m⁷GpppA cap analog are shown as ball and stick model. Modified from (Tomoo et al., 2005)

4EBP1 was reported to be regulated by ubiquitination that leads to its degradation (Elia et al., 2008), which could contribute to the difference in concentration of interacting proteins. Lastly, the sensitivity or dynamic range of FRET probes is usually not large and extensive optimization of linker sequences may be necessary to obtain a good signal. One striking example is a recent paper from fresh Nobel laureate Roger Tsien laboratory (Hires et al., 2008). While developing a FRET sensor for glutamate, the sensitivity of the original FRET construct was only around 7% change in the donor/acceptor ratio. After having screened through 176 truncation combinations by varying the length of linking regions between the glutamate binding domain and donor and acceptor, they found 1! combination with significantly increased sensitivity. Moreover, there was no rational explanation that could explain why this combination was so much better than others. This example demonstrates

how challenging the development of FRET probes can be and how unpredictable the process is.

It is impossible to exclude that FRET occurs in the probes that I have tried, it could as well be undetectable using the methods employed. All the results taken together for intermolecular FIAsh-based probe, suggest that even if FRET occurs, its magnitude is not big enough to make it a useful tool to monitor TOR activity. One possible direction for the future could be using FLIM to detect FRET, as this method has some advantages (see introduction) over intensity-based methods.

In conclusion, both intramolecular and intermolecular FRET probes were designed and tested using different FRET pairs and a number of cell lines. Several different constructs and a range of methods were utilized to assess FRET efficiency using FIAsh labeling but no acceptable probe was identified. Future studies using different strategies are needed to achieve the goal of developing a sensor for TOR activity *in vivo*.

4. Analysis of MAP4K3 function in *Drosophila melanogaster*

4.1. Introduction - amino acid signaling and fat metabolism

4.1.1. Nutrient signaling by TORC1

TOR kinase regulation by nutrients, specifically amino acids, is the most conserved functions of TOR, yet it is quite poorly understood. Amino acids withdrawal results in decreased TORC1 activity towards its substrates, S6K and 4EBP but the elements mediating this input remain largely unknown (Avruch et al., 2006). Of note is that insulin is able to induce activation of PI3K and AKT but not TORC1 in amino acid deprived cells. This indicates that there are two independent pathways converging on TORC1, with amino acid branch being dominant one, that is, it can block insulin induced TORC1 activation, and is necessary for insulin stimulation to be successful (Hara et al., 1998). This makes perfect sense in terms of cell physiology – growth promoting signals can only be executed, when there are enough building blocks to support growth.

A number of proteins have been reported to be involved in amino acids signaling to TORC1 but their interrelationship is not clear and they do not constitute a signal cascade, that could explain the signal flow from amino acids to TORC1 (as is the case for Insulin cascade). For example, a homolog of yeast Vps34 (vacuolar protein sorting 34), Type III PI3-kinase that produces PI(3)P was shown to participate in amino acid regulation of TORC1. Overexpression of hVps34 or the associated hVps15 kinase activates S6K1, and insulin stimulation of S6K1 is blocked by microinjection of inhibitory anti-hVps34 antibodies, overexpression of a FYVE domain construct that sequesters the hVps34 product PI(3)P, or small interfering RNA-mediated knock-down of hVps34 (Byfield et al., 2005; Nobukuni et al., 2005). This regulation is confusing, given that Vps34 is required for starvation-induced autophagy (Mizushima et al., 2002), while TORC1 is a negative regulator of autophagy (Lum et al., 2005).

Amino acids have been shown to act on TORC1 independently of TSC complex but they regulate Rheb binding to TOR, in a manner that is not completely understood (Long et al., 2005b). Overexpression of Rheb can

overcome amino acids starvation-induced TORC1 inhibition, supposedly by flooding the cell with very high concentrations of Rheb-GTP, that is able to activate TORC1 (Avruch et al., 2006).

Recently small GTPases called Rags were reported to mediate amino acids activation of TORC1 (Kim et al., 2008; Sancak et al., 2008). Rags function as heterodimers and interact with TORC1. Inactive GDP-bound Rag mutants can block amino acid activation of TORC1, while constitutively active GTP-bound mutants make TORC1 insensitive to amino acids deprivation. Sancak et al. propose that Rags act, similarly to amino acids, by promoting translocation of TORC1 from distributed cytoplasmic puncta to the perinuclear compartment containing its activator Rheb. Genetic studies in *Drosophila* demonstrated that Rag GTPases regulate cell growth, autophagy and viability during starvation (Kim et al., 2008).

Additional component recently discovered to play a role in amino acid signaling to TORC1 is a *Drosophila* gene CG7097, an ortholog of mammalian MAP4K3 (Findlay et al., 2007). It was discovered in an RNAi screen in *Drosophila* S2 cells looking for new kinases affecting phosphorylation of S6K in the sensitized background of TSC1 depletion. MAP4K3 was needed for phosphorylation of S6K induced by amino acids, MAP4K3 kinase activity was stimulated by amino acids but not insulin and overexpression of MAP4K3 promoted rapamycin-sensitive phosphorylation of S6K and 4EBP. In addition, knockdown of MAP4K3 levels caused a decrease in cell size, phenocopying Rapamycin treatment or Rheb knockdown. Taken together these results provide evidence that MAP4K3 plays a role in transducing nutrients availability signal to TORC1, but how it does so or its relationship to other components of nutrients-TORC1 pathway remains to be established.

We decided to use *Drosophila* model to investigate the function of MAP4K3 as a nutrient sensor on the organism level. Cell culture is a very convenient and widely used experimental system but it does not allow analysis of gene function in the context of intact organism. Artificial culturing conditions and absence of high level systemic regulation (e.g. hormonal) necessitate complementary studies in the whole organism. One recent example, highlighting importance of verification of cell culture studies in the model organism is Vps34 case. While Vps34 was reported crucial for amino acids

regulation of TORC1 in cultured cells (Byfield et al., 2005; Nobukuni et al., 2005), *Drosophila* animals lacking Vps34 gene product have normal TOR activity and Vps34 doesn't seem to activate TOR in this system (Juhász et al., 2008). This could either reflect differences between *Drosophila* and mammalian Vps34 functions or the results in cell culture do not reflect the physiological function of the protein in the organism.

Apart from the newly proposed function as an activator of TOR in response to amino acids, MAP4K3 has been poorly characterized and the literature about it is quite scarce. Mammalian MAP4K3 is also known as Germinal-center Like Kinase (GLK), it belongs to the GCK (Germinal Center Kinase) family (Kyriakis, 1999). *Drosophila* MAP4K3 is a large kinase of 1218 amino acids (947 for a smaller isoform B) with two defined domains: Ser/Thr kinase domain and a Citron homology domain (Figure 23). Citron homology domain is annotated as a small GTPase regulatory domain, pointing at small GTPases as possible interaction partners.

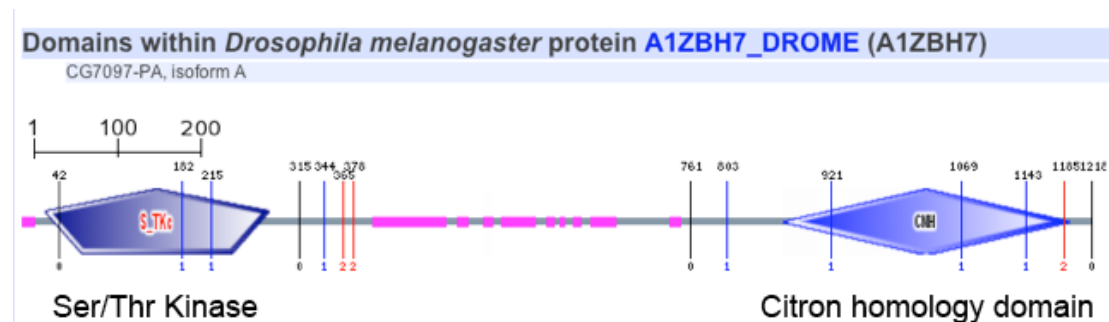


Figure 23 Domain structure of MAP4K3

Isoform A of MAP4K3 was annotated for known domains using SMART tool (Schultz et al., 1998).

Human MAP4K3 was identified as an interacting partner for endophilin 1, a protein involved in clathrin-mediated endocytosis. MAP4K3 can bind SH3 domain of endophilin 1 and is needed for activation of c-Jun N-terminal Kinase (JNK) by endophilin 1 (Ramjaun et al., 2001). JNK is one of the four main branches of the MAP (Mitogen Activated Protein kinase) pathway, along with ERK, p38 and ERK5. Interestingly, MAP kinase signaling, a vast signaling network regulating response to mitogens and stress, has been recently linked to TOR signaling. Several reports demonstrated crosstalk

between MAP kinase signaling and insulin/TOR signaling (Herbert et al., 2002; Ma et al., 2005; Roux et al., 2004). The later two of these show that TSC2 is the point where ERK (extracellular signal-regulated kinase) signaling is feeding into TOR pathway, modulating TOR activity, while Hebert et al show that 4EBP phosphorylation induced by ERK is TOR dependent.

Another study implicates p38 and ERK branches of MAPK pathway in amino acid signaling to S6K, surprisingly, in a seemingly TOR-independent way (Casas-Terradellas et al., 2008). This study shows that ERK and p38 are activated by amino acids and signal to their effector kinases called RSK (p90 ribosomal S6 kinases) and MSK (mitogen- and stress-activated kinases) in addition to activating S6K1 by phosphorylation on Thr421/Ser424.

Moreover, a component of TORC1, raptor, turns out to be a target of RSK kinase, effectively making TORC1 an effector of ERK signaling (Carriere et al., 2008). RSK is a family of four kinases in mammals, they can phosphorylate raptor *in vitro* and *in vivo* on 3 closely spaced Ser residues at the conserved region. Phosphorylated raptor is then able to significantly increase TORC1 kinase activity towards 4EBP1 and S6K1, presumably through promoting a catalytically more active conformation of TORC1.

Thus it appears that TOR and MAPK pathways have more in common than previously appreciated. ERK and p38 signaling feed into TORC1 signaling both up- (TSC2) and downstream (S6K) of TORC1 as well as affecting it directly (raptor). This co-ordination of two central pathways controlling growth and proliferation has a clear rational from cell point of view. How amino acids feed into this regulatory circuitry remains to be established. MAP4K3 as a kinase regulated by amino acids and affecting TORC1 and at the same time belonging to the family of MAP kinases may play an interesting role. We approached its function using genetic approach in *Drosophila*.

4.2. Results

4.2.1. Identification of the *Drosophila* MAP4K3 mutant

To analyze gene function in *Drosophila* many mutagenesis screens have been performed. One of the most popular methods is transposon mutagenesis, where a mobile genetic element is mobilized and randomly inserted in a genome (Adams and Sekelsky, 2002). If inserted into a gene or its regulatory region, an insertion can result in partial or complete mutation of a given gene. Many fly strain carrying specific insertions are available from various large-scale mutagenesis screens through fly stocks repository centers, such as Bloomington stock center (<http://flystocks.bio.indiana.edu>).

I characterized several insertions in the *Drosophila* ortholog of MAP4K3, which is a gene called CG7097 to see if any of them affects expression of the gene. Figure 24A shows the structure of a gene and its products as well as sites of transgenes insertions that I have tested. MAP4K3 is a large gene, spanning almost 50 Kb. It has 2 alternatively spliced isoforms that differ in the exon9 (isoform CG7097-RA has an alternative 5' splice site, which makes it some 800 bp longer than CG7097-RB). 3 stocks that have insertions in CG7097 were tested: P(EP)2445 which is a promoter insertion and two insertions in the intron2 – PBac(WH)CG7097(f04135) and P(lacW)l(2)SH1261. Compared to wild-type flies (strain w1118) P(lacW)l(2)SH1261 had almost no mRNA left (around 1%), while two other insertions had less dramatic decreases of mRNA level (Figure 24B). I concluded that P(lacW)l(2)SH1261 is a strong hypomorphic mutant of MAP4K3 (further named MAP4K3).

To investigate expression pattern of MAP4K3, quantitative PCR analysis was done on samples from different developmental stages and tissues of wandering 3rd instar larvae (Figure 24C). MAP4K3 is ubiquitously expressed throughout development with maximal expression levels in pupal stages and adult males. It is expressed in both proliferating (imaginal wing disc) and endoreplicative (fat body, body wall, salivary gland) larval tissues.

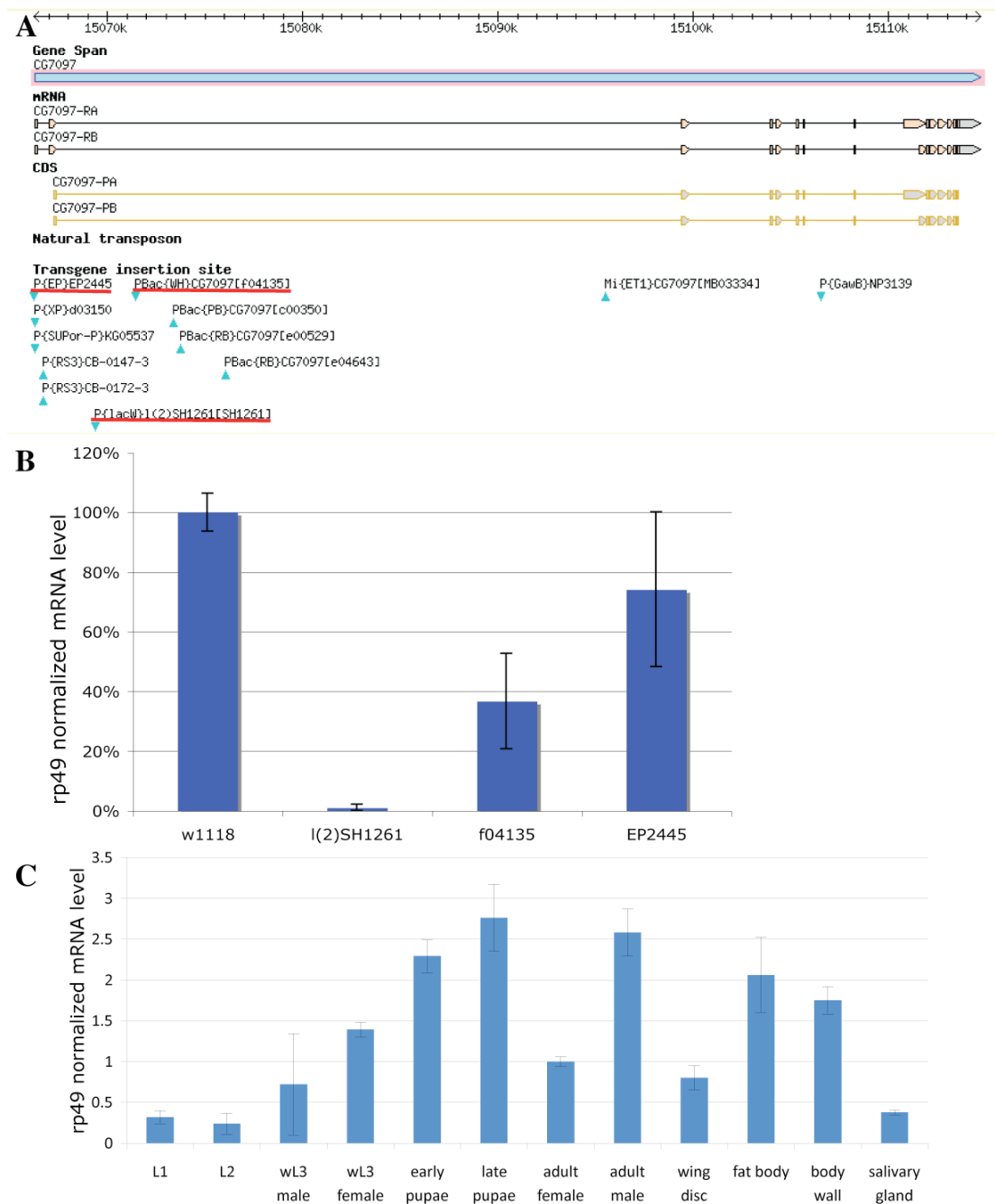


Figure 24 Genomic structure of MAP4K3, its expression in transgenic lines and developmental stages and tissues.

(A)CG7097 gene is shown in blue, mRNA transcripts in black, exons as boxes, introns as lines, coding sequence (CDS) is in yellow. Transposon insertion sites are indicated by blue triangles below. Three insertions underlined by a red line were ordered and analysed. Black scale at the top is a location on 2R chromosome arm. (B) MAP4K3 expression in transgenic lines indicated in (A). Note that I(2)SH1261 is a strong mutant. (C) MAP4K3 expression during development and in different tissues of Ore^R strain. L1 - 1st instar, L2 - 2nd instar, wL3 - wandering 3rd instar.

Interestingly, fat body had one of the highest levels of expression, suggesting a possible role in fat metabolism. Having confirmed that I(2)SH1261 is a mutant I went on to see what effects this mutation causes on the organism level.

4.2.2. Phenotypic characterization of MAP4K3 mutant

To study flies mutant for MAP4K3, I obtained flies harboring the I(2)SH1261 insertion, which was produced in a screen for lethal mutations on the 2nd chromosome (Oh et al., 2003). I initially assumed it to be lethal. Surprisingly, it turned out that it is homozygous viable and probably initial lethality phenotype was assigned because under crowded conditions very few homozygous animals survive. Under controlled growth conditions (50 animals/vial) most of the MAP4K3 mutant animals survived to adulthood, but appeared weak and many died upon hatching by getting stuck in the food (Figure 25A). There was also some pupal lethality, indicating that developmental program was compromised or perhaps the metabolic stores were not sufficient. Mutant MAP4K3 flies were fertile and produced viable progeny.

MAP4K3 has been shown to affect TORC1 activity in drosophila and mammalian cells (Findlay et al., 2007). Several mutants in the have been described in Drosophila affecting TOR pathway. Their phenotypes include lethality (dTOR itself, (Zhang et al., 2000) and rheb (Saucedo et al., 2003)), growth and metabolism (chico (Bohni et al., 1999), S6K (Montagne et al., 1999)) and , stress sensitivity (d4EBP (Teleman et al., 2005a)). Therefore, we tested MAP4K3 mutants for growth, metabolism and stress resistance.

As MAP4K3 is important for sensing amino acids in cells, we tested how MAP4K3 mutants survive under different starvation conditions. When starved (agarose with PBS) MAP4K3 mutants died faster than wild-type (wt) animals (Figure 25B). When reared on starvation medium supplemented with carbohydrates (1% Sucrose) or with amino acids (all 20 amino acids, at the concentrations equal to those in Drosophila Serum Free Medim – SFM) MAP4K3 mutants also died faster than wt flies(Figure 25C,D). Increased

starvation sensitivity could stem from lower energy stores or from increase energy expenditure (see below).

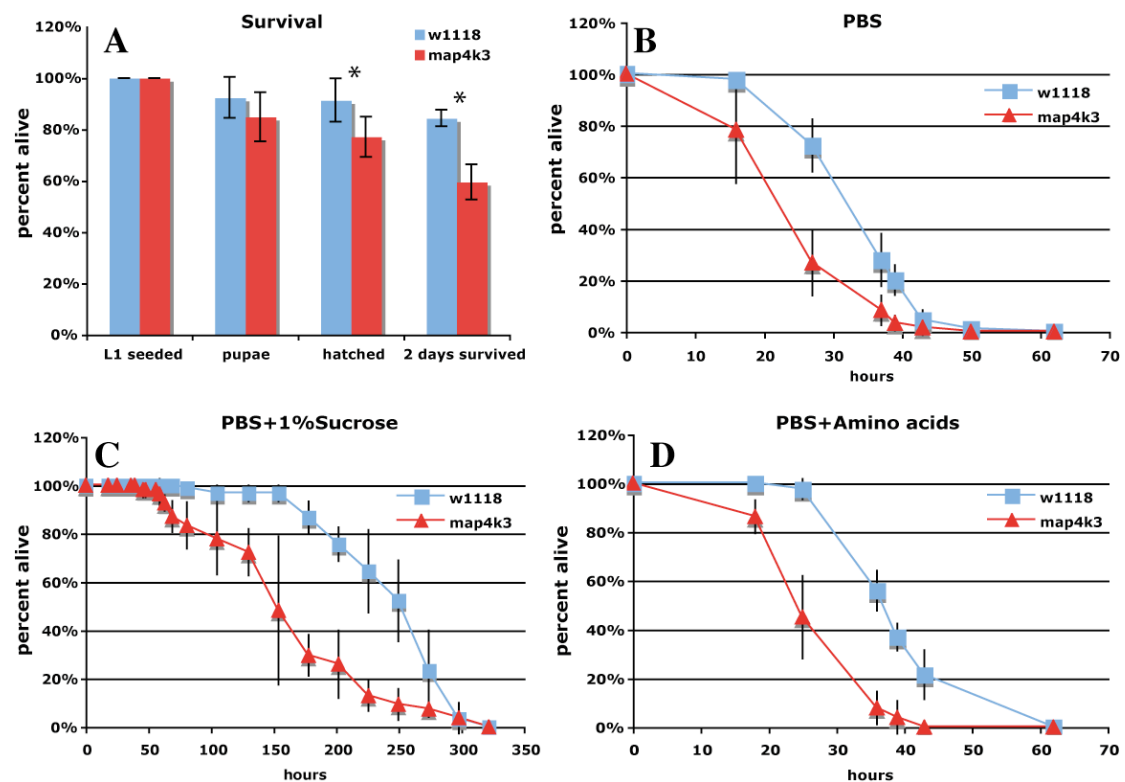


Figure 25 Survival of the MAP4K3 mutants under different conditions

(A) 50 first instar larvae (L1) were seeded into normal food and counted after reaching pupal stage, upon hatching and 2 days after hatching. (B-D) 20-30 first instar larvae were seeded into medium containing PBS (B), PBS+1% Sucrose (C) or PBS+Amino acids (D). Number of alive flies was monitored at the indicated time points. All experiments were done in triplicates. * indicates $p < 0.01$.

TOR is known to regulate cell and organ size (Oldham et al., 2000) and MAP4K3 was shown to be able to regulate size in cells (Findlay et al., 2007). I tested if MAP4K3 can regulate size *in vivo*. *Drosophila* wing is a very sensitive and well-defined system for size measurements. MAP4K3 mutants displayed a reduction in wing area, indicating that MAP4K3 is required for attaining normal organ size (Figure 26A). Final organ size is determined by the number of cells and the size of each cell. Wing cells of MAP4K3 mutant are smaller (Figure 26B), suggesting that it is the size of individual cells that results in the smaller wing. Weight measurement also hinted that MAP4K3 mutants are a bit smaller than wt, but these measurements are tricky to do and many flies

are needed, so the difference did not reach statistical significance. Thus MAP4K3 can regulate cell and organ size in *Drosophila*.

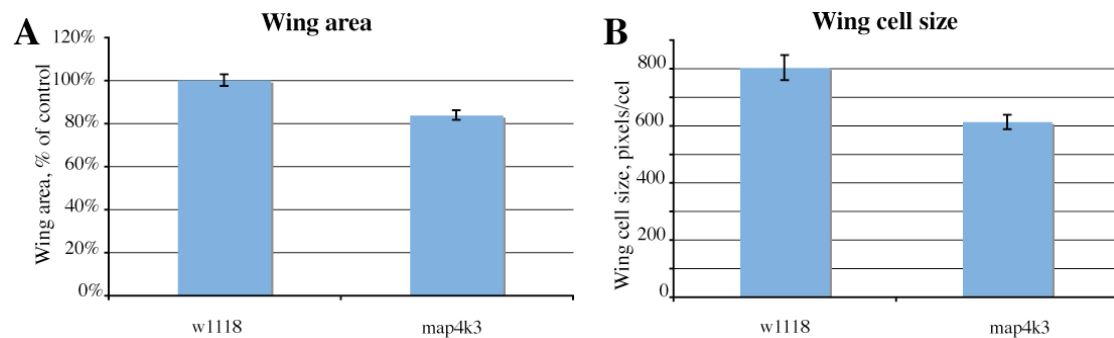


Figure 26 MAP4K3 regulates organ and cell size

(A) Wing area was measured using ImageJ software for wt and mutant male flies, grown under controlled conditions. $p=4.5 \cdot 10^{-8}$, $n=5$. (B) Cells hairs in the constant area in the posterior of the wing were counted and average cell size calculated by dividing the area by the number of cells. $p=3.1 \cdot 10^{-5}$, $n=5$.

Apart from being weak, MAP4K3 mutants develop slower than their wt counterparts. They grow slower and it takes them longer to reach pupation stage and to hatch (Figure 27A). There is quite a lot of variability in the population as evident from different sizes of mutant larvae in Figure 27C and also from the lower slope of the pupation curve (Figure 27A). While most wt animals pupate on the same day, MAP4K3 pupation spreads over a few days, reflecting heterogeneity in the population. Some animals are indistinguishable from wt while others are severely delayed. This suggests that there are other modulatory factors that in the absence of MAP4K3 modify growth rate. Interestingly, when grown on diluted (20% of normal food) MAP4K3 mutants develop at the same rate as the wt (Figure 27B). This may be surprising at the first sight, but it actually makes sense considering the role of MAP4K3 as a sensor for nutrients (amino acids). If we assume MAP4K3 functions to sense amino acids and fully activate growth, when growth is slowed down under low nutritional conditions, MAP4K3 is not active. Therefore under low nutritional conditions MAP4K3 function does not manifest itself and there is no difference between wt and mutant animals growth rate.

Metabolism is among the processes regulated by TOR (Britton et al., 2002). MAP4K3 mutant flies displayed reduced fat levels, as measured by the

amount of triglycerides, which are the main form of fat storage in *Drosophila* (Van der Horst, 2003).

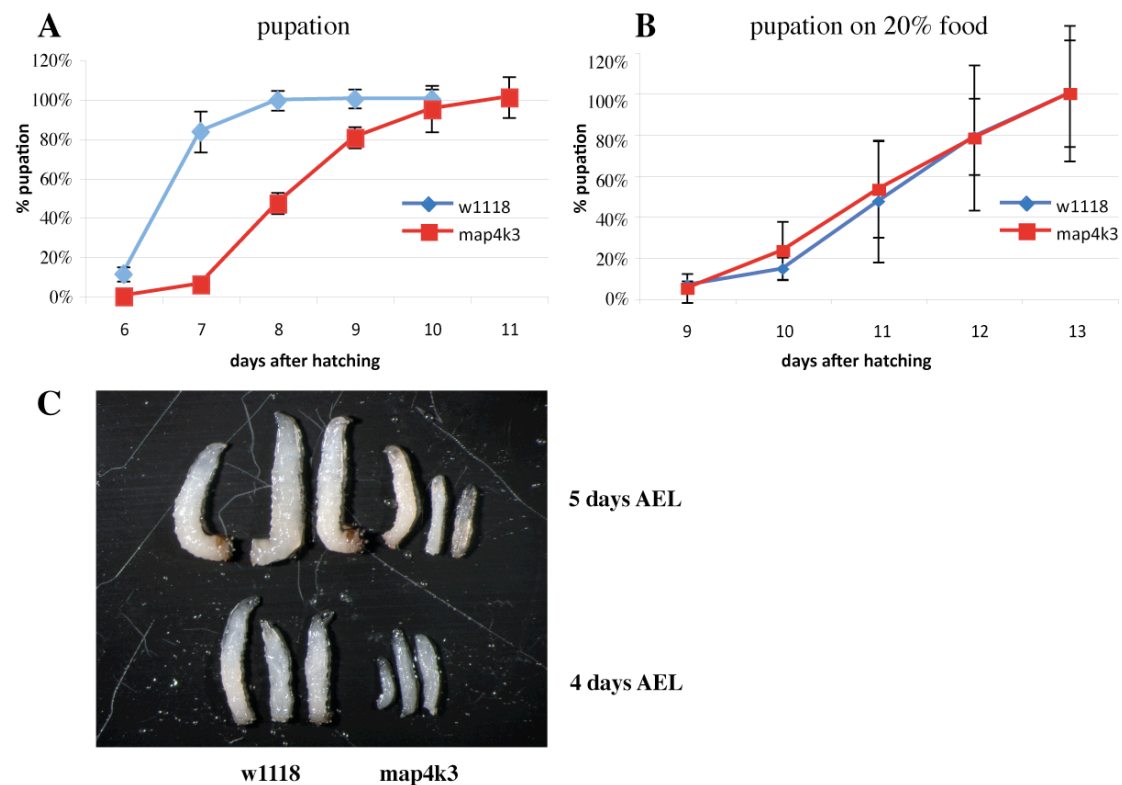


Figure 27 MAP4K3 mutant have a delay in growth

Representative pupation curve of MAP4K3 mutant compared to w1118 grown at controlled density on normal food (A) or 20% of normal food (B). (C) Examples of growth delay in 3rd instar larvae of MAP4K3 mutant (3 larvae on the right) vs. w1118 (3 larvae on the left) at 4 (bottom) and 5 (top) days after egg laying (AEL). Note the variability in size of MAP4K3 mutants.

This effect was most pronounced in adult flies (~40% reduction in 3 days old flies, up to 70% reduction in 5 days old flies) but also detectable in wandering 3rd instar larvae, although smaller in magnitude (Figure 28A,B). To make sure that the phenotype is caused by mutation of the MAP4K3 gene, we generated a precise excision of the P-element from the gene. Flies carrying I(2)SH1261 insertion were crossed to the strain carrying a transposase and in the next generation the progeny was screened for the absence of the marker gene (w^+) that is encoded by the insertion construct.

Excision of the transposon is not always a precise process, sometimes parts of the neighboring genomic sequence can be deleted as well. We verified the precision of the excision by PCR performed on the insertion site as shown in Figure 29A.

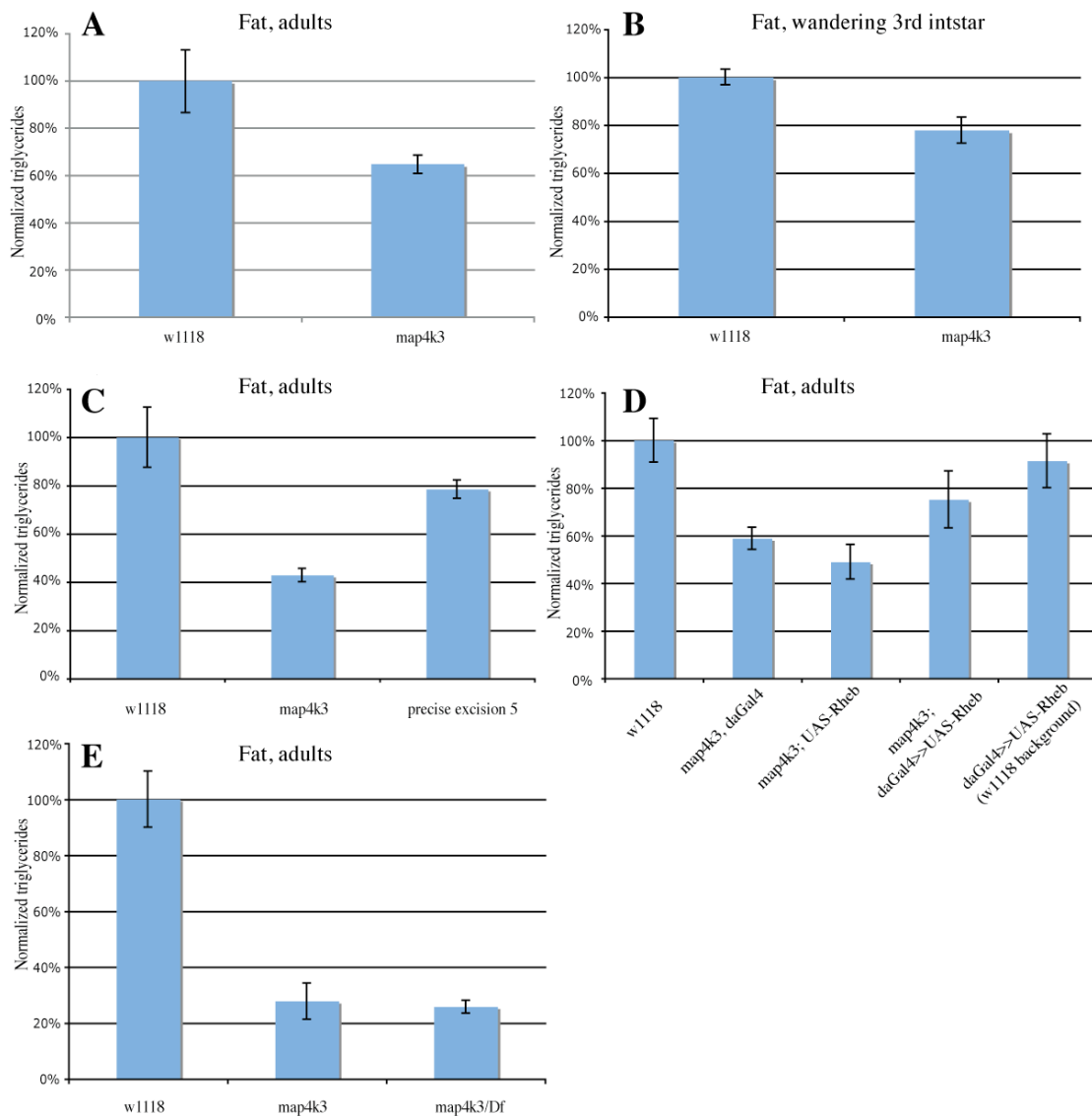


Figure 28 Fat levels are reduced in MAP4K3 mutants

Adult male flies (A,C,D) or wandering 3rd instar female larvae (B) grown under controlled conditions were homogenized and triglycerides levels measured and normalized to protein. (C) Precise excision of the P-element insertion in MAP4K3 gene rescues fat phenotype. (D) Driving Rheb ubiquitously rescues the fat at least partially. Driving Rheb in wt background does not increase fat. (E) Further reducing MAP4K3 levels by using deficiency allele Df(2R)Exel6069, does not decrease fat levels.

Out of four excision lines, two (lines 4 and 5) turned out to be precise and two imprecise (Figure 29B).

The fat phenotype is rescued by a precise excision but not completely (Figure 28C). It might be that the w1118 flies are fatter than the background in which P-element insertion was made. Another possibility is that the excision is not really precise, removing or leaving behind small number of nucleotides, which

one wouldn't see by running the PCR product on a gel, but would still affect the gene.

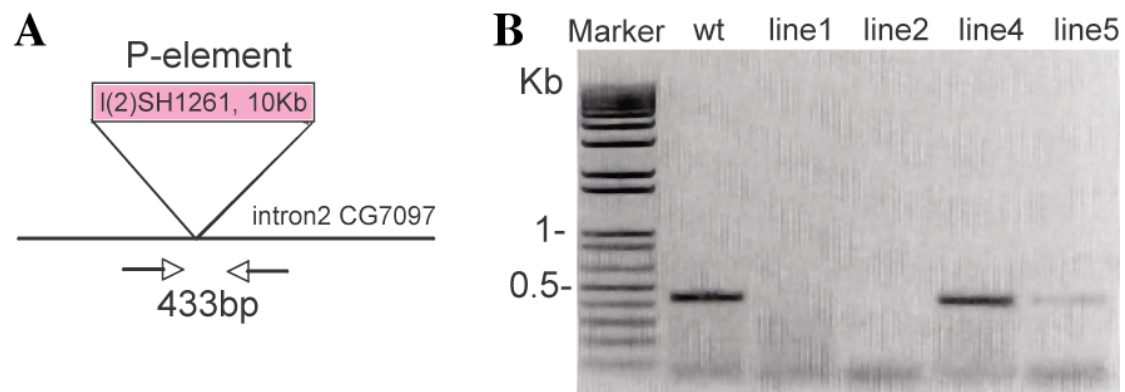


Figure 29 Excision lines test by PCR

(A) PCR design, primers spanning insertion site should produce a product of 433 bp for wt chromosome, meaning that excision was precise. (B) PCR was done on genomic DNA and resolved on agarose gel. Lines 1 and 2 are imprecise while lines 4 and 5 are precise.

If the phenotype is caused by reduced TOR signaling, as is seen in cell culture, then we would expect fat levels to be rescued via genetic manipulations that restore TOR activity. To test this, we used UAS-Rheb^{AV4} allele ((Patel et al., 2003)) to express Rheb in the MAP4K3 mutant background. Indeed, reduced levels of fat could be rescued by ubiquitous expression of Rheb, using UAS-Gal4 system that allows heterologous expression of a gene of interest in the tissue-specific manner. Driving expression under control of UAS (Upstream Activating Sequence) promoter with a Gal4 transcription factor under the control of *daughterless* promoter (ubiquitous, low level) resulted in a partial rescue of reduced fat levels (Figure 28D). This indicated that increasing TORC1 activity can restore the fat defect in MAP4K3 mutants at least partially. At the same time driving Rheb in a wt background does not make flies fatter indicating that MAP4K3 is a “sensitized” background and the rescue is specific. To assess the remaining minimal levels of MAP4K3 we made use of the deficiency deleting the gene entirely (Df(2R)Exel6069). Heteroallelic combination of MAP4K3/ Df(2R)Exel6069 should have 2-fold less MAP4K3 mRNA and still had the same fat levels as MAP4K3 mutant. This argues that the residual level of MAP4K3 are not

substantial, so that reducing it even more does not worsen the phenotype (Figure 28E).

Insulin regulates glucose and fat metabolism in mammals. Insulin-Like Peptides (ILPs) have the same function in *Drosophila*. In MAP4K3 mutant flies ILP levels are dramatically decreased (Figure 30). ILPs are responsive to nutritional conditions and go down upon starvation, suggesting that MAP4K3 mutant animals behave as if starved, even though nutrients are available. Rheb expression rescues ILP levels to some extent for two of the three measured ILPs, supporting the idea that reduced ILPs are consequences of low fat storage.

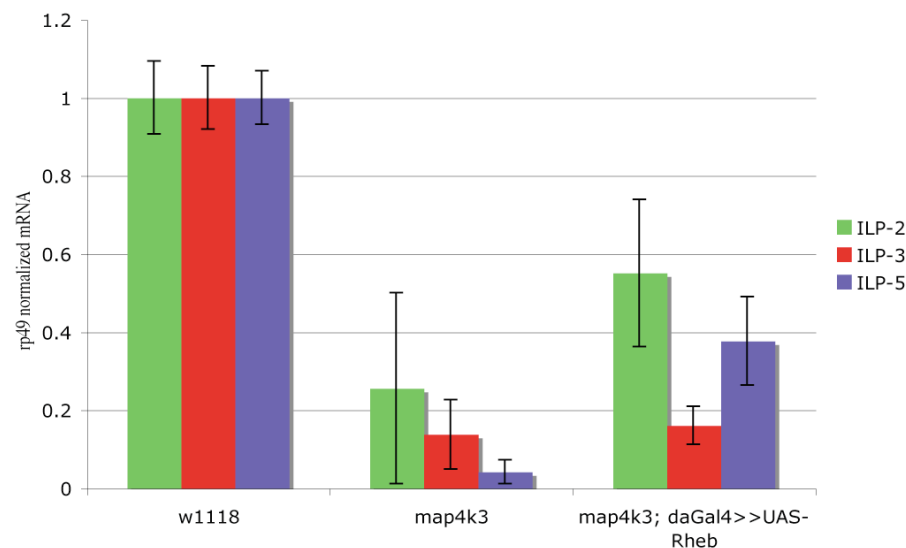


Figure 30 Insulin-like peptides are low in MAP4K3 mutants and can be partially rescued by Rheb

Quantitative PCR of Insulin-like peptides (ILP) in control, MAP4K3 mutant and daGal4>>UAS-Rheb rescue flies.

4.2.3. Overexpression of MAP4K3

Next we tested the effect of overexpression of MAP4K3, using a EP(2)2445 insertion containing UAS promoter, that can be used to activate expression with different Gal4 drivers.

Ubiquitous Gal4 drivers with strong expression turned out lethal with expression levels correlating well with lethality (Figure 31A). tubGal4 (tubulin) had highest expression and lethal at early larval stage, actGal4 (actin) had

weaker expression and partial lethality (~50-60%), while daGal4 (daughterless) had low expression similar to the wt and no lethality. Other weak drivers armGal4 (armadillo) and hsGal4 (heatshock) at 25 degrees also did not show lethality. These data imply that too much MAP4K3 product is deleterious for organism development.

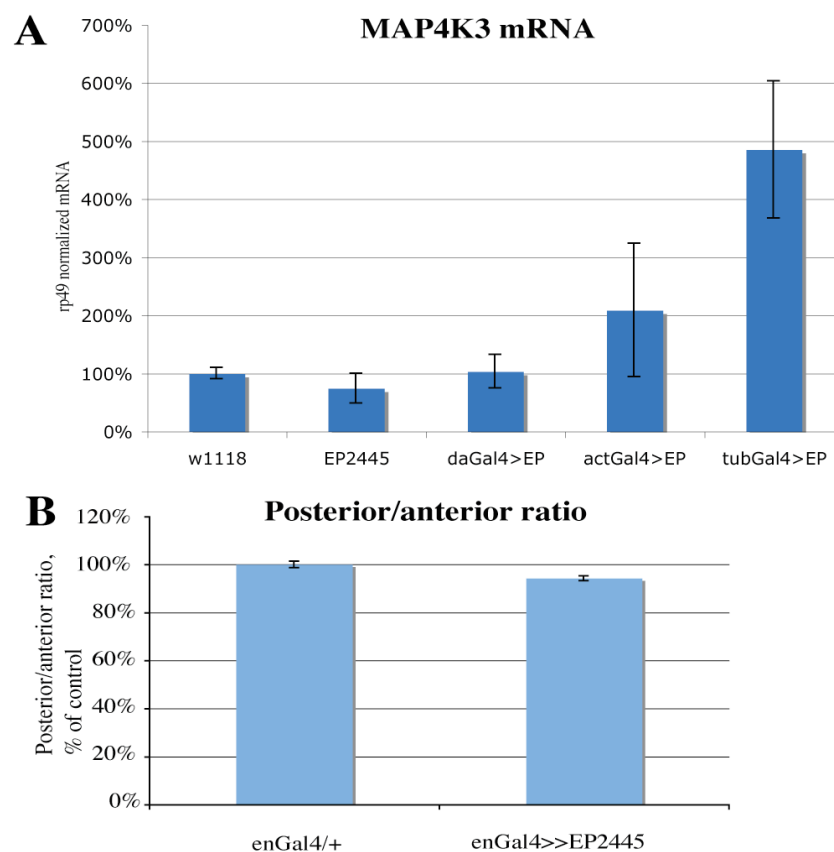


Figure 31 Overexpression of MAP4K3 with different Gal4 drivers

(A) RNA from adult flies, ectopically expressing sMAP4K3 using the EP2445 P-element insertion, was isolated and quantitative PCR on MAP4K3 performed. (B) EP2445 driving in the posterior compartment of the wing using enGal4 makes it smaller. Posterior compartment area was measured and normalized to anterior part. $p = 6.7 \times 10^{-5}$, $n=5$.

Overexpression with Gal4 driver driving expression in the specific tissues or domains such as eye (eyelessGal4) or wing (apterousGal4, nubbinGal4, patchedGal4) did not produce dramatic phenotypes. apGal4 is expressed in the dorsal part of the wing and resulted in slightly upwards curved (curly) wings but it was not highly penetrant. MAP4K3 ectopic expression in the posterior half of the wing, using engrailedGal4 (enGal4) resulted in the

decreased area of the expression compartment, suggesting reduced growth rate and/or size of the cells (Figure 31B). This could be the result of dominant-negative action on TORC1 by titrating out TORC1 activators (e.g. Rag GTPases, see below). enGal4 also caused posterior cross vein branching in some flies.

4.2.4. Genetic interactions

Since MAP4K3 was shown to affect TORC1 activity in cells, we tested if it can do so in the context of the whole organism. TSC2 mutant flies die at the early larval stage, presumably because of excess TOR activity (Ito and Rubin, 1999). We tried to rescue this lethality by combining this *gig*¹⁹² mutation with MAP4K3 mutant, which supposedly should decrease TOR activity. However, removing MAP4K3 did not rescue *gig*¹⁹² TSC2 mutant.

Rheb mutation causes developmental arrest and lethality at the first instar larval stage, because of the reduced TOR activity (Saucedo et al., 2003). We tried increasing TOR activity by overexpressing MAP4K3 in the Rheb mutant background (Rheb^{delta1/delta2}). MAP4K3 overexpression by driving EP(2)2445 with daGal4 could not rescue Rheb lethality. This is not very surprising, given that this allelic combination can only be rescued to the 2nd instar by introducing Rheb itself back (hsGal4>>UAS-Rheb (Saucedo et al., 2003)).

MAP4K3 mutant does not affect the phenotype of *chico* mutant (Drosophila ortholog of IRS), which is small size flies (Bohni et al., 1999).

Overexpression of Rheb in the dorsal side of the wing with apGal4 causes the wings to curve down, because Rheb promoting cell growth via TORC1 makes the area of the dorsal side larger, thus resulting in curved down wings. MAP4K3 mutant background cannot alter this phenotype. Taken together these results are suggesting that in the context of the whole organism MAP4K3 doesn't affect TORC1 or its effect on TORC1 is not large enough to modify phenotypes of other genes in the Insulin/TOR pathway.

4.2.5. MAP4K3 molecular mechanism

To address the mechanism of action of MAP4K3 in the whole animal, we first turned to TOR, since based on cell culture data MAP4K3 is mediating amino acids signaling to TORC1. Western blot analysis of fly protein extract to assess TORC1 activity in the mutant did not provide an insight into status of TORC1. An example of the Western blot is shown in Figure 32. TOR activity as measured by 4EBP and S6K phosphorylation for control (w1118) and MAP4K3 mutant flies, grown under controlled conditions. 4EBP phosphorylation was variable from sample to sample.

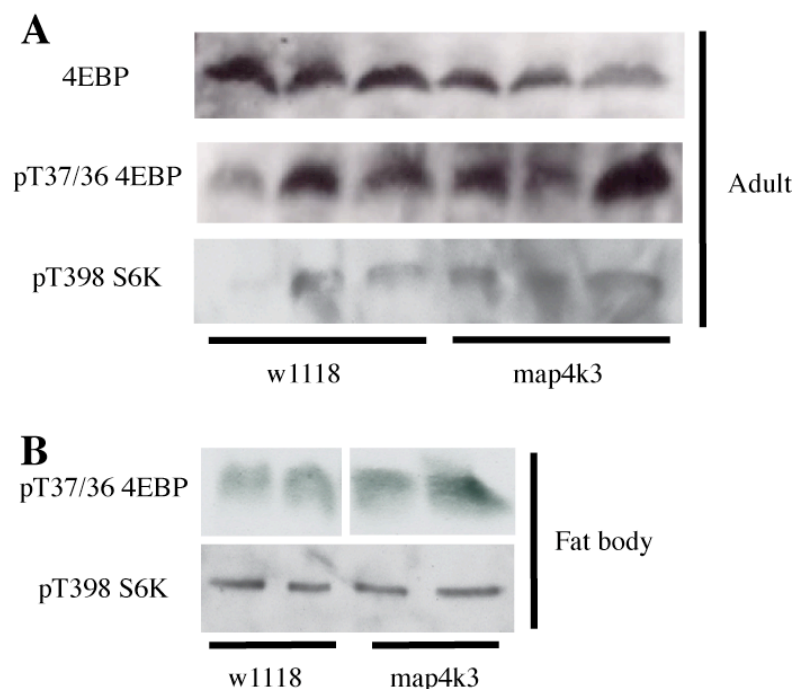


Figure 32 TOR activity in MAP4K3 mutant

(A) 10 male flies were homogenized in sample buffer and proteins were separated on SDS-PAGE and detected with indicated antibodies. (B) Pre-wandering 3rd instar larvae were dissected and fat body proteins were resolved on the SDS-PAGE and detected with indicated antibodies. Note variability in the signal of phospho 4EBP antibody.

After several trials we concluded that TORC1 activity is variable in the animals, it does not seem to be reduced, as might be expected from cell culture data. One possible reason for difficulties to define TORC1 activity is it may be different in different tissues and looking at the whole animal level is

not informative. Since MAP4K3 mutants are deficient in fat metabolism and fat body is the organ regulating fat, we asked whether TOR activity is altered in the fat body of the mutant pre-wandering 3rd instar larvae. Unfortunately, these results were also not informative, Western blot on fat body protein extracts worked badly; total 4EBP antibody failed to detect endogenous levels of 4EBP, phospho-specific 4EBP antibody varying levels in the mutant, while phospho-S6K antibody showed similar levels of active S6K in both wt and mutant (Figure 32B). Although not conclusive, these results do not support an idea of decreased TOR activity in the MAP4K3 mutant. We decided to focus our attention on genetic interactions that would provide a clue about TOR status in MAP4K3 mutants.

Recent reports connecting MAPK signaling and TORC1 raise the possibility that MAP4K3 may affect TORC1 through one or more of the MAP kinases branches. This is quite a complex question as there are 4 main branches of MAP kinases with partially overlapping inputs and outputs. MAP4K3 has been reported to activate JNK pathway (Diener et al., 1997; Shi and Kehrl, 1997), ERK has been implicated in signaling to TORC1, so I tested if these pathways are also affected by MAP4K3 in *Drosophila*. MAP4K3 knock-down by dsRNA in S2 cells resulted in the decrease in ERK and JNK activities, while MAP4K3 expression promoted their phosphorylation on activating residues (Figure 33A). Total protein for ERK and JNK was changing in a similar fashion, suggesting that the total protein levels also change, if the loading is equal. Loading is actually affected with knock-down having less total protein and MAP4K3 expression more, because knocking down MAP4K3 is decreasing cell growth and expressing it drives growth, so there are more cells in the well. Still comparing differences in loading from a background bands with differences in active ERK (pT202/204 ERK1/2) and active JNK (pT183/185 JNK), it is likely that MAP4K3 is able to regulate ERK and JNK activity and possibly protein levels in S2 cells. These results point out a possible mechanism by which MAP4K3 may affect TORC1, namely by modulation of TORC1 signaling through MAPK ERK and/or JNK branches.

Taken together, the results from *Drosophila* mutant of MAP4K3 indicate that MAP4K3 is not essential for viability, but important for optimal growth and metabolism. Surprisingly, one of its main phenotypes manifests in fat stores of the animal, highlighting the close connection between nutrient sensing and storage of fat as a main energy reserve. This is dependent on TORC1 activity because stimulating TORC1 can rescue the phenotype. Growth is affected as well, since it strongly depends on the availability of nutrients.

4.3. Discussion

4.3.1. MAP4K3 regulates growth

TOR signaling is critical regulator of growth. Flies lacking TOR arrest their growth and die as early stage larvae (Oldham et al., 2000; Zhang et al., 2000). Growth regulation by dTOR is primarily mediated by dS6K, since its overexpression can rescue TOR mutants. Phenotypes of TOR deficient animals are reminiscent of amino acids starved animals. MAP4K3 was proposed to function as a amino acid sensor, based on cell culture data and the fact that its activity is stimulated by amino acids. Our data support this notion, because in the organism MAP4K3 is regulating growth. MAP4K3 mutants develop slower than controls and have partial lethality at the pupal stage. In addition their viability is compromised as evident from lethality during the first 2 days. Furthermore, they display a small but highly significant reduction in wing size, indicating that their growth ability is compromised. Under conditions of low nutrients (20% of normal food), TOR signaling is reduced and growth is delayed. Interestingly, when TOR signaling does not need to be fully activated mutant and control animals develop at the same rate, supporting the idea that MAP4K3 is required under rich nutrient conditions to promote optimal growth.

In general phenotypes of MAP4K3 mutants are quite mild, compared to those of dTOR itself (Oldham et al., 2000; Zhang et al., 2000), dS6K (Montagne et al., 1999) or Rags (Kim et al., 2008), a new component in nutrient signaling, identified recently. All of these cause a growth arrest during the larval stages, as does amino acid starvation itself. Thus MAP4K3 is probably not a critical component of the amino acids sensing but rather has a modulatory role, providing maximal TORC1 activation under favorable conditions. Alternatively, we cannot exclude the possibility that the mutant we have analyzed is not a complete loss of function and the remaining 1 percent of mRNA is enough to provide residual function of the gene. The fact that further reducing the levels of MAP4K3 by half using a deficiency does not worsen the phenotype argues against this possibility.

MAP4K3 function, although not crucial for individual animal viability, has an important function for species survival. This is elegantly demonstrated by the fact that I(2)SH1261 insertion was isolated in a screen for mutations on chromosome 2 and was reported to be lethal (Oh et al., 2003). This happened most probably because under normal culturing conditions with competition between individual animals, homozygous mutants do not survive because they are slower and weaker heterozygous pals. In evolutionary sense, a gene providing a small competitive advantage (for example shorter developmental time) can be as important as a gene absolutely required for viability of the organism. In a real world, outside research lab, with fierce competition for limited resources, it is only a matter of a few generations until the progeny carrying a mutation in such a gene is extinct. That is probably the reason why these, seemingly “dispensable”, genes are conserved in evolution just as “viability” genes.

4.3.2. MAP4K3 affects fat metabolism

Growth is metabolically expensive process, a cell has to generate biomass and this requires energy and building blocks for protein and membrane synthesis (Edgar, 2006). Thus it is not very surprising that TOR as a regulator of growth also affects and is affected by metabolism. Both classical TOR effectors S6K and 4EBP have metabolic phenotypes in knockout animals: mutant S6K1 mice are protected from diet-induced obesity (Um et al., 2004), while 4EBP1 knockout mice are lean, hypoglycemic and have altered fat metabolism (Tsukiyama-Kohara et al., 2001). In addition, fly 4EBP mutants are starvation sensitive and lose fat faster under starvation (Teleman et al., 2005a). Low TOR activity in hypomorphic dTOR allele has been shown to be associated with reduced fat levels and reduce glucose levels (Luong et al., 2006).

Insulin regulates carbohydrates and lipid metabolism in response to nutrients. Although glucose homeostasis is most often associated with insulin, it is only one of many insulin-regulated processes. These also include synthesis and storage of fat, protein synthesis, and non-metabolic processes such as cell growth and differentiation (Biddinger and Kahn, 2006). Different tissues

respond in a different way to insulin. In response to high levels of glucose (fed conditions) insulin promotes glucose uptake by muscles. Liver responds by increasing glycogen synthesis and decreasing gluconeogenesis. Adipose tissue responds by promoting lipogenesis for fat storage and reducing lypolysis, that releases free fatty acids. Thus phenotypes of loss of function studies in the whole organism are difficult to predict and the outcome depends on the combination of effects from different tissues. For example insulin receptor substrate mutant *chico* flies are fat (Bohni et al., 1999), while hypomorphic dTOR mutants are lean (Luong et al., 2006). Systemic reduction in the insulin signaling has been associated with elevated lipids levels (Bohni et al., 1999; Broughton et al., 2005), while insulin signaling reduction in adipose tissue leads to the opposite, as is the case for FIRKO (fat insulin receptor knockout) mice (Bluher et al., 2002).

MAP4K3 mutants are lean and this phenotype can be rescued by driving Rheb, indicating that reduced TORC1 activity accounts for this phenotype. Fat body is the main site of adipose tissue and fat metabolism regulation. It is plausible that low TOR activity in fat body could mimic starvation, leading to inhibition of lypogenesis and activation of lypolysis, resulting in low fat stores. MAP4K3 mutants' phenotype are in accordance with low TOR activity and show similarity to FIRKO mice and flies with low TOR. Low ILPs are also consistent with low glucose reported for flies with reduced TOR (Luong et al., 2006). Furthermore, rescue of the fat phenotype by increasing TOR with Rheb overexpression is accompanied by a partial rescue of ILP levels. This suggests that low ILPs in the MAP4K3 mutant are the consequences of low fat levels and when those are normalized ILPs also recover. Alternative scenario where the the phenotype is caused by a defect in ILP production is not likely, because flies with ablated ILP producing cells are not lean but rather have slightly higher lipids (Broughton et al., 2005).

4.3.3. TOR activity status and possible mechanism

How is MAP4K3 acting in molecular terms? I tried to approach this question with biochemical and genetic approaches. Biochemical data from mutant flies did not provide a definitive answer as TORC1 activity, measured by

phosphorylation of 4EBP and S6K was variable (Figure 32). Although variable it did not appear to be reduced, as might be expected from cell culture data (Findlay et al., 2007). It was also possible that tissue specific effect of MAP4K3 reduction was not strong enough to be detected in the whole animal extracts. Fat body is a good candidate for tissue specific effects of MAP4K3, because it is the organ, whose function is to store fat and regulate fat metabolism (Colombani et al., 2003). We didn't see a change in TOR activity in fat body, although the analysis was complicated by the absence of total S6K antibody and poorly working total d4EBP antibody. Interestingly, TOR activity is also not changed in chico mutants (measured by S6K activity). Moreover, S6K protein levels are increased in dTOR mutant or by starvation, suggesting that S6K protein level in addition to activity are regulated by amino acids (Oldham et al., 2000). All this makes interpretation of biochemical data more difficult, especially given the lack of total S6K antibody.

Since I could not obtain clear data from biochemistry, I used genetic approach to ask whether MAP4K3 can interact with other genes in the Insulin/TOR pathway. Most of the genetic interaction I tried (Rheb, TSC2, chico) did not succeed. This could mean that MAP4K3 does not change TOR activity *in vivo* or alternatively that its effect on TOR is not as strong as those of the other genes tested. Indeed the phenotypes of Rheb and TSC2 genes are lethality and chico also has a strong effect on survival and size, while MAP4K3 phenotypes are relatively mild. Thus it may not be surprising that MAP4K3, whose effects are more modulatory in nature cannot change the dramatic phenotypes of critical TOR regulators. On the other hand, Rheb expression can efficiently rescue lean phenotype of MAP4K3 mutants. This suggests that most of the phenotypic effect of MAP4K3 mutant comes from reduced TOR activity. It would be interesting to see if driving Rheb in the fat body can rescue MAP4K3 phenotype.

I have started to look into the mechanism of action of MAP4K3 but did not have time to address this issue in detail. From belonging to the family of MAP kinase regulator it is tempting to speculate that MAP4K3 can affect TOR through activation of one or more branches of MAPK signaling. Indeed, initial experiments showed that MAP4K3 expression can activate ERK and JNK kinases and possibly affect their protein levels. This fits very well together with

recent report implicating ERK and p38 MAPK signaling branches in amino acid signaling to S6K (Casas-Terradellas et al., 2008). In addition ERK-activated RSK kinase has been shown to regulate TORC1 activity directly by activating phosphorylation on raptor (Carriere et al., 2008).

Another possible avenue for exploring mechanistic mode of action of MAP4K3 is to look for possible interacting proteins. Since MAP4K3 has a conserved GTPase regulating domain, it may interact with a small GTPase. We could not detect interaction with Rheb, suggesting Rheb is not an effector of MAP4K3, although not all transient interactions are detectable by immunoprecipitation. Rag GTPases have been independently identified by two groups and established as mediators of amino acids sufficiency in mammalian cells and *Drosophila* (Kim et al., 2008; Sancak et al., 2008). Rag GTPases function as a heterodimer and can bind to TORC1 and regulate its activity towards S6K following amino acids stimulation. Four Rag proteins exist in mammals (RagA, RagB, RagC, and RagD). RagA and RagB are very similar to each other and are orthologs of budding yeast Gtr1p, whereas RagC and RagD are similar and are orthologs of yeast Gtr2p. In yeast and in human cells, the Rag and Gtr proteins function as heterodimers consisting of one Gtr1p-like (RagA or RagB) and one Gtr2p-like (RagC or RagD) component (Hirose et al., 1998; Nakashima et al., 1999; Sekiguchi et al., 2001). Amino acids stimulate binding of Rags to raptor and promote TORC1 activity. Our preliminary data show that MAP4K3 can interact with Rags. This strongly suggests that it can modify their activity either by regulating their interactions with raptor and thus TORC1 or by regulating their GTPase activity. We are in the process of testing this hypothesis.

4.3.4. Metabolism and growth, a close relationship

MAP4K3 is a protein conserved in mammals and it is interesting if its function is also conserved. This is likely to be the case because mammalian cell culture work has shown human MAP4K3 also regulates TORC1 and cell size. These data agrees well with this work, but metabolic effects of MAP4K3 will have to be confirmed in a mammalian system. This is of interest because of the therapeutic potential of MAP4K3 as a metabolic regulator.

In general, this work exemplifies the utility of whole organism studies and complementarity of cell culture and model organism studies. It would be very difficult to discover metabolic phenotypes in the cell culture system. I would also like to argue that metabolic aspect of the MAP4K3 phenotype is a causal one and the growth aspect is a consequence of the metabolic deficiency. Growth is a final result that is easy to measure and is by its nature a very convenient visual phenotype. However, it is dependant on adequate supply of building blocks and energy to fuel accumulation of biomass. MAP4K3 mutants have a metabolic defect that does not allow them to accumulate normal amounts of adipose tissue and this may be the reason why they have mild growth defects. The literature presents TOR as a critical controller of growth and its role in metabolism is also well established (Harris and Lawrence, 2003; Hay and Sonenberg, 2004; Wullschleger et al., 2006). Growth and metabolism are two processes regulated by TOR, but the link between them is not always evident. Although TOR is a “classical” growth regulator, the exact mechanism of growth control remains elusive. TOR controls translation through 4EBP and ribosome biogenesis through S6K, thus regulating protein synthesis that is required for growth. However, looking closer at the data reveals some interesting facts. Firstly, 4EBP loss of function studies show that growth is normal in flies and mice lacking 4EBP; instead metabolism is deregulated (Teleman et al., 2005a; Tsukiyama-Kohara et al., 2001). Moreover, recently the theory of TOR control of translation of 5' tract of oligopyrimidine (TOP) mRNAs, thought to be important for growth, was challenged (Pende et al., 2004; Ruvinsky et al., 2005). In S6K1/S6K2 double knockout mice cells 5' TOP mRNAs were still responsive to mitogen signals and S6 protein was still phosphorylated on some residues by a MAPK pathway (Pende et al., 2004). Moreover in mice with knock-in of S6 protein with all its S6K phosphorylation sites mutated to alanines, translation of 5' TOP mRNAs is not affected. Interestingly, these mice in addition to growth defects suffer from diminished levels of pancreatic insulin, hypoinsulinemia, and impaired glucose tolerance (Ruvinsky et al., 2005). These results taken together with our findings in the MAP4K3 mutant flies suggest a general

model of metabolism deregulation underlying growth defects. This hypothesis can be put to the test by future studies.

In summary, this work identifies the physiological function of MAP4K3 in modulating growth during development and regulation of fat metabolism in *Drosophila*. We propose that it enables optimal activation of TORC1 in response of sufficient nutrients levels. Molecular mechanism most likely involves modulation of TORC1 activity and may involve inputs from MAPK pathway and/ or Rag GTPases. Given a role of MAP4K3 in fat metabolism and growth it may represent a new target for treatment of metabolic diseases such as obesity and diabetes and possibly for growth deregulated conditions such as cancer. It remains to be seen if MAP4K3 role in fat metabolism and growth is conserved to mammals as it may represent a new target for treatment of metabolic diseases and cancer.

5. Conclusions

The work presented in this thesis attempts to improve our understanding of how cells sense and coordinate external cues to grow and maintain energy homeostasis in a changing environment. To this end I tried developing a new tool to visualize TORC1 activity in cells and characterized an *in vivo* function of a new component in a nutrient sensing pathway in *Drosophila*.

Developing a FRET-based probe for TORC1 activity proved to be a challenging task. Although a number of approaches have been tried, including intramolecular and intermolecular FRET, several cell lines tested and various FRET detection methodologies implemented, we could not obtain a working FRET probe. The major difficulty I encountered, was abolishment of the biological regulation of the FRET probe compared with the regulation of the endogenous protein, because of the fusion to relatively large GFP domain/s. This is a general problem of introducing non-natural fusion protein into cells but I managed to overcome this obstacle by employing an *in vivo* labeling method utilizing a small tag. This probe was shown to be functional but produced no reliable FRET signal, when introduced into cells, even though several alternative fluorophore positions were tested. The reasons for FRET absence could include unfavorable orientation of fluorophores, differences in brightness or concentrations of the interacting partners. In conclusion, 4EBP1 does not seem to be a good starting point for FRET probe development, because of its small size and sensitivity to fusions and also because of lacking of defined three-dimensional structure that would allow rational probe design. MAP4K3 mutant analysis in *Drosophila* was performed and its functional significance on the level of the whole organism assessed. MAP4K3 is not crucial for individual animal viability, but it affects growth and development. Lacking MAP4K3 makes animals grow slower and attain smaller final size. This is most probably because the mechanism sensing nutrients is compromised, which manifest itself in reduced fat stores and altered insulin-like peptide levels. This deficiency can be rescued by increasing TORC1 activity, confirming a role of TORC1 as a main effector of MAP4K3. Molecular mechanism of MAP4K3 action is not yet clear but it may involve modulation of

MAP kinase signaling or function of Rag GTPases. These findings confirm a role for MAP4K3 in nutrients sensing and control of growth and metabolism and lay a foundation for further investigation of its function under normal and disease conditions.

6. Outlook

The ultimate level of understanding a complex biological system is its modeling *in silico*, which provides explanation of experimental data and prediction for manipulations. For modeling of TOR pathway we need more data that has to be quantitative and also dynamic. FRET sensors supply data in a temporal and spatial resolution, which is difficult to obtain otherwise. My attempts to generate a TOR FRET probe demonstrate many challenges that are associated with this approach. Nevertheless, many options for future development still exist. Methods for FRET detection are improving as well a palette of genetically encoded and synthetic fluorophores (Chudakov et al., 2005). TOR substrates other than 4EBP can be used as a starting point of probe development, one candidate could be S6K.

Alternative strategies can be considered, for example Rags proteins are small GTPases and their binding to TOR is dependent on GTP loading (Kim et al., 2008; Sancak et al., 2008), (unlike Rheb, whose binding is not dependent on GTP/GDP). Lots of experience has been accumulated for designing FRET probes for small GTPases (Aoki et al., 2008; Itoh et al., 2005; Mochizuki et al., 2001; Yoshizaki et al., 2003), which can be used to generate Rags-based probes.

MAP4K3 function analysis opens a lot of possibilities to extend the data presented here. More phenotypic data can be collected to characterize specific defects of the phenotype. Autophagy is among the most conserved phenotypes of amino acid starvation and it has not yet been looked at. More complete metabolic analysis (levels of sugars, etc) should be performed to figure out what is the mechanism of fat reduction in MAP4K3 mutants. Given conservation of MAP4K3 protein it is interesting if it controls metabolism in mammals.

Molecular mechanism also warrants further investigation. How MAP4K3 fits in the MAPK network and what is the significance of MAPK signaling in amino acid stimulation of TORC1 and its downstream effectors? Interaction with Rag GTPases is another lead. It has to be clarified how MAP4K3 affects Rags function. Additionally, MAP4K3 is a kinase, so what is its substrate/s? Is it

itself regulated by phosphorylation like many kinases in signaling cascades?
How exactly do amino acids affect MAP4K3 activity? In other words there is
still a lot to do 😊

7. Materials and Methods

7.1. Chemicals and solutions

Standard chemicals were purchased from Sigma-Aldrich AG (Steinheim, Germany) or Merck (Darmstadt, Germany).

Kits for DNA purification were purchased from Qiagen GmbH (Hilden, Germany).

Competent cells (XL1-Blue) were prepared by Eva Loeser in Cohen lab.

All buffers and chemical solutions, unless otherwise stated were prepared with sterile double distilled water, according to the standard molecular biology protocols (Maniatis et al., 1989), and filter sterilized.

7.2. Molecular biology and cloning

DNA primers and oligonucleotides were purchased from Sigma-Aldrich AG (Steinheim, Germany). Enzymes for recombinant DNA work were purchased from New England Biolabs (Ipswich, USA) or Fermentas (St. Leon-Rot, Germany).

Kits for purification of plasmid DNA, as well as for purification of PCR and restriction products, were used according to the protocol of the supplier. Restriction and ligations for cloning were performed using reagents from New England Biolabs and standard molecular biology protocols (Maniatis et al., 1989). DNA sequencing was performed by EMBL genomics core facility.

7.3. Plasmids

Plasmids described in this thesis are listed in Table 7.1, including source of the original vector backbone. Restriction sites used for cloning the insert are indicated, where necessary.

For FIAsh labeling tetracycline tag was introduced into 4EBP1 coding sequence either at N- or C-terminus by PCR using oligos containing tag and the PCR product was cloned into pcDNA3 vector. All final constructs were verified by sequencing. A list of oligonucleotides, used for cloning and PCR is provided in the Appendix.

Table 7.1 List of plasmids generated in this thesis

Name	Vector backbone	Insert	Restriction sites used for cloning	Original Vector Backbone Source
pBB14	pcDNA3.1	ECFP-Citrine	Starting point for cloning	from Bastiaens lab, EMBL
pBB15	pcDNA3.1	ECFP	Starting point for cloning	from Bastiaens lab, EMBL
pBB16	pcDNA3.1	monoECFP	Starting point for cloning	from Bastiaens lab, EMBL
pBB18	pcDNA3.1	ECFP-h4EBP1	made by removing Citrine from pBB19	from Bastiaens lab, EMBL
pBB19	pcDNA3.1	ECFP-h4EBP1-Citrine	BamHI- BglII	from Bastiaens lab, EMBL
pBB20	pcDNA3.1	h4EBP1-Citrine	made by removing ECFP from pBB19	from Bastiaens lab, EMBL
pBB21	pcDNA3	heIF4E	EcoRI-NotI	Cohen lab plasmid collection
pBB24	pEYFP-Clontech	YFP-dummy-GFP ²	Starting point for cloning	from Schultz lab, EMBL
pBB25	pEYFP-Clontech	mYFP-dummy-mGFP ²	Starting point for cloning	from Schultz lab, EMBL
pBB28	pBB24	h4EBP1	NcoI-BamHI	from Schultz lab, EMBL
pBB29	pBB25	h4EBP1	NcoI-BamHI	from Schultz lab, EMBL
pBB42	pcDNA3	4Cys-h4EBP1	EcoRI-NotI	Cohen lab plasmid collection
pBB43	pcDNA3	h4EBP1-4Cys	EcoRI-NotI	Cohen lab plasmid collection
pBB47	pBB15	heIF4E	EcoRI-XhoI	from Bastiaens lab, EMBL
pBB48	pBB15	heIF4E	KpnI-BamHI	from Bastiaens lab, EMBL
pBB49	pBB16	heIF4E	EcoRI-XhoI	from Bastiaens lab, EMBL
pBB50	pBB16	heIF4E	KpnI-BamHI	from Bastiaens lab, EMBL
pBB51	pUAST	MAP4K3	NotI-XhoI	Cohen lab plasmid collection
pBB53	pMT3b	MAP4K3	NotI-SalI	Cohen lab plasmid collection
pBB55	pOT2	MAP4K3 cDNA	EcoRI-XhoI	Drosophila Genomics Resource Center (DGRC)
pBB59	pMT3b	MAP4K3-HA	HA-tag is in NheI site	Cohen lab plasmid collection
pBB60	pMT3b	dRagA	NotI-XhoI	Cohen lab plasmid collection
pBB61	pMT3b	FLAG-dRagA	FLAG is in NotI	Cohen lab plasmid collection
pBB62	pMT3b	dRagC	NotI-XhoI	Cohen lab plasmid collection
pBB63	pMT3b	FLAG-dRagC	FLAG is in NotI	Cohen lab plasmid collection

7.4. PCR, RT-PCR and quantitative real-time PCR

Genomic DNA extraction for I(2)SH1261 P-element excision mapping:
Collect 10 adult flies in an eppendorf tube kept on ice. Crush flies in 100 μ l of Homogenizing Buffer (0.1 M Tris-HCl pH9.0, 0.1 M EDTA, 1 % SDS) using plastic pestle until no more large pieces of cuticle can be seen. Incubate samples at 65°C for 30 minutes, and then add in 22.5 μ l of 5 M KOAc and chill samples on ice for 30 minutes. Centrifuge samples for 10 minutes at 4°C and transfer supernatant to a new eppendorf tube. Add in 60 μ l of Isopropanol and incubate for 5 minutes at room temperature. Centrifuge again for 5 minutes at room temperature. Wash pellet with 1 ml of 70 % EtOH and air-dry pellet at room temperature. For PCR reactions afterwards, I resuspended pellet in 50 μ l of sterile distilled water instead of TE Buffer (10 mM Tris adjusted to pH8.0 with HCl, 1 mM EDTA). I also added in DNase-free RNase A at a final concentration of 10 μ g/ml to eliminate ribosomal RNA. Heating up to 65°C may help dissolve the pellet if necessary. Measure concentration in Nano-Drop spectrometer to assess the yield. Store DNA samples at -20°C.

7.4.1. PCR reaction

The PCR reaction was carried out in volume of 25 μ l and contained 1 μ l of extracted genomic DNA as amplification template, 1.25U Taq DNA polymerase (Roche), 1x PCR Buffer containing MgCl₂ (Roche), 0.2 mM dNTPs (PCR grade, Roche), 0.4 μ M of forward and reverse primers, and sterile distilled water. The PCR reaction was running on Thermal Cycler (PTC-200, MJ research) according to the following program:

Step 1 94°C for 3 minutes

Step 2 94°C for 30 seconds

Step 3 55 or 60°C for 30 seconds (depend on the T_m values of primers)

Step 4 72°C 30 seconds to 1 minute (depend on the length of the product)

Step 5 Repeat step 2-4 for 29 times

Step 6 72°C 10 min

Step 7 End at 4°C

The amplified products were separated by electrophoresis on 0.8 – 1.5 % agarose gel and visualized by Ethidium Bromide staining and UV light.

7.4.2. RNA isolation

Collect 5-10 adult flies or larvae into 1.5 ml eppendorf tube and keep on ice. Homogenize samples with 200 µl of TRIzol reagent (Invitrogen) first with plastic pestle until no more large pieces of cuticle can be seen. Rinse the pestle with additional 800 µl of TRIzol and kept samples at room temperature for 5 minutes. For cell sample, lyse by pipetting cells up and down several times in 1 ml of TRIzol and keep it standing for 5 minutes at room temperature. Then, add in 200 µl of Chloroform and vortex samples for 15 seconds. Incubate samples at room temperature for 15 minutes before a centrifugation at 14000 rpm at 4°C for 15 minutes. I carefully took the aqueous phase (top layer) into a new eppendorf tube and added in 500 µl of Isopropanol for precipitation RNA. Incubate samples at room temperature for 10 minutes, followed by a 15 minutes centrifugation at 4°C. Wash pellet with 75 % Ethanol (in RNase-free water) and dry pellet at room temperature for 15 minutes. Dissolve pellet in 50 µl of RNase-free water. Heating up to 60°C helps dissolve RNA into water if necessary. Store RNA samples at -80°C.

7.4.3. First-strand cDNA synthesis – Reverse Transcription

First-strand cDNA for PCR reaction was synthesized by reverse transcriptase using SuperScript II or III first-strand synthesis system (Invitrogen). Mix 1 µg RNA with oligo(dT) and dNTPs in a volume of 10 µl and heat up to 65°C to denature secondary structures of RNA, and then place them on ice for 1 minute. Prepare reaction mixture composed of reaction buffer, MgCl₂, DTT, RNase inhibitor, and SuperScript™ II RT and add 10 µl

of reaction mixture to each RNA/primer mix. Incubate samples at 42°C for 50 minutes. Terminate the reactions at 70°C for 15 minutes, and then chill them on ice for the next procedure or store them at -20°C.

7.4.4. PCR reaction on cDNA

As described in Section 7.4.1, only the PCR reaction was carried out using 2 µl of synthesized cDNA as amplification template instead.

7.4.5. Quantitative real-time RT-PCR

RNA isolation and first-strand cDNA synthesis:

RNA isolation and cDNA synthesis were performed as described in sections 7.4.2 and 7.4.3 for RT-PCR. Because the cDNA:RNA hybrid molecule decreases the sensitivity of real-time PCR reaction from cDNA templates, I added one more step to eliminate RNA template in cDNA samples with RNase H for 20 minutes at 37°C before proceeding to the PCR reaction.

Primers used for quantitative real-time RT-PCR

Primer pairs were designed on Oligo 6.0 software. Several criteria were used to select the primers for quantitative real-time PCR: about 20 nucleotides in length, annealing temperature of 58-60°C, GC content of 20-80%, in general with no more than two G or C residues among the last five bases at the 3' end. The PCR products had to be 100-150 base pairs long to minimize PCR cycle time, and no primer-dimers were predicted to be sure that the SYBR green dye incorporation was only due to the specific amplicon. If possible, intron spanning primer pairs were designed or one of the primer pair was designed on exon junction of the coding sequence by spanning 5-7 nucleotides on the next exon at the 3' end of the oligo so that the PCR product is only specific to cDNA template rather than contaminated genomic DNA. A primer pair specific to *Drosophila* ribosomal protein 49

(*rp49*) were used for normalization. Prior to real-time PCR, primer pairs were tested by conventional PCR using *Drosophila* cDNA to confirm that only one single amplicon at the right size was produced from cDNA template. Standard curves were run for each of the gene-specific primer pair to test for their efficiency in real-time PCR.

Real-time PCR

Real-time PCR is performed by monitoring the progress of the PCR as it occurs; therefore data is collected throughout the PCR process, rather than at the end of the PCR. It makes use of SYBR Green I dye which binds to any double-stranded DNA to detect PCR product as it accumulates during PCR. The reaction volume was 25 μ l containing 12.5 μ l 2X SYBR Green PCR Master mix (Applied Biosystems), 250 nM of each gene-specific primer, and diluted cDNA template which corresponds to 0.1 ng of the original total RNA. Reaction mixtures containing water, instead of the cDNA template, were used to check cross-reaction contamination. The reactions were run in a 96 well plate on an ABI Prism 7000 SDS according to the following program:

Stage	Cycle	Temperature	Time
1	Hold	50°C	2 min
2	Hold	95°C	10 min
3	40 cycles	95°C	15 sec
		60°C	1 min

Later I used LightCycler[®] 480 (Roche) using the same program and Master Mix but the reaction was scaled down to 10 μ l. Analysis was done using a The LightCycler[®] 480 Relative Quantification Software.

Quantification of gene expression

Real-time PCR results were analyzed using the ABI Prism SDS software. Firstly, I checked the dissociation curve of each run in order to make sure the CT (threshold cycle) was specific to amplicon rather than primer-dimers.

Secondly, I manually adjusted the baseline to the beginning of the amplification and threshold to the exponential phase of the amplification curve. Thirdly, all quantitations were normalized to an endogenous control (*rp49*) to account for variability in the initial concentration of the total RNA. It also takes it into account the quality of the total RNA and the conversion efficiency of the reverse transcription reaction. Finally, gene expression can be measured by the quantification of cDNA converted from mRNA corresponding to this gene relative to a calibrator samples. By this relative quantification, I could determine the fold change of mutant flies (experimental samples) to the wild type flies (calibrator sample) for all the normalized target cDNAs levels.

7.5. Western blot

Sample preparation

For cell samples, cells were lysed in 200 μ l of 1x Laemmli Sample Buffer. For whole larvae or adults extract, total protein was obtained by crushing 4-10 larvae or adults in 100 μ l of 1x Laemmli Buffer with plastic pestle. Boil samples at 95°C for 5 minutes and load 10 μ l in SDS-polyacrylamide gel.

Tissue samples were obtained by dissecting of fat body in cold *Drosophila*-SFM medium (Gibco) prior to lysing in 50 μ l of Lysis Buffer. Fat body samples were lysed by pipetting several times in Lysis Buffer on ice. Usually 10 μ l were loaded onto a gel, if necessary amount of sample was adjusted to achieve same amount protein loading.

Electrophoresis and blotting

- Make SDS-Polyacrylamide gel using mini-gel module (165-3302, Bio-Rad)
- Load 10 μ l of samples and one lane of protein size marker (161-0374, Bio-Rad) by Hamilton syringe or Geloader tip (Eppendorf)
- Separate proteins by electrophoresis with constant current at 25 mA per mini-gel for 60 minutes or until the dye front reaches the end of the gel

- Stack a sandwich with 3 pieces of Whatman 3MM Chr paper, gel, 0.45µm pore-size nitrocellulose membrane (10401196, Schleicher & Schuell), and another 3 pieces of Whatman 3MM Chr paper orderly
- Transfer proteins to membrane with constant current (65-150 mA, depending on the size of the protein) per mini-gel for 1 hour

Blocking and antibody incubation

- Rinse membrane with water
- Incubate with Ponceau S solution (#33427, Serva) for 1 minute
- Rinse with water several times and check total protein levels
- Block with 5 % not-fat milk/ PBST for 1 hour
- Incubate with primary antibody diluted in 5 % not-fat milk/ PBST at 4°C overnight (some antibodies require 5% BSA instead of milk)
- Rinse once and wash for 5 minutes 3 times with PBST
- Incubate with HRP-conjugated secondary antibody (Jackson ImmunoResearch) diluted in 5 % milk/ PBST at room temperature for 1 hour
- Rinse once and wash for 10 minutes 3 times with PBST

Chemiluminescent detection

- Rinse once with PBS
- Rinse with enhanced chemiluminescence reagent by mixing equal volumes of the Enhanced Luminol Reagent and the Oxidizing Reagent (NEL105, PerkinElmer)
- Expose to Kodak X-OMAT AR Film for 30 seconds to 15 minutes

Solutions

Laemmli Sample Buffer 4X: 200mM Tris-base, 40% glycerol, 16% SDS, 20% β- mercaptoethanol, 0.01% bromphenolblue.

PBST: 0.05 % Tween-20 in PBS

Antibodies used: Anti-HA (Roche, 11867423001); anti-FLAG (Sigma, F1804)

anti-pS6K(Thr398) (Cell Signaling 9209S); anti-tubulin (Developmental

Studies Hybridoma Bank, AA4.3); anti-4EBP1, anti-phosphoT37/46 4EBP1, anti-phosphoS656 4EBP1 (Cell Signaling); anti-GFP (Torrey Pines, New Jersey, USA). Secondary HRP-conjugated antibodies were from Jackson ImmunoResearch.

7.6. Cap pull-down and Co-immunoprecipitation

Cap pull-downs and co-immunoprecipitations were performed on mammalian or S2 cells, usually in a 6-well plate format.

- Harvest cells by scraping, centrifuge at 3000 rpm to pellet the cells, remove all the supernatant (sup)
- Lyse cells by fast pipetting up and down in 200 μ l IP lysis buffer, incubate 5' on ice, from now on all steps are on ice to avoid protein degradation
- Spin down the nuclei at maximum speed in the 4°C, transfer the sup to a new tube
- Remove 50 μ l for input, add 17 μ l 4X loading buffer (#R0891, Fermentas), boil for 5 min at 95°C, put on ice, freeze at -20°C
- To 150 μ l of sup add 350 μ l of IP buffer and 30 μ l of cap beads (m7GTP Sepharose 4B, Amersham), prewashed with 300 μ l of IP buffer.
- Incubate rocking for 1 hour at 4°C
- Wash 3 times with 500 μ l of IP buffer, spinning the beads down for 1 min at 2000 rpm at 4°C
- Remove as much buffer as possible, add 60 μ l of 2X sample buffer, boil for 5min at 95° C, put on ice, freeze at -20°C
- run Western blot

For immunoprecipitation, cells were lysed by pipetting up and down in ice-cold IP lysis Buffer with protease and phosphatase inhibitors. Lysates were cleared by centrifugation at 4°C at maximum speed for 15 min and incubated with antibody for 2 hr at 4°C. 50 μ l of 50% agarose-protein A or G bead slurry was washed twice in lysis buffer and added to the antibody/cell-lysate mixture for

30 min. After three washes with cold lysis buffer, proteins were recovered with 2X protein-gel loading buffer and heating for 5 min at 95°C.

Solutions

IP lysis Buffer: 50 mM Tris pH7.5, 150 mM NaCl, 1 % Triton X-100.
Supplementary protease inhibitors: Protease Inhibitor Cocktail (Roche).
Supplementary phosphatase inhibitors: 25 mM NaF, 1 mM Vanadate, and 25 mM beta-Glycerolphosphate

7.7. Cell culture

Cell lines

Cell lines used were obtained from ATCC (American Tissue Culture Collection).

HeLa Kyoto (human)

HEK-293 (human)

COS-7 (monkey)

S2 (Drosophila)

Chemicals and solutions for cell culture were purchased from Gibco (Eggenstein, Germany). Transfection reagent, Fugene6, was purchased from Roche (Mannheim, Germany).

Cell dishes with glass bottoms were purchased from MaTek (Ashland, USA) and well covered slides (LabTek) from Nunc (Wiesbaden, Germany).

Mammalian cell cultures were cultured at 37°C and 5% CO₂. Mammalian cells were cultured in DMEM with 10% FCS (Foetal Calf Serum, Sigma) and 2mM L-glutamine and 100 µg/ml Penicillin/Streptomycin antibiotics (Gibco). S2 cells were cultured in Drosophila SFM medium (Invitrogen) at 25°C and 100 µg/ml Penicillin/Streptomycin. S2 cells were transfected with Cellfectin (Invitrogen), according to the manufacturer instructions.

Transient transfection of mammalian cells

Cells were transfected at 40-60% confluency with 1 µg of total DNA using

Fugene6 in Optimem, according to the protocol of the manufacturer. Cells were incubated at 37°C and 5% CO₂ to allow for protein expression. Expression time was usually between 15 and 48 h. If necessary cells were starved of serum overnight.

7.8. Microscopy and FRET

For imaging and detecting FRET two microscope setups were used. These were provided and maintained by EMBL Advanced Light Microscopy Facility (ALMF).

Visitron System – widefield microscope Zeiss Axiovert from Carl Zeiss Mikroskopiesysteme (Jena, Germany) equipped with CCD camera Coolsnap HQ from Photometrics, Roper Scientific, Inc. (Trenton, USA) and Filter wheel system from Visitron Systems GmbH (Puchheim, Germany)

Leica AOBIS SP2 - confocal microscope from Leica Microsystems (Heidelberg, Germany).

7.8.1. Ratiometric FRET measurement

Ratiometric imaging was done using an automated Axiovert 135 microscope (Zeiss) equipped with a 63x/1.4 NA oil immersion lens or a 40x/1.2 NA water immersion lens. Images were recorded with Cool Snap HQ cooled charge-coupled device camera (Photometrics) using Metamorph software. Cell medium was replaced by Imaging medium (MEM, Sigma, M3024), with 30mM HEPES buffer, pH 7.2. The experiments were performed at 37°C in a heating chamber. The Insulin and Rapamycin were pre-dissolved in 100 µl medium before addition to the experiment. Samples were illuminated by a 100-watt mercury arc lamp through a D436/10 excitation filter and a CFP/YFP/Cy5 triple-band beam splitter and imaged sequentially through 470/30 (ECFP) and 535/30 (YFP) emission filters with the charge-coupled device camera set to 4 x 4 binning. If expression levels and fluorescence intensities were high enough, a 90% neutral grey filter was used to dim the excitation light. Exposure times were adjusted for each experiment, but were usually not

higher than 200 ms. Five different stage positions were usually recorded in one experiment.

7.8.2. Image analysis

If not otherwise mentioned, live cell FRET experiments were analyzed as follows: the fluorescence intensities of both channels (donor and acceptor) were directly taken from the unprocessed original microscope data set. Regions of interest (ROI) were defined, usually a whole cell and the background without cells. Mean fluorescence intensities were calculated using ImageJ (Rasband, 1997–2008). The background was subtracted for each time point and the ratio of acceptor/ donor mean intensities in the chosen ROI were calculated using Excel software. Cells chosen for analysis were visually healthy and usually expressed the probes to a medium level.

7.8.3. Acceptor photobleaching

Experiments were performed on a Leica AOBS SP2 equipped with strong lasers for photo-bleaching and making use of the FRET acceptor photo-bleaching module provided by the Leica software. First, reference pre-bleaching pictures of the two fluorophores were taken. ECFP was excited with a 405 nm laser, FIAsh was excited using a 514 nm laser. Emission for ECFP was measured between 416 to 486 nm; for FIAsh between 520 to 600 nm. Subsequently, the acceptor was bleached using 514 nm laser at maximum power. Finally, images of both fluorophores were taken again after bleaching. Laser and PMT power were adjusted for each FRET experiment, but PMT values were set the same for both channels. To remove noise 4-line average was used.

7.8.4. Sensitized emission

Experiments were performed on a Leica AOBS SP2 making use of the FRET sensitized emission macro module provided by the Leica software. Initially sample containing only donor and acceptor fluorophores are used to calculate the correction factor for calculation of FRET efficiency. They describe the crosstalk between the channels. Three channels are recorded: channel A – donor channel (donor excitation/donor emission), channel B – FRET channel

(donor excitation/acceptor emission), channel C – acceptor channel (acceptor excitation/ acceptor emission). Correction factors are defined as following:

a = share of acceptor signal in the donor channel (channel A). Correction factor from the acceptor sample = donor emission (donor excitation) / acceptor emission (acceptor excitation).

b = share of donor signal in the FRET channel (channel B). Correction factor from the donor sample = acceptor emission (donor excitation) / donor emission (donor excitation).

c = share of acceptor signal in the FRET channel (channel B). Correction factor from the acceptor sample = acceptor emission (donor excitation) / acceptor emission (acceptor excitation).

After the correction factors are calculated it is crucial to leave the detection parameters (lasers power, PMTs and detectors windows) unchanged when FRET is measured. There is a bug in the Leica confocal software, using sequential acquisition, the software does not change PMTs and detectors windows when switching from the first to the next acquisition step, and only laser is changed. Thus PMTs and detectors had the same settings for acquisition on all channels. ECFP was excited with a 405 nm laser, FIAsH was excited using a 514 nm laser. Emission for ECFP was measured between 430 to 510 nm; for FIAsH between 530 to 600 nm. After background subtraction, FRET efficiency was calculated according to the following formula:

$$\text{FRET}_{\text{eff}} = (B - b \cdot A - (c - a \cdot b) \cdot C) / C$$

where A,B,C are detection channels and a,b,c are correction factors as explained above.

Finally to ensure that the Leica module was functioning properly I used raw data to analyze data manually using ImageJ and the same algorithm. The results were very similar to those produced by Leica software.

7.8.5. FIAsH labeling and BAL experiments

HeLa Kyoto cells were transiently transfected with DNA. The cells were labeled with FIAsH 24-48 h after transfection, according to the following

procedure (protocol from Cristiane Jost, Schultz lab, EMBL). FIAsh was a kind gift of Carsten Schultz lab (EMBL, Heidelberg).

FIAsh was first incubated with 12.5 μ M EDT, giving FIAsh-EDT₂. FIAsh-EDT₂ was then used at a final concentration of 1 μ M in a (microscope) dish and cells were incubated for 1 h at 37°C in Hank's Balanced Salt Solution (HBSS: 10 mM HEPES, 140 mM NaCl, 5.4 mM KCl, 1 mM MgCl₂, 2 mM CaCl₂ and 1 g/L Glucose at pH 7.3) supplemented with 1 g/L D-Glucose. After incubation, unbound and non-specifically bound FIAsh was removed by three 10 min washing steps with 200 μ M EDT in Imaging medium. Finally, cells were left in the imaging medium at 37°C until imaging on the Leica AOBS SP2 confocal microscope. ECFP and FIAsh channels were monitored every 30sec for 6 min. PMTs and detectors had the same settings for acquisition on both channels. ECFP was excited with a 405 nm laser, FIAsh was excited using a 514 nm laser. Emission for ECFP was measured between 430 to 510 nm; for FIAsh between 530 to 630 nm. FIAsh labeling was destroyed by adding 5 mM British-Anti-Lewisite, (BAL, 2,3-dimercaptopropanol).

7.9. Fly genetics

7.9.1. Fly husbandry

Flies were grown on standard corn meal molasses agar. All crosses were carried out at 25°C unless indicated otherwise. Fly stock were stored at 18 °C and flipped once a month.

Fly food recipe:

12 g agar, 18 g dry yeast, 10 g soy flour, 22 g turnip syrup, 80 g malt extract, 80 g corn powder, 6.25 ml propionic acid, and 2.4 g methyl 4-hydroxybenzoate (Nipagin) per liter.

7.9.2. Fly strains

All the fly strains used in this thesis are listed and annotated in Table 7.2 including source or creator. Common stock means stocks propagated at

common EMBL fly room or from Cohen lab collections with not traceable origin.

Table 7.2. Fly strains used for experiments

Genotype	Source	Description
tub-GAL4	Common stock	tubulin-GAL4
en-GAL4	Common stock	engrailed-GAL4
P(EP)2445	Bloomington	CG7097 promoter insertion
PBac(WH)CG7097(f04135)	Bloomington	CG7097 insertion
	Szeged stocks	
P(lacW)l(2)SH1261	center	CG7097 insertion
W ¹¹¹⁸	Common stock	<i>white</i> mutant, used as control
Ore ^R	Bloomington	wildtype
Df(2R)Exel6069	Bloomington	deficiency of CG7097 region
l(2)SH1261excision lines		
1,2	Boris Bryk	excision lines 1,2 imprecise
l(2)SH1261excision lines		
4,5	Boris Bryk	excision lines 4,5 precise
daGAL4	Common stock	daughterlessGAL4
UAS-Rheb ^{AV4}	Bloomington	UAS-Rheb
actGal4	Common stock	actin-GAL4
armGal4	Common stock	armadillo-GAL4
hsGal4	Common stock	heatshock-GAL4
eyeGal4	Common stock	eyelessGal4
apGal4	Common stock	apterousGal4
nubGal4	Common stock	nubbinGal4
ptcGal4	Common stock	patchedGal4
<i>gig</i> ¹⁹²	Bloomington	TSC2 null
Rheb ^{delta1}	Bruce Edgar	Rheb deletion
Rheb ^{delta2}	Bruce Edgar	Rheb deletion
<i>chico1</i>	Bloomington	chico mutant

7.9.3. Ectopic expression using GAL4/UAS system

GAL4/UAS system allows to express genes of interest in a temporally and spatially regulated manner in *Drosophila* (Brand and Perrimon, 1993). This system makes use of the yeast transcription activator, GAL4. GAL4 binds to its target sequence, UAS (upstream activation sequence), and thus activates transcription of attached gene. GAL4 can be expressed in many different patterns by placing it under the control of various *Drosophila* promoter sequences and activates expression of target gene or reporter placed downstream of UAS. In order to get ectopic expression of target gene according to the pattern of a specific promoter, transgenic line carrying GAL4 driver under the specific promoter is crossed to another transgenic line carrying UAS followed by the coding sequence of target gene.

7.10. Fat measurements

Growth controlled males or wandering L3 larvae were used for triglycerides measurements in a two-step protocol. In the first step, homogenized triglycerides are hydrolysed by Lipoprotein Lipase (Sigma cat.62333) to fatty acids and glycerol and then glycerol amount is measured in a colorimetric reaction using Free Glycerol Reagent (Sigma cat. F6428). Amount of triglycerides was normalized to protein to account for differences in size and sample preparation.

- Homogenize 5-8 flies in 200 μ l of ice-cold Homogenization buffer using plastic tip, first smash the flies by hand and then 30 sec by electric homogenizer
- add 300 μ l of ice-cold Homogenization buffer to have a final volume of 500 μ l
- incubate 5 min at 70°C, cool to room temperature
- take out 100 μ l for Bradford (protein) measurement
- spin debris 14000rpm for 3min, use 20 μ l of the supernatant to measure proteins (add 1ml of Bradford reagent (Bio-Rad), wait 5min, read absorbance at 595nm)

- to the remaining 400µl add 10µl of 10mg/ml Lipoprotein Lipase stock, mix
- incubate overnight at 37°C
- spin debris 5000rpm for 1min
- transfer 200µl to a new tube and spin at 14000rpm for 3 min
- add 50µl sample (from the middle of liquid) to 800µl Free Glycerol Reagent (Sigma cat. F6428), incubate 6min at 37°C
- read absorbance at 540nm

Solutions:

Homogenization buffer - 0.05% Tween20 in H₂O

7.11. Size measurement

7.11.1. Growth controlled condition

In order to reduce the variation of growth caused by environmental factors (limited food and space), flies grew under controlled conditions. I collected embryos on apple juice agar plate from each cross for 12 hours. On the next day, I picked up first instar larvae and placed 50 larvae into a vial with fresh food. Flies grew up at 25°C until adulthood. Depending on the number of animals needed several collections were done. If not all progeny is of required genotype, scale up the collection according to Mendel's Law.

7.11.2. Body weight

Flies grew under controlled conditions as described in Section 7.10.1. Once the adult flies eclosed, I separated males and females into vials containing fresh food. I weighted two-day-old flies in a group of 50 males by microbalance.

7.11.3. Growth rate/pupation

First instar larvae were collected within 12 hours interval and placed in a batch of 50 into one vial of food as described in Section 7.10.1. The collection was done in triplicate. Pupae were counted every day from the day the pupation started.

7.11.4. Wing size and cell size measurement

Flies grew in a controlled condition as describe in Section 7.10.1. Matured adult flies were fixed in Glycerol/Ethanol for at least one day before dissection. Rinse fixed flies with distilled water several times and dissect out wings from main body in water. Mount wings in de Faure's medium, leave a weight on top of coverslip, and allow it to dry overnight. Pictures were taken using 2.5X objective and digital camera (Leica DC 500) on Zeiss Axiophot Microscope. Wing areas were measured using ImageJ. At least 7 wings were measured to estimate experimental errors.

For cell size, number of hairs in a fixed area between vein 5 and the posterior of the wing were counted in a 20X magnification image. Each cell in the wing epithelium produces a hair. To calculate cell size, the area was divided by the hair number.

Reagents:

Glycerol/ Ethanol

20 % pure Glycerol in absolute Ethanol

de Faure's medium

50 g Chloral hydrate (toxic), 30 g Gum Arabic, 20 ml Glycerol, and 50 ml distilled water

7.12. Statistics

All error bars in the graphs represent standard deviation. Significance was estimated by a two-tailed Student's test, assuming unequal variance.

Appendix

List of Figures

FIGURE 1 MODEL OF MAMMALIAN TOR SIGNALING	12
FIGURE 2 4EBP1 BINDING TO EIF4E IS REGULATED BY TORC1 MEDIATED PHOSPHORYLATION	15
FIGURE 3 JABLONSKI DIAGRAM	23
FIGURE 4 RIBBON DIAGRAM OF THE WTGFP STRUCTURE	28
FIGURE 5 STRUCTURE OF FRET PROBES	31
FIGURE 6 FLASH LABELING AND COMPARISON TO GFP	33
FIGURE 7 SCHEMATIC OF A CONFORMATIONAL ECFP-4EBP1-CITRINE FRET PROBE	36
FIGURE 8 REGULATION OF ENDOGENOUS 4EBP1 IN HEK 293 CELLS	37
FIGURE 9 REGULATION OF ECFP-4EBP1-CITRINE IN HEK 293 CELLS	39
FIGURE 10 RATIOMETRIC FRET MEASUREMENT OF THE ECFP-4EBP1-CITRINE SENSOR IN HEK 293 CELLS	40
FIGURE 11 RATIOMETRIC FRET MEASUREMENT OF THE ECFP-4EBP1-CITRINE SENSOR IN STABLE HEK 293 CELLS.....	41
FIGURE 12 BIOCHEMICAL ANALYSIS AND FRET MEASUREMENT OF THE ECFP-4EBP1-CITRINE SENSOR IN HELA CELLS.....	43
FIGURE 13 RATIOMETRIC FRET MEASUREMENT OF THE YFP-4EBP1-GFP2 SENSOR IN HELA CELLS	45
FIGURE 14 REGULATION OF ECFP-4EBP1 AND 4EBP1-CITRINE IN MCF7 CELLS	46
FIGURE 15 BIOCHEMICAL ANALYSIS OF THE FLASH-4EBP1 FUSION IN HELA CELLS	48
FIGURE 16 EIF4E FUSIONS BIND CAP AND 4EBP1 IN HELA CELLS	49
FIGURE 17 FRET MEASUREMENT BY ACCEPTOR PHOTOBLEACHING	52
FIGURE 18 FRET MEASUREMENT BY SENSITIZED EMISSION	55
FIGURE 19 FRET MEASUREMENT BY SENSITIZED EMISSION – NEGATIVE CONTROL	56
FIGURE 20 FRET TEST BY DESTROYING FLASH WITH BAL – KCP-F	58
FIGURE 21 4EBP1 FUSIONS TO FLASH DO NOT SHOW FRET	59
FIGURE 22 STRUCTURE OF EIF4E WITH 4EBP1 PEPTIDE AND CAP ANALOG	64
FIGURE 23 DOMAIN STRUCTURE OF MAP4K3.....	69
FIGURE 24 GENOMIC STRUCTURE OF MAP4K3, ITS EXPRESSION IN TRANSGENIC LINES AND DEVELOPMENTAL STAGES AND TISSUES.....	72
FIGURE 25 SURVIVAL OF THE MAP4K3 MUTANTS UNDER DIFFERENT CONDITIONS	74
FIGURE 26 MAP4K3 REGULATES ORGAN AND CELL SIZE.....	75
FIGURE 27 MAP4K3 MUTANT HAVE A DELAY IN GROWTH	76
FIGURE 28 FAT LEVELS ARE REDUCED IN MAP4K3 MUTANTS.....	77
FIGURE 29 EXCISION LINES TEST BY PCR.....	78
FIGURE 30 INSULIN-LIKE PEPTIDES ARE LOW IN MAP4K3 MUTANTS AND CAN BE PARTIALLY RESCUED BY RHEB	79
FIGURE 31 OVEREXPRESSION OF MAP4K3 WITH DIFFERENT GAL4 DRIVERS.....	80
FIGURE 32 TOR ACTIVITY IN MAP4K3 MUTANT.....	82
FIGURE 33 MAP4K3 IS ABLE TO REGULATE ERK AND JNK AND BIND RAG GTPASES.....	84

List of oligonucleotides used for cloning and PCR

Name	Gene/Restriction site	strand/position	Primer sequence 5' to 3'
OBB021	d4e-bp +Bgl II	+	agatctATGTCCGCTTCACCCACC
OBB022	d4e-bp +Bgl II	-	agatctCAGATCCAGTTGGAAGTTC
OBB031	h4ebp1+BamH I	+	ggatccATGTCCGGGGCAGCAGCTG
OBB032	h4ebp1+Bgl II	-	agatctAATGTCCATCTCAAAGTACTCT
OBB034	hum eIF4E	-	gaattcGTGGTGGAGCCGCTCTTAGT
OBB035	hum eIF4E+EcoRI	+	gaattcGCGTTGTGCGATCAGATC
OBB036	hum eIF4E+NotI	-	gcggccgcGCTTGACGAGTCTCCTATGA
OBB037	hum eIF4E+NotI	-1556	gcggccgcGGTTCAGCTCCCAAATCTC
OBB038	h eIF4E 28-217+NcoI	+937	ccatgGTTGCTAACCCAGAACAAC
OBB039	h eIF4E 28-217+KpnI	-1487	gggtaccTTAAACAACAACCTATTTTTAGTG
OBB040	h eIF4E +NdeI	+856	catATGGCGACTGTCTGAACCG
OBB041	h eIF4E +Xho I	-1487	ctcgagTTAAACAACAACCTATTTTTAGTG
OBB042	4EBP1 +Nco I+2	+	ccatggcgTCCGGGGCAGCAGCTG
OBB043	4EBP1 +Kpn I	-	gggtaccTTAAATGTCCATCTCAAAGTGA
OBB044	h eIF4E +NcoI	+856	ccATGGCGACTGTCTGAACCG
OBB045	HAtag-NcoI up		catggcgtaccctacgacGTCCCGACTATGCCGG
OBB046	HAtag-NcoI bot		CATGCCGGCATAGTCCGGGACgctcgtaggggtacgc
OBB047	Afl III h4ebp1	+	acatgtATGTCCGGGGCAGCAGCTG
OBB048	BamH I h4ebp1	-	GGATCCAATGTCCATCTCAAAGTACTCTTCAC
OBB049	Afl III h4ebp1 new	+	acATGTCCGGGGCAGCAGCTG
OBB063	rp49 for qPCR	+	GCTAAGCTGTCGCACAAA
OBB064	rp49 for qPCR	-	TCCGGTGGGCAGCATGTG

Name	Gene/Restriction site	strand/position	Primer sequence 5' to 3'
OBB077	EcoRI-4Cys-h4EBP1	+	gaattcATGttcctgaactgctgccccggctgctgcatggagcccA TGTCCGGGGGCAGCAGCTG
OBB078	NotI 4EBP1 stop	-	gcggccgcTTAaatgtccatctcaaactgtg
OBB079	EcoRI-h4EBP1	+	gaattcATGTCCGGGGGCAGCAGCTG
OBB080	NotI -4Cys 4EBP1 stop	-	gcggccgcTTAgggctccatgcagcagccggggcagcagttcag gaaAATGTCCATCTCAAACCTGTG
OBB081	Age1 hefF4E	+	tcatctACCGTggaATGGCGACTGTGCGAACCG
OBB082	XhoI hefF4E	-	tcatctctcgagTTAAACAACAAACCTATTTTTAGTG
OBB083	KpnI hefF4E	+	ggtaccATGGCGACTGTGCGAACCG
OBB084	BamH I hefF4E	-	ggatccAACAACAAACCTATTTTTAGTG
OBB085	EcoRI hefF4E	+	gaattcATGGCGACTGTGCGAACCG
OBB086	CG7097	+	AACGTGGACAGCATTGTTTTG
OBB087	CG7097	-	CTCTCCAAGGCCACAACC
OBB088	CG5373	+	CTGATGCCAGCCAAGCTC
OBB089	CG5373	-	CCTGGCGCAGATCATCAC
OBB090	CG7097	-	GCCTGTAGGTGCGACTCA
OBB091	CG7097-RA	+15	GCGTTGACGAAGTGCATGTG
OBB092	CG7097-RA	+505	GGCTGCCATCAAGGTCATCA
OBB093	CG7097-RA	+994	CAATCGAACTGGCTGAACTG
OBB094	CG7097-RA	+1492	CGACCTTGCCACTGAACAAC
OBB095	CG7097-RA	+1989	GATGCCGACGACGATGAACT
OBB096	CG7097-RA	+2445	GGCTTCTCGCATTCCAATAG
OBB097	CG7097-RA	+2998	CCGAGGAGGCATCTACAAC
OBB098	CG7097-RA	+3493	CGATTGTGTGTACGGGTGTG

Name	Gene/Restriction site	strand/position	Primer sequence 5' to 3'
OBB099	CG7097-RA	+4022	CCCGCCAATCCACTGTTAT
OBB100	CG7097-RA	+4496	AGTCAGCCAGCAGGAGAATC
OBB101	HAtag-NheI up		ctagctaccctacgacgtcccgactatgcctaa
OBB102	HAtag-NheI bot		ctagttaggcatagtcgggacgtcgtaggggtag
OBB103	SH1261up	2224+	TCGGTTTCAATCCACCATGC
OBB104	SH1261bot	2657-	GGAGCAAACAAATTGGAGCAG
OBB105	MAP4K3	7444-	AAGATAGCGATTCGGGTCGAG
OBB106	MAP4K3	7419-	CCCGTCAGTGTGCATGGTAGT
OBB107	MAP4K3	+	GCTGCGACAACAACCTTGAGAT
OBB108	MAP4K3	-	CGCAGGAGCCACAAATAAGTA
OBB109	MAP4K3	+	TGTGCTTGTGTGGGTTTGTTA
OBB110	MAP4K3	-	CCTTGCCCGTTACATTTACAT
OBB111	MAP4K3	+	CCTCGTTCTGCTCCACTGTGT
OBB112	MAP4K3	-	GCACAGCTCCTTCCTTCACTT
OBB113	MAP4K3	+	AGGAAGGGAAAGGCAAAAACCT
OBB114	MAP4K3	-	GCGTGGTGAGCAATAATGATA
OBB115	MAP4K3	+	TTTGAGAACCATCGGTATTGA
OBB116	MAP4K3	-	CCACCGAAAATGTTATAAGGA
OBB117	MAP4K3	+	GCAAACAAAAGGCAAAGAAAT
OBB118	MAP4K3	-	CAATCCAATGAGGCAATAGTG
OBB119	CG11968+NotI	+	gcggccgcAAGAAAAGGTGTTACTGATGGG
OBB120	CG11968+XhoI	-	ctcgagCGGCAAATGGAGTTATGGAA
OBB121	CG8707+NotI	+	gcggccgcAGCTACGATGATGATGACTATCC
OBB122	CG8707+XhoI	-	ctcgagTTTTTTACGCTGCTCTGTGA
OBB123	FLAGtag-NotI up	+	ggccATGGACTACAAGGACGACGACAAG

Name	Gene/Restriction site	strand/position	Primer sequence 5' to 3'
OBB124	FLAGtag-NotI bot	-	ggccCTTGTCGTCGTCGTCCTTGTAGTCCAT

Note: Lower case usually denotes restriction site sequence followed by a gene specific sequence in upper case.

References

- Adams, M.D., and Sekelsky, J.J. (2002). From sequence to phenotype: reverse genetics in *Drosophila melanogaster*. *Nat Rev Genet* 3, 189-198.
- Adams, S.R., Campbell, R.E., Gross, L.A., Martin, B.R., Walkup, G.K., Yao, Y., Llopis, J., and Tsien, R.Y. (2002). New biarsenical ligands and tetracysteine motifs for protein labeling in vitro and in vivo: synthesis and biological applications. *Journal of the American Chemical Society* 124, 6063-6076.
- Adams, S.R., Harootunian, A.T., Buechler, Y.J., Taylor, S.S., and Tsien, R.Y. (1991). Fluorescence ratio imaging of cyclic AMP in single cells. *Nature* 349, 694-697.
- Andresen, M., Schmitz-Salue, R., and Jakobs, S. (2004). Short tetracysteine tags to beta-tubulin demonstrate the significance of small labels for live cell imaging. *Molecular biology of the cell* 15, 5616-5622.
- Aoki, K., Kiyokawa, E., Nakamura, T., and Matsuda, M. (2008). Visualization of growth signal transduction cascades in living cells with genetically encoded probes based on Forster resonance energy transfer. *Philosophical transactions of the Royal Society of London* 363, 2143-2151.
- Avruch, J., Hara, K., Lin, Y., Liu, M., Long, X., Ortiz-Vega, S., and Yonezawa, K. (2006). Insulin and amino-acid regulation of mTOR signaling and kinase activity through the Rheb GTPase. *Oncogene* 25, 6361-6372.
- Baker, K.D., and Thummel, C.S. (2007). Diabetic larvae and obese flies—emerging studies of metabolism in *Drosophila*. *Cell metabolism* 6, 257-266.
- Bastiaens, P.I., and Squire, A. (1999). Fluorescence lifetime imaging microscopy: spatial resolution of biochemical processes in the cell. *Trends in cell biology* 9, 48-52.
- Berney, C., and Danuser, G. (2003). FRET or no FRET: a quantitative comparison. *Biophysical journal* 84, 3992-4010.
- Bhaskar, P.T., and Hay, N. (2007). The two TORCs and Akt. *Developmental cell* 12, 487-502.

- Biddinger, S.B., and Kahn, C.R. (2006). From mice to men: insights into the insulin resistance syndromes. *Annual review of physiology* 68, 123-158.
- Bjornsti, M.A., and Houghton, P.J. (2004a). Lost in translation: dysregulation of cap-dependent translation and cancer. *Cancer cell* 5, 519-523.
- Bjornsti, M.A., and Houghton, P.J. (2004b). The TOR pathway: a target for cancer therapy. *Nature reviews* 4, 335-348.
- Bluher, M., Michael, M.D., Peroni, O.D., Ueki, K., Carter, N., Kahn, B.B., and Kahn, C.R. (2002). Adipose tissue selective insulin receptor knockout protects against obesity and obesity-related glucose intolerance. *Developmental cell* 3, 25-38.
- Bohni, R., Riesgo-Escovar, J., Oldham, S., Brogiolo, W., Stocker, H., Andruss, B.F., Beckingham, K., and Hafen, E. (1999). Autonomous control of cell and organ size by CHICO, a Drosophila homolog of vertebrate IRS1-4. *Cell* 97, 865-875.
- Brand, A.H., and Perrimon, N. (1993). Targeted gene expression as a means of altering cell fates and generating dominant phenotypes. *Development (Cambridge, England)* 118, 401-415.
- Brejck, K., Sixma, T.K., Kitts, P.A., Kain, S.R., Tsien, R.Y., Ormo, M., and Remington, S.J. (1997). Structural basis for dual excitation and photoisomerization of the Aequorea victoria green fluorescent protein. *Proceedings of the National Academy of Sciences of the United States of America* 94, 2306-2311.
- Britton, J.S., Lockwood, W.K., Li, L., Cohen, S.M., and Edgar, B.A. (2002). Drosophila's insulin/PI3-kinase pathway coordinates cellular metabolism with nutritional conditions. *Developmental cell* 2, 239-249.
- Brogiolo, W., Stocker, H., Ikeya, T., Rintelen, F., Fernandez, R., and Hafen, E. (2001). An evolutionarily conserved function of the Drosophila insulin receptor and insulin-like peptides in growth control. *Curr Biol* 11, 213-221.
- Broughton, S.J., Piper, M.D., Ikeya, T., Bass, T.M., Jacobson, J., Driege, Y., Martinez, P., Hafen, E., Withers, D.J., Leever, S.J., and Partridge, L. (2005). Longer lifespan, altered metabolism, and stress resistance in Drosophila from ablation of cells making insulin-like ligands. *Proceedings of the National Academy of Sciences of the United States of America* 102, 3105-3110.

- Brugarolas, J., Lei, K., Hurley, R.L., Manning, B.D., Reiling, J.H., Hafen, E., Witters, L.A., Ellisen, L.W., and Kaelin, W.G., Jr. (2004). Regulation of mTOR function in response to hypoxia by REDD1 and the TSC1/TSC2 tumor suppressor complex. *Genes & development* 18, 2893-2904.
- Byfield, M.P., Murray, J.T., and Backer, J.M. (2005). hVps34 is a nutrient-regulated lipid kinase required for activation of p70 S6 kinase. *The Journal of biological chemistry* 280, 33076-33082.
- Carriere, A., Cargnello, M., Julien, L.A., Gao, H., Bonneil, E., Thibault, P., and Roux, P.P. (2008). Oncogenic MAPK signaling stimulates mTORC1 activity by promoting RSK-mediated raptor phosphorylation. *Curr Biol* 18, 1269-1277.
- Casas-Terradellas, E., Tato, I., Bartrons, R., Ventura, F., and Rosa, J.L. (2008). ERK and p38 pathways regulate amino acid signalling. *Biochimica et biophysica acta*.
- Chalfie, M., Tu, Y., Euskirchen, G., Ward, W.W., and Prasher, D.C. (1994). Green fluorescent protein as a marker for gene expression. *Science (New York, N.Y)* 263, 802-805.
- Chen, H., Puhl, H.L., 3rd, Koushik, S.V., Vogel, S.S., and Ikeda, S.R. (2006). Measurement of FRET efficiency and ratio of donor to acceptor concentration in living cells. *Biophysical journal* 91, L39-41.
- Chudakov, D.M., Lukyanov, S., and Lukyanov, K.A. (2005). Fluorescent proteins as a toolkit for in vivo imaging. *Trends in biotechnology* 23, 605-613.
- Colombani, J., Raisin, S., Pantalacci, S., Radimerski, T., Montagne, J., and Leopold, P. (2003). A nutrient sensor mechanism controls *Drosophila* growth. *Cell* 114, 739-749.
- Diener, K., Wang, X.S., Chen, C., Meyer, C.F., Keesler, G., Zukowski, M., Tan, T.H., and Yao, Z. (1997). Activation of the c-Jun N-terminal kinase pathway by a novel protein kinase related to human germinal center kinase. *Proceedings of the National Academy of Sciences of the United States of America* 94, 9687-9692.
- Edgar, B.A. (2006). How flies get their size: genetics meets physiology. *Nat Rev Genet* 7, 907-916.
- Elia, A., Constantinou, C., and Clemens, M.J. (2008). Effects of protein phosphorylation on ubiquitination and stability of the translational inhibitor protein 4E-BP1. *Oncogene* 27, 811-822.

- Feng, Z., Zhang, H., Levine, A.J., and Jin, S. (2005). The coordinate regulation of the p53 and mTOR pathways in cells. *Proceedings of the National Academy of Sciences of the United States of America* 102, 8204-8209.
- Findlay, G.M., Yan, L., Procter, J., Mieulet, V., and Lamb, R.F. (2007). A MAP4 kinase related to Ste20 is a nutrient-sensitive regulator of mTOR signalling. *The Biochemical journal* 403, 13-20.
- Förster, T. (1948). Zwischenmolekulare Energiewanderung und Fluoreszenz. *Annalen der Physik* 437, 55-75.
- Gangloff, Y.G., Mueller, M., Dann, S.G., Svoboda, P., Sticker, M., Spetz, J.F., Um, S.H., Brown, E.J., Cereghini, S., Thomas, G., and Kozma, S.C. (2004). Disruption of the mouse mTOR gene leads to early postimplantation lethality and prohibits embryonic stem cell development. *Molecular and cellular biology* 24, 9508-9516.
- Gingras, A.C., Raught, B., Gygi, S.P., Niedzwiecka, A., Miron, M., Burley, S.K., Polakiewicz, R.D., Wyslouch-Cieszyńska, A., Aebersold, R., and Sonenberg, N. (2001). Hierarchical phosphorylation of the translation inhibitor 4E-BP1. *Genes & development* 15, 2852-2864.
- Gingras, A.C., Raught, B., and Sonenberg, N. (1999). eIF4 initiation factors: effectors of mRNA recruitment to ribosomes and regulators of translation. *Annual review of biochemistry* 68, 913-963.
- Griesbeck, O., Baird, G.S., Campbell, R.E., Zacharias, D.A., and Tsien, R.Y. (2001). Reducing the environmental sensitivity of yellow fluorescent protein. Mechanism and applications. *The Journal of biological chemistry* 276, 29188-29194.
- Griffin, B.A., Adams, S.R., and Tsien, R.Y. (1998). Specific covalent labeling of recombinant protein molecules inside live cells. *Science (New York, N.Y)* 281, 269-272.
- Hara, K., Yonezawa, K., Weng, Q.P., Kozłowski, M.T., Belham, C., and Avruch, J. (1998). Amino acid sufficiency and mTOR regulate p70 S6 kinase and eIF-4E BP1 through a common effector mechanism. *The Journal of biological chemistry* 273, 14484-14494.
- Harris, T.E., and Lawrence, J.C., Jr. (2003). TOR signaling. *Sci STKE* 2003, re15.

- Hay, N., and Sonenberg, N. (2004). Upstream and downstream of mTOR. *Genes & development* 18, 1926-1945.
- Heim, R., Cubitt, A.B., and Tsien, R.Y. (1995). Improved green fluorescence. *Nature* 373, 663-664.
- Heim, R., Prasher, D.C., and Tsien, R.Y. (1994). Wavelength mutations and posttranslational autoxidation of green fluorescent protein. *Proceedings of the National Academy of Sciences of the United States of America* 91, 12501-12504.
- Heim, R., and Tsien, R.Y. (1996). Engineering green fluorescent protein for improved brightness, longer wavelengths and fluorescence resonance energy transfer. *Curr Biol* 6, 178-182.
- Heitman, J., Movva, N.R., and Hall, M.N. (1991). Targets for cell cycle arrest by the immunosuppressant rapamycin in yeast. *Science (New York, N.Y)* 253, 905-909.
- Herbert, T.P., Tee, A.R., and Proud, C.G. (2002). The extracellular signal-regulated kinase pathway regulates the phosphorylation of 4E-BP1 at multiple sites. *The Journal of biological chemistry* 277, 11591-11596.
- Hires, S.A., Zhu, Y., and Tsien, R.Y. (2008). Optical measurement of synaptic glutamate spillover and reuptake by linker optimized glutamate-sensitive fluorescent reporters. *Proceedings of the National Academy of Sciences of the United States of America* 105, 4411-4416.
- Hirose, E., Nakashima, N., Sekiguchi, T., and Nishimoto, T. (1998). RagA is a functional homologue of *S. cerevisiae* Gtr1p involved in the Ran/Gsp1-GTPase pathway. *Journal of cell science* 111 (Pt 1), 11-21.
- Hoffmann, C., Gaietta, G., Bunemann, M., Adams, S.R., Oberdorff-Maass, S., Behr, B., Vilardaga, J.P., Tsien, R.Y., Ellisman, M.H., and Lohse, M.J. (2005). A FIAsh-based FRET approach to determine G protein-coupled receptor activation in living cells. *Nature methods* 2, 171-176.
- Inoki, K., Zhu, T., and Guan, K.L. (2003). TSC2 mediates cellular energy response to control cell growth and survival. *Cell* 115, 577-590.
- Ito, N., and Rubin, G.M. (1999). *gigas*, a *Drosophila* homolog of tuberous sclerosis gene product-2, regulates the cell cycle. *Cell* 96, 529-539.
- Itoh, R.E., Kurokawa, K., Fujioka, A., Sharma, A., Mayer, B.J., and Matsuda, M. (2005). A FRET-based probe for epidermal growth factor receptor bound

- non-covalently to a pair of synthetic amphipathic helices. *Experimental cell research* 307, 142-152.
- Jares-Erijman, E.A., and Jovin, T.M. (2003). FRET imaging. *Nature biotechnology* 21, 1387-1395.
- Jost, C.A., Reither, G., Hoffmann, C., and Schultz, C. (2008). Contribution of fluorophores to protein kinase C FRET probe performance. *Chembiochem* 9, 1379-1384.
- Juhasz, G., Hill, J.H., Yan, Y., Sass, M., Baehrecke, E.H., Backer, J.M., and Neufeld, T.P. (2008). The class III PI(3)K Vps34 promotes autophagy and endocytosis but not TOR signaling in *Drosophila*. *The Journal of cell biology* 181, 655-666.
- Kahn, B.B. (1996). Lilly lecture 1995. Glucose transport: pivotal step in insulin action. *Diabetes* 45, 1644-1654.
- Kim, E., Goraksha-Hicks, P., Li, L., Neufeld, T.P., and Guan, K.L. (2008). Regulation of TORC1 by Rag GTPases in nutrient response. *Nature cell biology* 10, 935-945.
- Kim, S.K., and Rulifson, E.J. (2004). Conserved mechanisms of glucose sensing and regulation by *Drosophila corpora cardiaca* cells. *Nature* 431, 316-320.
- Kurokawa, K., Mochizuki, N., Ohba, Y., Mizuno, H., Miyawaki, A., and Matsuda, M. (2001). A pair of fluorescent resonance energy transfer-based probes for tyrosine phosphorylation of the CrkII adaptor protein in vivo. *The Journal of biological chemistry* 276, 31305-31310.
- Kurokawa, K., Takaya, A., Terai, K., Fujioka, A., and Matsuda, M. (2004). Visualizing the Signal Transduction Pathways in Living Cells with GFP-Based FRET Probes. *Acta Histochemica et Cytochemica* 37, 347-355.
- Kyriakis, J.M. (1999). Signaling by the germinal center kinase family of protein kinases. *The Journal of biological chemistry* 274, 5259-5262.
- Lakowicz, J.R., Szmacinski, H., Nowaczyk, K., Berndt, K.W., and Johnson, M. (1992). Fluorescence lifetime imaging. *Analytical biochemistry* 202, 316-330.
- Lee, G., and Park, J.H. (2004). Hemolymph sugar homeostasis and starvation-induced hyperactivity affected by genetic manipulations of the adipokinetic hormone-encoding gene in *Drosophila melanogaster*. *Genetics* 167, 311-323.

- Li, Y., Inoki, K., Vacratsis, P., and Guan, K.L. (2003). The p38 and MK2 kinase cascade phosphorylates tuberlin, the tuberous sclerosis 2 gene product, and enhances its interaction with 14-3-3. *The Journal of biological chemistry* 278, 13663-13671.
- Long, X., Lin, Y., Ortiz-Vega, S., Yonezawa, K., and Avruch, J. (2005a). Rheb binds and regulates the mTOR kinase. *Curr Biol* 15, 702-713.
- Long, X., Ortiz-Vega, S., Lin, Y., and Avruch, J. (2005b). Rheb binding to mammalian target of rapamycin (mTOR) is regulated by amino acid sufficiency. *The Journal of biological chemistry* 280, 23433-23436.
- Long, X., Spycher, C., Han, Z.S., Rose, A.M., Muller, F., and Avruch, J. (2002). TOR deficiency in *C. elegans* causes developmental arrest and intestinal atrophy by inhibition of mRNA translation. *Curr Biol* 12, 1448-1461.
- Lum, J.J., DeBerardinis, R.J., and Thompson, C.B. (2005). Autophagy in metazoans: cell survival in the land of plenty. *Nat Rev Mol Cell Biol* 6, 439-448.
- Luong, N., Davies, C.R., Wessells, R.J., Graham, S.M., King, M.T., Veech, R., Bodmer, R., and Oldham, S.M. (2006). Activated FOXO-mediated insulin resistance is blocked by reduction of TOR activity. *Cell metabolism* 4, 133-142.
- Ma, L., Chen, Z., Erdjument-Bromage, H., Tempst, P., and Pandolfi, P.P. (2005). Phosphorylation and functional inactivation of TSC2 by Erk implications for tuberous sclerosis and cancer pathogenesis. *Cell* 121, 179-193.
- Maniatis, T., Fritsch, E.F., and Sambrook, J. (1989). *Molecular cloning : a laboratory manual* / J. Sambrook, E.F. Fritsch, T. Maniatis. (New York : Cold Spring Harbor Laboratory Press).
- Manning, B.D. (2004). Balancing Akt with S6K: implications for both metabolic diseases and tumorigenesis. *The Journal of cell biology* 167, 399-403.
- Marcotrigiano, J., Gingras, A.C., Sonenberg, N., and Burley, S.K. (1999). Cap-dependent translation initiation in eukaryotes is regulated by a molecular mimic of eIF4G. *Molecular cell* 3, 707-716.
- Miyawaki, A. (2003). Visualization of the spatial and temporal dynamics of intracellular signaling. *Developmental cell* 4, 295-305.

- Miyawaki, A., Llopis, J., Heim, R., McCaffery, J.M., Adams, J.A., Ikura, M., and Tsien, R.Y. (1997). Fluorescent indicators for Ca²⁺ based on green fluorescent proteins and calmodulin. *Nature* 388, 882-887.
- Mizushima, N., Ohsumi, Y., and Yoshimori, T. (2002). Autophagosome formation in mammalian cells. *Cell structure and function* 27, 421-429.
- Mochizuki, N., Yamashita, S., Kurokawa, K., Ohba, Y., Nagai, T., Miyawaki, A., and Matsuda, M. (2001). Spatio-temporal images of growth-factor-induced activation of Ras and Rap1. *Nature* 411, 1065-1068.
- Montagne, J., Stewart, M.J., Stocker, H., Hafen, E., Kozma, S.C., and Thomas, G. (1999). *Drosophila* S6 kinase: a regulator of cell size. *Science* (New York, N.Y. 285, 2126-2129.
- Mothe-Satney, I., Yang, D., Fadden, P., Haystead, T.A., and Lawrence, J.C., Jr. (2000). Multiple mechanisms control phosphorylation of PHAS-I in five (S/T)P sites that govern translational repression. *Molecular and cellular biology* 20, 3558-3567.
- Nagai, Y., Miyazaki, M., Aoki, R., Zama, T., Inouye, S., Hirose, K., Iino, M., and Hagiwara, M. (2000). A fluorescent indicator for visualizing cAMP-induced phosphorylation in vivo. *Nature biotechnology* 18, 313-316.
- Nakashima, N., Noguchi, E., and Nishimoto, T. (1999). *Saccharomyces cerevisiae* putative G protein, Gtr1p, which forms complexes with itself and a novel protein designated as Gtr2p, negatively regulates the Ran/Gsp1p G protein cycle through Gtr2p. *Genetics* 152, 853-867.
- Nobukuni, T., Joaquin, M., Rocco, M., Dann, S.G., Kim, S.Y., Gulati, P., Byfield, M.P., Backer, J.M., Natt, F., Bos, J.L., Zwartkruis, F.J., and Thomas, G. (2005). Amino acids mediate mTOR/raptor signaling through activation of class 3 phosphatidylinositol 3OH-kinase. *Proceedings of the National Academy of Sciences of the United States of America* 102, 14238-14243.
- Oh, S.W., Kingsley, T., Shin, H.H., Zheng, Z., Chen, H.W., Chen, X., Wang, H., Ruan, P., Moody, M., and Hou, S.X. (2003). A P-element insertion screen identified mutations in 455 novel essential genes in *Drosophila*. *Genetics* 163, 195-201.
- Oldham, S., Montagne, J., Radimerski, T., Thomas, G., and Hafen, E. (2000). Genetic and biochemical characterization of dTOR, the *Drosophila* homolog of the target of rapamycin. *Genes & development* 14, 2689-2694.

- Ormo, M., Cubitt, A.B., Kallio, K., Gross, L.A., Tsien, R.Y., and Remington, S.J. (1996). Crystal structure of the *Aequorea victoria* green fluorescent protein. *Science (New York, N.Y)* 273, 1392-1395.
- Patel, P.H., Thapar, N., Guo, L., Martinez, M., Maris, J., Gau, C.L., Lengyel, J.A., and Tamanoi, F. (2003). *Drosophila* Rheb GTPase is required for cell cycle progression and cell growth. *Journal of cell science* 116, 3601-3610.
- Pende, M., Um, S.H., Mieulet, V., Sticker, M., Goss, V.L., Mestan, J., Mueller, M., Fumagalli, S., Kozma, S.C., and Thomas, G. (2004). S6K1(-/-)/S6K2(-/-) mice exhibit perinatal lethality and rapamycin-sensitive 5'-terminal oligopyrimidine mRNA translation and reveal a mitogen-activated protein kinase-dependent S6 kinase pathway. *Molecular and cellular biology* 24, 3112-3124.
- Piston, D.W., and Kremers, G.J. (2007). Fluorescent protein FRET: the good, the bad and the ugly. *Trends in biochemical sciences* 32, 407-414.
- Prasher, D.C., Eckenrode, V.K., Ward, W.W., Prendergast, F.G., and Cormier, M.J. (1992). Primary structure of the *Aequorea victoria* green-fluorescent protein. *Gene* 111, 229-233.
- Proud, C.G. (2007). Signalling to translation: how signal transduction pathways control the protein synthetic machinery. *The Biochemical journal* 403, 217-234.
- Ramjaun, A.R., Angers, A., Legendre-Guillemain, V., Tong, X.K., and McPherson, P.S. (2001). Endophilin regulates JNK activation through its interaction with the germinal center kinase-like kinase. *The Journal of biological chemistry* 276, 28913-28919.
- Rasband, W.S. (1997–2008). ImageJ, U. S. National Institutes of Health, Bethesda, Maryland, USA, <http://rsb.info.nih.gov/ij/>.
- Reiling, J.H., and Hafen, E. (2004). The hypoxia-induced paralogs Scylla and Charybdis inhibit growth by down-regulating S6K activity upstream of TSC in *Drosophila*. *Genes & development* 18, 2879-2892.
- Rizzo, M.A., and Piston, D.W. (2005). High-contrast imaging of fluorescent protein FRET by fluorescence polarization microscopy. *Biophysical journal* 88, L14-16.
- Rosen, E.D., and Spiegelman, B.M. (2006). Adipocytes as regulators of energy balance and glucose homeostasis. *Nature* 444, 847-853.

- Roux, P.P., Ballif, B.A., Anjum, R., Gygi, S.P., and Blenis, J. (2004). Tumor-promoting phorbol esters and activated Ras inactivate the tuberous sclerosis tumor suppressor complex via p90 ribosomal S6 kinase. *Proceedings of the National Academy of Sciences of the United States of America* 101, 13489-13494.
- Rulifson, E.J., Kim, S.K., and Nusse, R. (2002). Ablation of insulin-producing neurons in flies: growth and diabetic phenotypes. *Science (New York, N.Y)* 296, 1118-1120.
- Ruvinsky, I., Sharon, N., Lerer, T., Cohen, H., Stolovich-Rain, M., Nir, T., Dor, Y., Zisman, P., and Meyuhas, O. (2005). Ribosomal protein S6 phosphorylation is a determinant of cell size and glucose homeostasis. *Genes & development* 19, 2199-2211.
- Sabatini, D.M. (2006). mTOR and cancer: insights into a complex relationship. *Nature reviews* 6, 729-734.
- Sancak, Y., Peterson, T.R., Shaul, Y.D., Lindquist, R.A., Thoreen, C.C., Bar-Peled, L., and Sabatini, D.M. (2008). The Rag GTPases bind raptor and mediate amino acid signaling to mTORC1. *Science (New York, N.Y)* 320, 1496-1501.
- Sarbassov, D.D., Ali, S.M., and Sabatini, D.M. (2005). Growing roles for the mTOR pathway. *Current opinion in cell biology* 17, 596-603.
- Sasaki, K., Sato, M., and Umezawa, Y. (2003). Fluorescent indicators for Akt/protein kinase B and dynamics of Akt activity visualized in living cells. *The Journal of biological chemistry* 278, 30945-30951.
- Saucedo, L.J., Gao, X., Chiarelli, D.A., Li, L., Pan, D., and Edgar, B.A. (2003). Rheb promotes cell growth as a component of the insulin/TOR signalling network. *Nature cell biology* 5, 566-571.
- Schleifenbaum, A., Stier, G., Gasch, A., Sattler, M., and Schultz, C. (2004). Genetically encoded FRET probe for PKC activity based on pleckstrin. *Journal of the American Chemical Society* 126, 11786-11787.
- Schultz, J.r., Milpetz, F., Bork, P., and Ponting, C.P. (1998). SMART, a simple modular architecture research tool: Identification of signaling domains. *Proceedings of the National Academy of Sciences of the United States of America* 95, 5857-5864.

- Sekar, R.B., and Periasamy, A. (2003). Fluorescence resonance energy transfer (FRET) microscopy imaging of live cell protein localizations. *J. Cell Biol.* 160, 629-633.
- Sekiguchi, T., Hirose, E., Nakashima, N., Li, M., and Nishimoto, T. (2001). Novel G proteins, Rag C and Rag D, interact with GTP-binding proteins, Rag A and Rag B. *The Journal of biological chemistry* 276, 7246-7257.
- Shaner, N.C., Patterson, G.H., and Davidson, M.W. (2007). Advances in fluorescent protein technology. *Journal of cell science* 120, 4247-4260.
- Shi, C.S., and Kehrl, J.H. (1997). Activation of stress-activated protein kinase/c-Jun N-terminal kinase, but not NF-kappaB, by the tumor necrosis factor (TNF) receptor 1 through a TNF receptor-associated factor 2- and germinal center kinase related-dependent pathway. *The Journal of biological chemistry* 272, 32102-32107.
- Shimomura, O., Johnson, F.H., and Saiga, Y. (1962). Extraction, purification and properties of aequorin, a bioluminescent protein from the luminous hydromedusan, *Aequorea*. *Journal of cellular and comparative physiology* 59, 223-239.
- Stroffekova, K., Proenza, C., and Beam, K.G. (2001). The protein-labeling reagent FLASH-EDT2 binds not only to CCXXCC motifs but also non-specifically to endogenous cysteine-rich proteins. *Pflugers Arch* 442, 859-866.
- Stryer, L. (1978). Fluorescence energy transfer as a spectroscopic ruler. *Annual review of biochemistry* 47, 819-846.
- Tee, A.R., and Proud, C.G. (2002). Caspase cleavage of initiation factor 4E-binding protein 1 yields a dominant inhibitor of cap-dependent translation and reveals a novel regulatory motif. *Molecular and cellular biology* 22, 1674-1683.
- Teleman, A.A., Chen, Y.W., and Cohen, S.M. (2005a). 4E-BP functions as a metabolic brake used under stress conditions but not during normal growth. *Genes & development* 19, 1844-1848.
- Teleman, A.A., Chen, Y.W., and Cohen, S.M. (2005b). *Drosophila* Melted modulates FOXO and TOR activity. *Developmental cell* 9, 271-281.
- Tomoo, K., Matsushita, Y., Fujisaki, H., Abiko, F., Shen, X., Taniguchi, T., Miyagawa, H., Kitamura, K., Miura, K., and Ishida, T. (2005). Structural basis for mRNA Cap-Binding regulation of eukaryotic initiation factor 4E by 4E-

binding protein, studied by spectroscopic, X-ray crystal structural, and molecular dynamics simulation methods. *Biochimica et biophysica acta* 1753, 191-208.

Tsien, R.Y. (1998). The green fluorescent protein. *Annual review of biochemistry* 67, 509-544.

Tsukiyama-Kohara, K., Poulin, F., Kohara, M., DeMaria, C.T., Cheng, A., Wu, Z., Gingras, A.C., Katsume, A., Elchebly, M., Spiegelman, B.M., Harper, M.E., Tremblay, M.L., and Sonenberg, N. (2001). Adipose tissue reduction in mice lacking the translational inhibitor 4E-BP1. *Nature medicine* 7, 1128-1132.

Um, S.H., Frigerio, F., Watanabe, M., Picard, F., Joaquin, M., Sticker, M., Fumagalli, S., Allegrini, P.R., Kozma, S.C., Auwerx, J., and Thomas, G. (2004). Absence of S6K1 protects against age- and diet-induced obesity while enhancing insulin sensitivity. *Nature* 431, 200-205.

Van der Horst, D.J. (2003). Insect adipokinetic hormones: release and integration of flight energy metabolism. *Comparative biochemistry and physiology* 136, 217-226.

Villardaga, J.P., Bunemann, M., Krasel, C., Castro, M., and Lohse, M.J. (2003). Measurement of the millisecond activation switch of G protein-coupled receptors in living cells. *Nature biotechnology* 21, 807-812.

Vogel, S.S., Thaler, C., and Koushik, S.V. (2006). Fanciful FRET. *Sci. STKE* 2006, re2-.

Wang, X., Beugnet, A., Murakami, M., Yamanaka, S., and Proud, C.G. (2005). Distinct signaling events downstream of mTOR cooperate to mediate the effects of amino acids and insulin on initiation factor 4E-binding proteins. *Molecular and cellular biology* 25, 2558-2572.

Wolf, D.E. (2003). Fundamentals of fluorescence and fluorescence microscopy. *Methods in cell biology* 72, 157-184.

Wouters, F.S., Verveer, P.J., and Bastiaens, P.I. (2001). Imaging biochemistry inside cells. *Trends in cell biology* 11, 203-211.

Wullschleger, S., Loewith, R., and Hall, M.N. (2006). TOR signaling in growth and metabolism. *Cell* 124, 471-484.

Yoshizaki, H., Ohba, Y., Kurokawa, K., Itoh, R.E., Nakamura, T., Mochizuki, N., Nagashima, K., and Matsuda, M. (2003). Activity of Rho-family GTPases

during cell division as visualized with FRET-based probes. *The Journal of cell biology* 162, 223-232.

Zacharias, D.A. (2002). Sticky caveats in an otherwise glowing report: oligomerizing fluorescent proteins and their use in cell biology. *Sci STKE* 2002, PE23.

Zacharias, D.A., Violin, J.D., Newton, A.C., and Tsien, R.Y. (2002). Partitioning of lipid-modified monomeric GFPs into membrane microdomains of live cells. *Science (New York, N.Y)* 296, 913-916.

Zhang, H., Stallock, J.P., Ng, J.C., Reinhard, C., and Neufeld, T.P. (2000). Regulation of cellular growth by the *Drosophila* target of rapamycin dTOR. *Genes & development* 14, 2712-2724.

Zhang, J., Ma, Y., Taylor, S.S., and Tsien, R.Y. (2001). Genetically encoded reporters of protein kinase A activity reveal impact of substrate tethering. *Proceedings of the National Academy of Sciences of the United States of America* 98, 14997-15002.

Zimmermann, T., Rietdorf, J., Girod, A., Georget, V., and Pepperkok, R. (2002). Spectral imaging and linear un-mixing enables improved FRET efficiency with a novel GFP2-YFP FRET pair. *FEBS letters* 531, 245-249.